M-Pos107
LOW TEMPERATURE RECOMBINATION OF MbO_2 USING FOURIER TRANSFORM INFRARED SPECTROSCOPY. ((M. Halterman, L. M. Miller, and M. R. Chance)) Albert Einstein College of Medicine., Bronx, NY 10461.

The binding of oxygen to hemoglobin and myoglobin is one of the most important reactions in human cells. Essential to understanding the binding process is the study of intermediate states. To date, the intermediate states involved in carbon monoxide binding are much better understood than those of oxygen binding. However, recent studies have shown that O_2 and CO have significantly different rebinding intermediates (M. Chance, et. al., *Biochemistry*, 29, 1990, p. 5537). Vibrational spectroscopic methods have indicated several bands for MbO_2 ligand stretching modes (Potter, et. al., *Biochemistry*, 26, 1987, p. 4699). However, it is uncertain whether these bands correspond to various protein conformations, as they do for MbCO. If the multiple bands have different rebinding kinetics, this supports multiple steric and electronic environments of the distal histidine.

We present the results of low temperature recombination of O_2 with myoglobin using Fourier Transform Infrared Spectroscopy (FTIR). The bound state of oxymyoglobin exhibits three infrared bands of interest at 1090 cm^{-1}, 1115 cm^{-1}, and 1135 cm^{-1}. Upon photolysis, the intensity of each band is reduced. After warming, the O_2 and myoglobin recombine and the bands reappear. Kinetic analysis of these bands helps to identify the presence of various protein conformations involved in the recombination process. Low-temperature recombination of samples at various pH's will demonstrate various protonation states of the distal histidine. Also, we will present studies using isotopically labelled O_2 in order to identify those stretching modes directly related to the Fe-O_2 bond. This research is supported by a grant from the NIH, #HL-45892.

M-Pos108
TIME-RESOLVED X-RAY ABSORPTION SPECTROSCOPY ON A 5 μs TIMESCALE. ((M.R. Chance, M.D. Wirt, L.M. Miller, E.M. Scheuring, A. Xie, D.E. Sidelinger)) Albert Einstein Col of Med., Bronx, NY 10461

X-ray absorption spectroscopy (XAS) is unmatched in measuring metal-ligand distances in solution while the dynamics of evolving systems is a subject of intense interest in biophysics currently. We report the design and successful testing of a system for collecting time-resolved XAS data on a 5 μs timescale. The system is based on the use of a germanium energy resolving detector and a fast multichannel scaling (FMS) board, both from Canberra Ind. The output of a single Ge channel is amplified and connected to the FMS board. The data acquisition sequence is controlled by a digital delay generator, which also controls the firing of a (doubled) Nd-YAG laser (output 100 mW, 532 nm, 10 Hz). Software control allows the windowing of the x-ray fluorescence peak of interest, which is then laid down in directly accessed memory with specified time widths. A typical experiment laid down 8192 channels of data, each counting a 5 μs interval. For testing of the system, we used a well characterized chemical system, that of rebinding of carbon monoxide with myoglobin after a laser flash at low-temperature. To date, we are aware of only one previous attempt to perform XAS in a time-resolved fashion on (300) μs timescales (D. Mills, et. al., *Science*, 223, 1984, p. 811). In one experiment, an excellent x-ray edge was collected on 5μs timescales (4 mM MbCO, data collected every 4 eV, and 5000 sweeps at each energy). In a second experiment, we demonstrated that with a 1 mM sample and 20 μs time resolution we could sit at a single x-ray wavelength, where the difference between the photolyzed and ligand bound spectra is the largest (kinetic spectrophotometry), and observe the photolysis and recombination of the sample. This work is supported by NIH grant HL-45892.

M-Pos109
X-RAY ABSORPTION SPECTROSCOPY OF MBO_2 AND MBCO REBINDING INTERMEDIATES. ((L.M. Miller, M.R. Chance M.D. Wirt, E.M. Scheuring)) Albert Einstein Col. of Med., Bronx, NY 10461

Recent studies have shown that MbO_2 and MbCO have significantly different rebinding intermediates. For example, the quantum yield of MbO_2 photolysis at low temperature is 0.4 whereas that of MbCO is 1.0. X-ray absorption spectroscopy (XAS) can be used to study the differences between these two rebinding processes. XAS is especially sensitive to iron displacement from the heme plane and charge density on the iron atom. When a ligand is photolyzed from hemoglobin and myoglobin, the displacement and charge density of the iron change, resulting in changes in the x-ray edge position and the XANES region of bound versus photolyzed hemoglobin or myoglobin. The x-ray absorption spectrum of bound MbO_2 was obtained at high resolution using 0.5 eV steps across the x-ray edge. First derivatives of the edge spectra are used to accurately define the charge density on the central metal. The position of the MbO_2 edge can now be well defined at 7125.4 eV. In comparison, we find the x-ray edge position of MbCO to be at 7123.9 eV, indicating a significant difference in iron environments between the bound MbCO and MbO_2. This result is consistent with studies that have shown a hydrogen bond between oxygen (but not CO) and the distal histidine of myoglobin. This hydrogen bond is stabilized by charge reorganization from the iron to the oxygen, resulting in a loss of charge density on the iron. This loss of charge density is reflected in the x-ray edge by a shift to higher energy. Additionally, we have collected x-ray edge and EXAFS spectra of photolyzed MbO_2; both the x-ray edge and the XANES region show differences between the photolyzed and unphotolyzed MbO_2.This work has been supported by NIH grant HL-45892.

M-Pos110
LIGAND CONCENTRATION DEPENDENCE OF THE REBINDING RATE OF CO TO MYOGLOBIN. ((R. G. Philipp, R. M. Ernst, G. U. Nienhaus, R. D. Young, H. Frauenfelder)) University of Illinois at Urbana-Champaign, Urbana, IL 61801.*

We compare the rate of rebinding of CO to myoglobin with the rate predicted for a bimolecular process. The measurements probe rebinding kinetics in a glycerol/water solvent using flash photolysis over a wide range of time and temperature. We have used a pressure cell which allows CO pressures of 0-200 atm, with a corresponding CO concentration which ranges from the low to high concentration limits.

*This work supported by the Office of Naval Research.

M-Pos111
A- AND B-STATE TRANSITIONS IN MYOGLOBIN ((K. Chu, J.R. Mourant, Y. Abadan, H. Frauenfelder, G.U. Nienhaus and R.D. Young)) Department of Physics, University of Illinois, 1110 W. Green St., Urbana, IL 61801.

FTIR spectroscopy on low temperature photoproducts of sperm whale carbonmonoxymyoglobin has revealed much information about ligand rebinding dynamics in proteins. Several spectroscopic lines are observed around 1950 cm^{-1} and 2150 cm^{-1}; these are CO stretch bands corresponding to conformational substates of the ligand bound (A substates) and photolysed (B substates) protein-ligand system. The A and B substates undergo three separate classes of transitions following photolysis. Upon absorption of a visible photon by the heme, the ligand - heme bond breaks, resulting in an A→B transition. The resulting B substates are not in thermal equilibrium and a B→B exchange occurs. Finally, the ligand rebinds to the protein (B→A). We use isothermal kinetics and temperature derivative spectroscopy to identify and characterise the tunneling and thermally activated transitions. (This work supported by the NSF and the NIH.)

M-Pos112
INFRARED FLASH PHOTOLYSIS EXPERIMENTS ON THE TAXONOMIC SUBSTATES OF MYOGLOBIN ((Don C. Lamb, Bradley T. Banko, Hans Frauenfelder, G. Ulrich Nienhaus and Robert D. Young)) Department of Physics, University of Illinois at Urbana-Champaign, 1110 W. Green St., Urbana, Illinois 61801

Sperm whale carbonmonoxymyoglobin exhibits at least three spectroscopically distinguishable infrared stretch bands. They are interpreted as three different taxonomic substates,[1] referred to as A_0, A_1 and A_3. Flash photolysis experiments have been performed on the individual A substates by monitoring at selected wavelengths in the infrared. The three temperature-independent distributions of activation enthalpies for ligand rebinding after photolysis, g(H), are determined from the low temperature kinetics (60K - 160K) for the different A substates. These g(H) distributions are compared for samples at different pH. The g(H) distributions are also compared to those determined using temperature derivative spectroscopy. At temperatures above 180K, we describe the kinetics with temperature-dependent distributions of rate coefficients, f(λ). The maximum entropy method was used to calculate the f(λ) for temperatures above 180K. The f(λ) distributions provide additional insight into the entrance and escape of carbon monoxide from the heme pocket as well as protein motions. This work is supported with grants from the NIH, the NSF and the ONR.

[1] H. Frauenfelder, S.G. Sligar and P.G. Wolynes, *Science* 254, 1598 (1991).

M-Pos113

MOLECULAR DYNAMICS SIMULATIONS OF LIGAND DISSOCIATION AND REBINDING IN MYOGLOBIN. ((Olivier Schaad, Huan-Xiang Zhou, Eric R. Henry, Attila Szabo and William A. Eaton)) Laboratory of Chemical Physics, NIDDK, NIH, Bethesda, MD 20892

We have begun to study the kinetics of NO rebinding to myoglobin following photodissociation by molecular dynamics simulations. The simulations included the complete protein molecule with all hydrogen atoms plus a layer of 350 water molecules. Ligand dissociation was induced by instantaneously switching to a dissociative potential which forces the ligand away from the heme. Rebinding was simulated using a potential function which switches smoothly between an unliganded and a liganded heme potential as a function of the position and orientation of the ligand, with no barrier arising from the crossing of potential surfaces of different electronic configurations. In 93 of 100 trajectories the ligand rebound in less than 15 ps. The kinetic progress curve was calculated from the simulations as the fraction of unbound ligands as a function of time. The calculated relaxation time of 2 ps at 300°K is about 50 times shorter than the experimental value of Petrich et al. (*Biochemistry 30*, 3975, 1991), presumably because of the absence of the electronic barrier. The calculated progress curve also exhibits a lag phase of about 0.5 ps before the onset of ligand binding because of the finite time required to thermalize the initial ligand velocity.

M-Pos114

OXYGEN BINDING TO SINGLE CRYSTALS OF HEMOGLOBIN IN THE T QUATERNARY STRUCTURE. ((A. Mozzarelli, C. Rivetti, G. L. Rossi, E. R. Henry*, and W. A. Eaton*)) Institute of Biochemical Sciences, University of Parma, and *Laboratory of Chemical Physics, NIDDK, NIH, Bethesda, MD 20892.

Microspectrophotometry was used to measure reversible oxygen binding curves for single crystals of hemoglobin in the T quaternary structure. Measurements of the visible spectra were made on the orthorhombic crystal grown from polyethylene glycol with light polarized parallel to the *a* and *c* crystal axes. The α and β heme planes make different projections onto these crystal axes, making it possible to determine their saturations separately from the two spectra in wavelength regions where hemes behave like nearly perfect circularly symmetric absorbers of linearly-polarized light. The α subunits bind oxygen with an affinity that is about 5-fold greater than that of the β subunits. This difference in affinity is almost exactly compensated by a small amount of cooperativity to produce a binding curve for the tetramer in the crystal with a Hill *n* of 1.0. The cooperativity is only about 10% of that observed in solution, and therefore represents only a slight perturbation on the essential feature of the two-state allosteric model that binding to the T quaternary structure be perfectly non-cooperative. The low affinity and absence of the Bohr effect in the crystal can be explained by a model in which both high and low affinity tertiary conformations, with broken and unbroken salt bridges, respectively, are populated in the T quaternary structure in solution.

M-Pos115

Homogeneous Nucleation Initiates the Formation of Domains in Hemoglobin S Gels. ((James Hofrichter, Garrott W. Christoph, William A. Eaton)) Laboratory of Chemical Physics, NIH, NIDDK, Bethesda, Maryland 20892.

Upon deoxygenation hemoglobin S forms a gel in which polymers organize into closely packed structures called domains. An interesting prediction based on the double nucleation model is that the formation of each domain is initiated by the homogenous nucleation of a single polymer. However, experiments on the kinetics of gel formation show that the number of domains is 10-100 fold smaller than the number of homogeneous nucleation events predicted by numerically integrating the rate equations of the model. To study this problem we have carried out computer simulations of domain formation using the double nucleation mechanism. In these simulations, homogeneous nuclei were deposited at a constant rate; all polymers, described as rigid rods, were allowed to lengthen; and heterogeneous nuclei were deposited at angles of ±26° onto all preexisting polymers. The results of these simulations show that domains with optical properties similar to those observed experimentally develop around isolated homogeneous nuclei. They further show that as many as 10 homogeneous nucleation events can occur within the borders of each optically distinguishable domain, thereby accounting for at least part of the difference between the experimental results and the results of the numerical integrations.

M-Pos116

FRAGILITY OF HEMOGLOBIN S (HbS) FIBERS & GELS AND ITS EFFECT IN ACCELERATING GELATION. ((Robin W. Briehl & Alexandria E. Guzman)) Albert Einstein College of Medicine, Bronx, NY 10461.

HbS fibers were observed in real time by differential interference contrast (DIC) microscopy. Light taps on the slide far from the sample produced fiber breakage. Broken fibers grow at both ends. Breakage is enhanced if there is already a cross-linked network, compared to relatively flexible isolated fibers, which are more resistant to fracture. After breakage the increased number of growing fiber-ends vastly accelerates polymerization and cross-linking; a dense gel can form in minutes under conditions in which little polymerization would occur in an hour in the absence of fracture. Fracturing a gel again causes an even more marked increase in gel density and cross-linking. These results explain the acceleration of gelation by shear and may be important in determining gelation rates in the microcirculation. Fibers have affinity for each other as judged by formation of X-shaped junctions and rapid "zippering" together to form bundles; a competing, repulsive, process of branching also occurs. Fibers are heterogeneous, ranging from single fibers to bundles of many fibers, as judged by image contrast, oscillation rates, and junctional and branching patterns. Gels are highly non-uniform, regions nearly devoid of fibers lying near dense regions. Fiber growth rates at 13.5 mM (heme), pH 7.2 and 25° are about 2000 monomers/sec; using reaction progress rates the heterogeneous nucleation rate calculates to about 10^{-9}/monomer·sec.

M-Pos117

SOLVENT PERTURBATION AND UNFOLDING OF HEMOGLOBINS A, S, AND F. ((John P. Harrington)), Department of Chemistry/Comprehensive Sickle Cell Center, University of South Alabama, Mobile, AL 36688.

The physiological role of hemoglobin is dependent upon the proper orientation of each of the four heme moieties in this protein. Each heme,located in a hydrophobic region of the α and ß globin chains, binds an Fe(II) ion at the center of the porphyrin ring and is covalently linked to the proximal histidine of the F helix segment. Alterations of the hemoglobin structure by solvent perturbation or changes in the globin sequences has a direct effect on the stability of the tetrameric molecule, resulting in the unfolding and possible release of the heme moiety from individual globin chains. Many investigators have shown that release of heme-iron is related to the greater tendency of red cell membranes to undergo lipid oxidation. Isothermal and thermal unfolding studies have been carried out on several hemoglobins. The following observations resulted: 1) analysis of the Soret spectra (450-350 nm) of hemoglobin is useful in determining the extent of heme exposure in the presence of different solvent perturbants, 2)oxy Hb S unfolding in the presence of urea or propyl urea resulted in greater heme exposure than either oxy Hb A or F, 3)met Hb formation resulted in lower unfolding midpoints for each hemoglobin compared to the oxy Hb state; met Hb F had the lowest unfolding midpoint under isothermal conditions, and 4) rate of heme exposure was greater for oxy Hb S than oxy Hb A in the presence of sodium dodecyl sulfate. (Supported by AHA Grant AL-G-910033-R)

M-Pos118

LIGHT SCATTERING FROM SICKLE HEMOGLOBIN SPHERULITIC DOMAINS IN THE MIE SCATTERING REGIME. ((Kaustuv L. Das and Marilyn F. Bishop)) Department of Physics, Virginia Commonwealth University, 1020 West Main Street, Richmond, Virginia 23284-2000

We have calculated the light scattering from a spherulitic domain of sickle hemoglobin (HbS) polymers, where the size of the domain is comparable to the wavelength of light, i.e., the Mie scattering regime. Inside the spherulite, we have used a model uniform anisotropic dielectric tensor in which the dielectric constant for an electric field oriented along the radius of the spherulite is different than that for the electric field perpendicular to the radius. The form of this dielectric tensor is derived using a model medium inside the spherulite composed of polymers, monomers, and solution, where the polarizabilities of the three entities relative to the effective dielectric tensor add to zero. The alignment of polymers in the radial direction in the domain gives rise to the anisotropy in dielectric properties. Outside the spherulite, we have assumed an isotropic effective medium composed of monomers and solution. For simplicity, we have assumed that the wavelength of light is in the red where the absorption is negligible. For plane polarized incident light, we have calculated the intensity and angular distribution of polarized scattered light and compared the results for various degrees of alignment of polymers, from fully aligned to random. Since the uniform nature of this dielectric model neglects the scattering from individual polymers, we compare these results for the spherulite with scattering from individual HbS fibers that are well separated compared with the wavelength of light.

M-Pos119

MEASUREMENT OF SICKLE HEMOGLOBIN POLYMERIZATION AND DIFFUSION IN FINITE VOLUMES ((Zhiqi Cao, Qun Dou, and Frank A. Ferrone)) Department of Physics and Atmospheric Science, *Drexel University*, Philadelphia, PA 19104

When sickle hemoglobin polymerizes the immobilization of the polymers allows solution phase monomers to enhance the total concentration in polymer rich regions. This can have profound effects in the red cell by redistributing the concentration within the cell. Measurements of difference in concentration in regions of red cells i are difficult since polymer formation clearly creates distortion of the cell changing its thickness. Moreover, the initial solution conditions in the cell are difficult to quantify, and hemoglobin S polymerization is highly sensitive to solution conditions, especially initial concentration. Consequently, we have begun to examine diffusion in constrained volumes of sizes close to those found in red cells. Nucle-pore filters are used to trap hemoglobin in volumes of size 785 μm^3, which is viewed by microspectrophotomer in polarized light to monitor polymer formation following thermally induced polymerization.

M-Pos120

SICKLE HEMOGLOBIN POLYMER DOMAIN DENSITY STUDIED BY FLUORESCENCE AND POLARIZATION OPTICAL MICRO-SCOPY ((Qun Dou and Frank A. Ferrone)) Department of Physics and Atmospheric Science, *Drexel University*, Philadelphia, PA 19104

Polymerization of sickle hemoglobin produces arrays called domains. The hemoglobin polymerized is immobile, allowing monomers to diffuse into the domain, and increasing the net concentration. While aligned polymers can be measured by linear dichroism, it is difficult to quantitate the total mass of polymers. To explore this we have employed fluorescent optical microscopy using fluorescent labelled bovine albumin (TRITC) as a tracer molecule. The albumin molecules, whose molecular weight is approximately that of HbS molecules, are excluded from the polymers, thus the fluorescent image gives a measurement of the distribution of the unpolymerized HbS in the domain. Spatially resolved absorption and polarized absorption (linear dichroism) is measured in the same region, which determines the total amount of Hbs and the amount of aligned polymers in the domain. From these measurements the distribution of polymers in the domain and the diffusion of monomers induced by polymerization can be studied.

M-Pos121

EFFECT OF WATER ON THE ALLOSTERIC EQUILIBRIUM OF HEMOGLOBIN ((Jie Jiang and Frank A. Ferrone,)) Department of Physics and Atmospheric Science, *Drexel University*, Philadelphia, PA 19104

Colombo, Rau and Parsegian[1] have demonstrated that water interacts with hemoglobin's oxygen binding properties, increasing the p50 with increased osmotic pressure. We have examined this behavior in detail using precise ligand binding equilibrium measurements and modulated excitation studies. Modulated excitation measures the forward and reverse rate of transition between alternative structures R and T with three ligands bound, and hence allows determination of the allosteric equilibrium constant L_3. We find no change in L_3 for O_2 or CO as ligands, with or without 0.1 M Cl^-, when the osmotic pressure is changed by addition of 2 M sucrose. We do find the binding curves are changed in a manner consistent with changes only in the R state binding constant, K_R. This is consistent with the modulated excitation data, and suggests that the effects of osmotic pressure are more subtle that first supposed.

1. Colombo, Rau & Parsegian, Science, 256, 655 (1992)

M-Pos122

MODULATED EXCITATION STUDIES OF IRON-COBALT HYBRID HEMOGLOBINS WITH 2 AND 3 OXYGENS BOUND. ((Frank A. Ferrone, Jie Jiang, Mingdi Zhao, Dan Liao, Qun Dou, Antonio Tsuneshige, and Takashi Yonetani)), Department of Physics and Atmospheric Science, *Drexel University*, and Department of Biochemistry and Biophysics, *University of Pennsylvania*, (A. T and T. Y.) Philadelphia, PA 19104

Iron cobalt hybrids are a useful laboratory for investigating the effects of subunit inequivalences, since subunits can be selectively chosen as Fe or Co. We have used the method of modulated excitation to excite at most one subunit of oxygenated hybrid molecules. We have performed experiments at both 100% O_2 and atmospheric O_2 pressure. Since the cobalt subunits have lower affinity, lowering the partial pressure selectively deoxygenates the cobalt subunits. In 100% O_2, there is no evidence of conformational switching, while clear signals emerge at atmospheric O_2 pressures. Because of the low quantum yield for reaching the ligand-free state, laser photolysis produces a thermal modulation that appears to cause the ligand to be released from the cobalt subunits. Different ligand binding rates are seen depending on whether the Fe chains are α or β.

M-Pos123

MODULATED EXCITATION STUDY OF THE FIRST LIGATION STEP: THE SEARCH FOR MULTIPLE *T* STATES ((Dan Liao, Mingdi Zhao, Jie Jiang, Qun Dou, Frank A. Ferrone)) Department of Physics and Atmospheric Science, *Drexel University*, Philadelphia, PA 19104

In a dramatic result, Mozzarelli et al.[1] have observed the ligand binding to single crystals of hemoglobin, and found that the affinity is lower than solution measurements, with no evidence of a Bohr effect. They have proposed as an explanation that Hb might exist in the T state in two conformations which differ in the formation of a number of salt bridges, first proposed by Perutz. The T state affinity is lowered for the ligand CO in both a diminished on rate and off rate. Hence we have attempted to investigate where there is evidence of a second affinity state in the presence of multiple relaxations and/or spectral changes in the binding of the first ligand. We see little evidence for multiple ligand rebinding rates, but preliminary spectral data shown spectral changes which may indicate a structural relaxation.

1. Mozzarelli, Rivetti, Rossi, Henry & Eaton, *Nature*, 351, 416 (1991)

M-Pos124

THE ALKALINE BOHR EFFECT IN HEMOGLOBIN STUDIED BY MODULATED EXCITATION WITH FLUORESCENT DETECTION ((Mingdi Zhao and Frank A. Ferrone)) Department of Physics Atmospheric Science, *Drexel University*, Philadelphia PA 19104

The transformation between high and low affinity states of hemoglobin (R and T, respectively) is linked with the uptake and release of protons (Bohr effect). To follow the Bohr effect at the final ligation step we have employed the method of modulated excitation which uses a small periodic excitation to remove a single ligand from hemoglobin. Typically less than 1% of the hemes are photolyzed in this method. The detected signals are tuned relative to the excitation signal, to reveal relaxations distinct from the ligand rebinding event. The 3-liganded structure typically has a significant mixture of both R and T quaternary structures, which can be distinguished kinetically and spectroscopically. By the use of the fluorescent pH sensitive indicator dye BCECF-dextran, we have followed [H^+] changes with three CO ligands bound. The signal to noise is excellent, with very little bleaching, and is not synchronous with the ligand rebinding.

M-Pos125

ALLOSTERIC FUNCTIONS OF Co-SUBSTITUTED HEMOGLOBIN: OXYGENATION, NMR, AND CD STUDIES OF Fe-Co HYBRID HEMOGLOBINS. ((A. Tsuneshige, Y.-x. Zhou, and T. Yonetani)) Biochem. & Biophys., Univ. of Penn., Philadelphia, PA 19104-6089

Five α,α-crosslinked symmetric and asymmetric Fe-Co hybrid hemoglobins (Hb) were prepared by appropriate combinations of HbA, CoHbA, Fe-Co hybrids, HbC, and CoHbC, followed by crosslinking of the tetramers with bis(3,5-dibromosalicyl)fumarate between two α subunits to prevent dimer formation and separation by ion exchange chromatography. These hybrids are, according to the notation of $\alpha_1\beta_1\alpha_2\beta_2$: FCCC, CFCC, FCFC, CFCF, FFCC, where F and C represent Fe- and Co-containing subunits, respectively. Since only the Fe-containing subunits can bind CO, partially CO-ligated derivatives were easily prepared by exposing the samples to CO. Precise oxygen equilibrium isotherms were measured for these hybrids in the presence of CO at different pH values at 15°C and were compared with those of CCCC. FCCC. CFCC, and FCFC exhibited several different "T-state" like characteristics and were sensitive to IHP, although the degree of variations depended on the nature and the number of CO-ligated subunits. On the other hand, both CFCF and FFCC showed truly "R-state"-like behaviors at any pH studied. The effect of IHP on these hybrids was minimal. Proton NMR and CD data were consistent with those obtained from oxygenation experiments. Supported by Research grant (HL14508 from NIHLB, NIH).

M-Pos126

DISTRIBUTIONS OF COOPERATIVE FREE ENERGY IN PARTIALLY-LIGATED Co(II)/Fe(II)-CO AND Co(II)/Co(II)-O_2 HEMOGLOBINS. MICHAEL DOYLE‡, TAKASHI YONETANI¶ AND GARY ACKERS‡. ‡Dept. Biochem./Mol. Biophysics, Washington Univ. School of Medicine, St. Louis, MO 63110 and ¶Dept. Biochem./Biophysics, Univ. Pennsylvannia School of Medicine, Philadelphia, PA 19104-6089.

Cooperative free energies of all ten Co(II)/Fe(II)-CO microstates of human Hb have been determined at pH 6.5 and 21.5°C. These determinations were made through measurements of dimer-tetramer subunit assembly by analytical gel permeation chromatography, cryogenic isoelectric focusing of equilibrium distributions of ligation microstate tetramers, and forward and reverse reaction rates for subunit assembly. The results exemplify the general partition function for cooperative ligand binding by Hb [Ackers, Doyle, Myers & Daugherty (1992) *Science* 255, 54-63]: the distribution shows five distinct cooperative free energy levels and the consensus combinatorial code for cooperative switching of the doubly-ligated species. The data are consistent with the concept that allosteric regulation is achieved at the level of both tertiary and quaternary structure changes. Quaternary switching is governed by a "Symmetry Rule" whereby placement of at least one hemesite ligand on both of the $\alpha^1\beta^1$ and $\alpha^2\beta^2$ dimers induces quaternary transition. Good agreement was found between the Co(II)/Fe(II)-CO distribution and the Co(II)/Co(II)-O_2 distribution (determined by subunit assembly and O_2 equilibrium measurements under the same conditions).

M-Pos127

ENTHALPIC AND ENTROPIC COMPONENTS OF COOPERATIVITY FOR THE CYANOMET LIGATION MICROSTATES OF HEMOGLOBIN. Yingwen Huang & Gary K. Ackers, Dept. of Biochemistry and Molecular Biophysics, Washington University School of Medicine, St. Louis, MO 63110. (Spon. by P. Stahl).

Cooperative free energies ($^{ij}\Delta G_a$) of the 10 ligation species of cyanomet-hemoglobin were found to distribute into three levels according to a combinatorial code (i.e. dependent on both the number and configuration of ligated subunits) (Smith, F.R., and Ackers, G.K. (1985) PNAS 82, 5347). We have investigated the temperature dependence of these assembly free energies in order to partition $^{ij}\Delta G_a$ into enthalpic and entropic contributions using analytical gel chromatography, cryogenic isoelectric focusing, and haptoglobin binding kinetics. It was found that the assembly enthalpies ($^{ij}\Delta H_a$) of 8 species studied distribute into 3 discrete enthalpic levels. The 4 doubly-ligated tetramers distribute into 2 separate levels. The species 21 spacing is half-way between those of unligated and fully ligated species, while $^{ij}\Delta H_a$ levels of the other 3 doubly-ligated species fall into the level of 41. Thus the enthalpic and entropic components of cooperative free energy are controlled primarily by the configuration of ligated heme sites. The system exhibits combinatorial switching with respect to enthalpic and entropic effects. Comparison between $^{ij}\Delta H_a$ for singly, triply, or fully cyanomet ligation microstates with $^{i}\Delta H_a$ for the corresponding oxygen ligation states indicates that the effects of temperature on ΔG_a are very similar between the two systems. These results provide strong support for the existence of general rules of intersubunit coupling among the CN-met and oxygen ligation systems.

M-Pos128

IS QUATERNARY ENCHANCEMENT IN HUMAN HEMOGLOBIN DUE TO A THIRD QUATERNARY STRUCTURE? ((Jo H. Hazzard, Michael L. Doyle, Margaret A. Daugherty and Gary K. Ackers)) Dept. of Biochem./Molec. Biophys., Washington Univ. Sch. of Med., St. Louis, MO 63110.

Assembly of unliganded Hb dimers results in a quaternary structure with reduced affinity for binding the first three oxygen molecules. In contrast, the affinity of triply-liganded tetramer is increased relative to dimer, an effect known as "quaternary enhancement" (Mills, F.C. & Ackers, G. K., PNAS 76, 273 (1979)). Quaternary enhancement in each of the four binding steps has recently been found for oxygen binding to mutant Hb Ypsilanti (Doyle et al., Proteins, in press). Fully liganded Hb Ypsilanti assumes a unique quaternary structure which is distinct from both the R and T structures (Smith et al., Proteins 10, 81 (1991)). These findings strongly suggest a relationship between the "Y" structure and the functional property of quaternary enhancement. Specifically, does the triply-ligated normal human Hb tetramer exist primarily in quaternary Y? That this quaternary structure is accessible in normal, fully liganded Hb has recently been demonstrated by crystallographic analysis at physiological ionic strength and low pH (Silva et al., JBC 267, 17248 (1992)). Comparison of oxygen binding by normal Hb and Hb Ypsilanti under these and similar conditions provides a direct means of testing these correlations. Supported by NIH GM24486.

M-Pos129

BOHR EFFECTS OF THE PARTIALLY-LIGATED MICROSTATES OF HUMAN HEMOGLOBIN ((Margaret A. Daugherty, Madeline A. Shea and Gary K. Ackers)) Dept. of Biochemistry and Molecular Biophysics, Washington University Sch. of Medicine, St. Louis, MO 63110. Dept. of Biochemistry, Univ. of Iowa, Col. of Medicine, Iowa City, Iowa 52242. (Spon. by C. Blazynski)

To understand the detailed role of protons in the molecular mechanism of hemoglobin, we determined the energetics of dimer-tetramer assembly for the 10 unique ligation species of cyanomet-hemoglobin over the pH range 7.4-9.5. The Bohr proton release that accompanies hemesite binding to each species was deduced from the pH-dependence of dimer-tetramer assembly. We find that the two singly-ligated species and the asymmetric doubly-ligated species $(\alpha^{+CN}\beta^{+CN})(\alpha\beta)$ have Bohr Effects similar to the unligated (quaternary T) molecule while the remaining three doubly-ligated species and the two triply-ligated species exhibit Bohr Effects similar to the fully-ligated (quaternary R) molecule. These results are highly consistent with the proton-linked assembly reactions found with oxygen [Chu et al., (1984) Bioch. 23, 604]. With new levels of precision, we find that the microstates distribute into five cooperativity levels, consistent with results of the Co(II)/Fe(II)-CO system [Speros et al., (1991) Bioch. 30, 7254]. The cyanomet ligation system shows a quaternary enhancement effect [Mills, F.C. & Ackers, G.K. (1974) J. Biol. Chem. 254, 2881] at the final ligation step. These results strongly support a common set of rules for the various hemesite ligands whereby the tertiary and quaternary switches govern cooperativity.

M-Pos130

ORIGINS OF THE SYMMETRY RULE FOR QUATERNARY SWITCHING IN HEMOGLOBIN. Gary K. Ackers and Jo H. Hazzard. Dept. of Biochemistry and Molecular Biophysics, Washington University School of Medicine, St. Louis, MO 63110.

Recent work with cyanomet human hemoglobin has led to the first experimental determination of an allosteric mechanism through: (a) resolution of the energetics of cooperativity for transitions among the 8 intermediate ligation states and (b) assignment of the corresponding structural transitions (tertiary and quaternary) [Ackers et al. Science 255, 54-63 (1992)]. These studies reveal a "Symmetry Rule" that translates configurations of hemesite ligation into switchpoints of quaternary transition: the T→R switchover occurs when a ligation step creates a tetramer with ligands bound on both dimeric half-molecules. The origins of this empirical rule lie in three fundamental effects: (1) quaternary structure is influenced by the configuration of ligated vs unligated hemesites, (2) sequential cooperativity arises from tertiary-quaternary mismatch within each quaternary structure, and (3) additional dimer-dimer anticooperativity arises when ligands are bound subsequently to a second dimer. The Symmetry Rule results from a particular balance of these effects. A general partition function has been developed which incorporates these features and provides insights into the molecular basis of the symmetry rule, the conditions where it operates and where it will fail. The relationships between these factors and the possible switchpoint transitions has been explored. Experimental failure of the symmetry rule is observed at high salt and with mutational perturbation.

M-Pos131
EFFECT OF CHLORIDE ON THE CO_2 BINDING OF HEMOGLOBIN.

((Mark D. Chávez, Joan S. Carducci, and Robert L. Berger))Laboratory of Biophysical Chemistry, NHLBI-NIH, Bethesda, MD 20892.

The binding of chloride to hemoglobin is known to lower the oxygen affinity. Several binding sites are present for the chloride, of which only the highest affinity site is not sensitive to oxygen binding. One proposal locates this chloride binding site in the vicinity of the four α-NH_2-terminal residues of hemoglobin. These sites are also where the binding of CO_2 as carbamate contributes both to CO_2 transport. This CO_2 binding is partly responsible for lowering the oxygen affinity of hemoglobin. The exact mechanism by which the chloride or CO_2 binding influences the hemoglobin is not known. Specifically, it is not clear whether the lower oxygen affinity is due to the liberation of a proton resulting in an overall Böhr effect or is a direct consequence of binding to the protein. With differential calorimetry, we have determined to what extent the presence of chloride affects the binding of CO_2. The extent of the chloride effect has been observed by varying the concentration of the chloride relative to the CO_2 and hemoglobin concentrations and will be discussed in detail.

M-Pos132
TIME-RESOLVED STUDIES OF THE PHOTOLYSIS REACTION OF (CARBONMONOXY) HEMOGLOBIN.

((S. J. Paquette, S. B. Bjorling, C. F. Zhang, D. S. Kliger))
University of California Santa Cruz, Santa Cruz, CA 95064.

Time-resolved optical density (trOD) studies were used in conjunction with time-resolved circular dichroism (trCD) studies to study the recombination of hemoglobin with CO following photolysis of (carbonmonoxy)Hb (HbCO). Kinetic analysis of the absorption data shows that the heme relaxation and recombination reported in the Soret-band can be described with five exponentials in agreement with previous nanosecond flash-photolysis measurements [Hofrichter, J., J. H. Sommer, E. R. Henry, & W. A. Eaton (1983) *Proc. Natl. Acad. Sci. USA* 80, 2235]. The transient changes in the UV spectral region are analysed separately and compared to the changes in the Soret-band.

The trCD spectra were monitored at probe times corresponding to the maximum population of the intermediate species of interest. The UV trCD spectra showed subtle evidence of a recently reported intermediate with a 10 us lifetime [Su., C., Y. D. Park, G. Y. Liu, & T. G. Spiro (1989) *J. Am. Chem. Soc.* 111, 3457].

M-Pos133
Ligand Recombination in Photodissociated O_2 Hemoglobin Subsequent to One and Two Pulse Excitations. M. Yang, J. Wang, Y. Lu, M. Chance and J.M. Friedman. Dept. of Physiology & Biophysics, Albert Einstein College of Medicine, Bronx, NY 10461. (Spon. by M. Yang).

Ligand recombination occurring from 30ps out to over 100 milliseconds is monitored in photodissociated oxyHb as a function of temperature. The amplitude of both the subnanosecond and 100ns geminate phases first increased substantially in going from RT to 200K and then slowly decreases in going to 100K. The seemingly distinct geminate phases are also monitored as a function of temperature using a two pulse protocol in which the sample is rephotodissociated with an identical second 30ps pulse arriving 1.2ns subsequent to the first pulse. Preliminary results indicate that even at RT the geminate phase of the rephotolyzed fraction contains a higher fraction of "fast" recombining molecules. The second pulse also adds to the slower(>2ns) recombining population. The relative fraction of slow recombining material in the rephotolyzed population decreases substantially in going from RT to 200K. At the lowest temperatures the second pulse does not increase the "instantaneous" yield of photolysis over that of the first pulse; however, at RT there is a 15% increase subsequent to the second pulse at 1.2ns. The above results suggest: (1) that complete thermal conformational averaging is not complete at 1.2ns even at RT and (2) that at least partial averaging by 1.2ns occurs as evidenced by the observation of pumping of both the slow recombining population and the non photolyzable population by the second pulse.

M-Pos134
Conformational Dynamics in MbCO: Nanosecond Time Resolved Near IR Absorption Studies. J. Huang, S.C. Huang and J.M. Friedman. Department of Physiology and Biophysics, Albert Einstein College of Medicine, Bronx, NY 10461. (Spon. by J. Friedman).

Several groups studying geminate recombination in MbCO above the glass transition have obtained results that have implications regarding both the thermal averaging times and the tertiary relaxation time in the photoproduct. These studies either have focussed on the distal heme pocket or were structually non-specific. A major fraction of the enthalpic barrier for GR is derived from proximal control. Band III at -760nm is a charge transfer absorption band of the heme in the MbCO photoproduct whose spectral properties are sensitive to elements of the proximal heme pocket that have been implicated in the control of ligand recombination. Several protocols using up to two temporally separated photolysis pulses(10ns) and a variably delayed(10ns to 100 milliseconds) continuum probe pulse(10ns) are used to generate band III in photodissociated MbCO as a function of temperature(170K to RT) and time delay. Different protocols are used to separated out kinetic hole burning from tertiary relaxation. In addition the time evolution of a highly skewed distribution of conformational substates is monitored using the very red shifted band III obtained by the partial photolysis of MbCO using a red edge excitation of the α band. Together these studies provide a window on the time scale of both thermally driven conformation averaging and tertiary relaxation associated with the functionally relevant structural parameters of the proximal heme pocket.

M-Pos135
HEMOGLOBIN DYNAMICS FROM TIME-RESOLVED UV RESONANCE RAMAN SPECTRA OF TRYPTOPHAN AND TYROSINE SIDE CHAINS.

((Kenton R. Rodgers, Ishita Mukerji, Shankar Subramaniam, and Thomas G. Spiro))
Department of Chemistry, Princeton University, Princeton, N.J. 08544.

In recent years ultraviolet resonance Raman (UVRR) and time-resolved UVRR spectroscopy have become powerful tools for investigating the details of protein conformation as well as conformational dynamics via. We are interested in the interplay between protein function and conformational dynamics. Hence, we have undertaken a UVRR study of the oxygen carrying protein, hemoglobin (Hb), with the goal of understanding the role of protein dynamics in the allosteric and cooperative process of oxygen binding by Hb. Towards this end, we have been temporally and spatially mapping the protein motions that culminate in the transition between the high (R) and low (T) O_2- affinity states of Hb. Herein we demonstrate that conformational differences in Trp and Tyr environments that result from conformational differences between the R and T states can indeed be observed via UVRR even though the changes are only felt by one of a number of the same type of residue. We also present time-resolved UVRR difference spectra that show sequential tertiary and quaternary conformational dynamics in the R→T transition for Hb A and a natural mutant, Hb Kempsey (Hb_K). An interdimer contact critical to T-state stability is lost in Hb_K due to the Asp 899 → Asn mutation. The resulting destabilization of the T state is reflected in the quaternary dynamics of Hb_K. Finally, by locking Hb in a partially-ligated conformational state using Co/Fe Hb hybrids, we have clearly shown that the nanosecond time-resolved UVRR transients arise from tertiary motions that precede the quaternary R→T transition. Hence, it is clear that the mechanism of Hb cooperativity is best interpreted in terms if at least three conformational states, the R and T states and a third intermediate state that results from tertiary conformational motion within the quaternary R state.

M-Pos136
UV RESONANCE RAMAN STUDY OF FLUROMETHEMOGLOBIN.

((V.Jayaraman, K.R.Rodgers, I.Mukerji, T.G.Spiro)) Dept. of Chemistry, Princeton University, Princeton, NJ 08544.

Hemoglobin (HbA) co-operativity results from a switch between low and high oxygen affinity states, T and R respectively, upon partial ligation of the four heme sites. One approach towards understanding the mechanism of co-operativity has been to study the structural changes in the ferric derivatives of HbA. These changes are brought about by the binding of allosteric effectors such as diphosphoglycerate (DPG) and inositolhexaphosphate (IHP). In pursuance of this we have performed UV resonance Raman spectroscopy on fluromet Hb, a ferric derivative of HbA with a fluoride ligand, in the presence and absence of IHP. The difference between the spectra of the two states has been compared with that of the T-R state difference UV resonance Raman spectra of HbA. The difference spectra exhibit similar features indicating that their quaternary states are similar. However, we observe an increase in intensity of the Trp W3 mode in the difference spectrum of fluromet Hb which is absent in the HbA difference spectrum. This could be attributed to changes at the α14/β15 Trp residues located in the A helices of the α and β subunits. These could be attributed to tertiary structural changes induced by the presence of the fluoride ligand in the T state.

M-Pos137

Raman dispersion spectroscopy probes central and peripheral heme-protein interactions in deoxygenated Hb trout IV.

((R. Schweitzer-Stenner, M. Bosenbeck and W. Dreybrodt)), Inst. of Exp. Phys., University of Bremen, 2800 Bremen 33, Germany

In heme proteins the symmetry of the heme macrocycle (D_{4h}) is lowered by heme-protein interactions which can be changed by protonation of distinct amino acid residues (Bohr groups). In this case the conformation of the heme depends on the protonation state of the protein. Informations on heme distortions can be derived from the dispersion of the depolarization ratio (DPD) of prominent Raman lines [1]. In order to examine the allosteric coupling between the Bohr groups and the heme in deoxyHb-trout IV we have measured and analyzed the DPD of its ν_4- and ν_{10}-lines as a function of pH between 6.0 and 9.0. From the pH-dependence of the thus obtained apparent vibronic coupling parameters (VCP) we found the pK-values of the protonable groups involved. They turned out to be identical to those of the Bohr groups which were earlier obtained from the analysis of corresponding O_2-binding isotherms [1] (i.e $pK_{\alpha 1}=pK_{\alpha 2}=8.5$ for the α-subunits and $pK_{\beta 1}=7.5$, $pK_{\beta 2}=7.4$ for the β-subunits). A group theoretical analysis of the VCPs shows, that the protonation of the Bohr groups via allosteric interactions affects the central part of the heme (N, C_α) by changing the azimuthal angle of the Fe^{2+}-His F8 bond also and its peripheral part (C_β) by interactions between the peripheral substituents (in particular vinyl I and III) and amino acid residues located in the FG-helix.

1. R. Schweitzer-Stenner, Quart. Rev. Biophys. 22, 381, 1989

M-Pos138

STRUCTURAL HETEROGENITY OF THE Fe^{2+}-N_ϵ(HIS F8)-BOND IN HEMOGLOBIN PROBED BY THE RAMAN ACTIVE FE-HIS-STRETCHING MODE.

((H. Gilch, R. Schweitzer-Stenner and W. Dreybrodt)) Institute of Experimental Physics, University of Bremen, 2800 Bremen 33, Germany.

We have measured the Stokes- and anti-Stokes-band of the Fe^{2+}-N_ϵ (His F8)-mode for deoxy-HbA with high resolution. In both cases the band can be decomposed into 5 sublines (SL) similar to observations on Hb-trout-IV (Bosenbeck et al. Biophys.J. 61, 31, 1992). The line positions are at 195 cm^{-1}, 202 cm^{-1}, 212 cm^{-1}, 218 cm^{-1} and 226 cm^{-1}. The halfwidths are 12 cm^{-1}. We also have decomposed the Fe^{2+}-N_ϵ-band of the α- and β-subunits, of R-state HbA and several mutants. In all cases the line shapes of the Fe^{2+}-N_ϵ-bands are determined by one common set of SLs, with differing intensities, but the same halfwidths and similar frequencies ($\pm$ 2 cm^{-1}).

By lowering the temperature a shift of the peak positions of the Fe^{2+}-N_ϵ-band in HbA to higher frequencies is observed. Decomposing these data in a similar way, we find that to explain the temperature dependence of the relative intensities of the SLs a complex energy landscape is needed in which at least two configurational coordinates of the Fe^{2+}-N_ϵ-bond are involved. The first one determines the frequencies, the second one the intensities of the SLs. In a vibronic coupling model these coordinates may be attributed to the polar angle θ of the Fe^{2+}-N_ϵ-bond with respect to the heme plane and the corresponding azimuthal angle φ respectively. In all cases shifts of the peak frequencies of the Fe^{2+}-N_ϵ-bands result from a redistribution of the SL-intensities.

M-Pos139

CHARACTERIZATION OF THE VIBRATIONAL AND ELECTRONIC SPECTROSCOPIC PROPERTIES OF COHBA SOLUBILIZED IN DMSO.

((E.W. Findsen, K. Burnham and B.S. Wicks))
Department of Chemistry, University of Toledo, Toledo OH 43606
(spon. E.W. Findsen)

The dynamic behavior of proteins in non-aqueous solvents is of interest in the understanding of the role of solvation in protein activity. We report the results of preliminary studies of COHBA which has been lyophilized and dissolved in neat (but not dried) dimethyl sulfoxide. The protein is found to be stable at room temperature for up to three days before changes in the absorption spectrum indicative of sample degradation occur. Absorption spectra parameters are very similar to those reported for COHBA in buffered aqueous solutions. Resonance Raman spectra obtained using Soret excitation at low powers show vibrational modes at positions in very close agreement to those observed for COHBA in aqueous solution. At high incident laser powers new modes are observed which are in agreement with the formation of the five-coordinate HbA* species.

M-Pos140

NITRIC OXIDE EPR OF MYOGLOBIN DISTAL HEME POCKET MUTANTS.

((H. Hori, E.W. Singleton, J.S. Olson, and M. Ikeda-Saito)) Dept. of Physiol. and Biophys. Case Western Reserve Univ. Sch. of Med., Cleveland, OH 44106-4970, Dept. of Biophys. Eng., Osaka Univ. Osaka 560 Japan, and Dept. of Biochem. and Cell Biol., Rice Univ., Houston, TX 77251

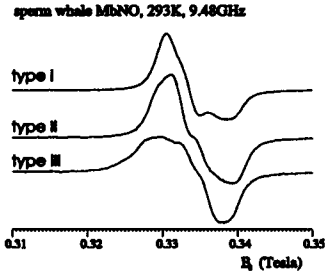

EPR spectra of NO complexes of recombinant human and sperm whale Mb with mutations at His64, Val68 and Leu29 sites are categorized into three groups, as represented in the Figure. Type I, axial symmetric with $g_\perp > g_{//}$, includes the wild-type, Thr64, Gly64, Gln64, Val64, Ala29, Val29, and Leu68 mutants. Ala64, Leu64, Ile68, and Phe29 mutants belong to Type II, which is rhombic with $g_1 > g_2 > g_3$. The bound NO is less mobile in these mutants. Type III NO spectrum, which is axial symmetric with $g_{//} > g_\perp$, indicates drastic changes in the Fe-NO coordination due to restrictions imposed by His64→Tyr, and Val68→Phe mutations. These indicate that the Fe-NO geometry in Mb might not depends simply on the side chain volume of the distal amino acid residues. Supported by NIH (GM39492, GM35649), Northeast Ohio AHA, and the Government of Japan.

M-Pos141

REDOX REACTIVITY OF NITRIC OXIDE WITH HUMAN METHEMOGLOBIN AND TWO CROSS-LINKED HEMOGLOBIN DERIVATIVES

((A.I. Alayash, J.C. Fratantoni, C. Bonaventura, J. Bonaventura,and R.E. Cashon)) Center for Biologics Evaluation and Research, FDA, Bethesda, MD 20892 and Duke University Marine Lab, Beaufort, NC 28516

We have examined the interactions between nitric oxide (NO) and oxidized human hemoglobin, comparing the behavior of unmodified HbA_0 with that of two chemically cross-linked hemoglobins. The latter are promising blood substitute candidates due to their lower oxygen affinity and greater stability of the tetrameric structures. The modified forms examined were HbA-DBBF, cross-linked between the alpha chains with bis(3,5-dibromosalicyl) fumarate, and HbA-FMDA, modified between the beta chains with fumaryl mono-dibromoaspirin. Biphasic kinetics of NO binding to the ferric hemes were observed, attributable to differing reactivities of alpha and beta chains. The rates of the two phases were altered in the modified hemoglobins. In a much slower subsequent process, the ferric hemes became reduced. The reduction occurred at differing rates for the hemoglobins studied, with the fastest time courses shown by the modified forms. The endogenously produced NO is now recognized as the endothelium derived relaxing factor (EDRF) because of its role in the relaxation of vascular smooth muscles. Initial oxidation of hemoglobin occurs extremely rapidly when exposed to NO in vivo. Subsequent redox cycling of hemoglobin however, may further deplete nitric oxide as a biological transducer leading to altered vascular tone with variable effects observed for different Hb preparations.

M-Pos142

ZINC INDUCED DIMERIZATION OF FERRIMYOGLOBIN.

B. Cunningham, M. Mulkerrin, L. Presta, and S. J. Shire.

Genentech, Inc., S. San Francisco, CA 94080.

Size exclusion chromatography and analytical ultracentrifugation experiments show that zinc promotes dimerization of horse ferrimyoglobin at physiologically relevant concentrations. Schatchard analysis of zinc binding to equine myoglobin shows that the binding is highly cooperative with a 1:1 stoichiometry indicating that a pair of zinc atoms is bound per myoglobin dimer. Sedimentation equilibrium analysis of the dimerization as a function of pH suggests that the amino acids involved in the binding of zinc have a pK_a value consistent with that of histidine imidazole groups. The involvement of specific histidine side chains is further supported by experiments with canine myoglobin. This myoglobin lacks histidine residues at positions 113 and 116 (His--->Gln) and does not dimerize in the presence of zinc. A molecular model for equine myoglobin in which these histidine residues are coordinated with two zinc atoms is also presented. Together these data show that zinc can induce species specific dimerization of myoglobin at concentrations normally found in muscle tissue. This suggests a possible role for zinc as a regulator and mediator of oxygen storage and/or transport in muscle.

M-Pos143

RATE OF DISSOCIATION OF THE HUMAN APOHEMOGLOBIN DIMER
((Daniel P. Moulton and Melisenda J. McDonald)) Biochemistry Program, Department of Chemistry, University of Massachusetts at Lowell, Lowell MA 01854

Here we report studies aimed at measuring the rate of dissociation of the dimer ($\alpha^0\beta^0$) of apohemoglobin A. It is well documented that when $\alpha^0\beta^0$ is incubated with α^h (or β^h) chains *heme-chain exchange* occurs yielding a semihemoglobin ($\alpha^h\beta^0$ or $\alpha^0\beta^h$) and a precipitated globin (α^0 or β^0) subunit. This exchange is relatively slow and likely to be limited by $\alpha^0\beta^0$ dissociation rather than $\alpha\beta$ chain combination. To test this hypothesis incubation mixtures were prepared which contained $\alpha^0\beta^0$ and either α^h or β^h chains in 0.01 M potassium phosphate buffer, pH 7 and 20° C. During incubation aliquots were taken and subjected to electrophoresis which readily separated the globin, semihemoglobin and heme-chain species. Subsequent quantitation by densitometry revealed that the production of semi-α- and semi-β-hemoglobins was identical (within experimental error) and coincided with the disappearance of the heme chain. The reaction time course was indeed exponential and appeared to follow first order kinetics yielding a rate constant of 0.5 h^{-1}. This dissociation rate presumably reflects the stability of the $\alpha^0\beta^0$ monomer interface in the absence of heme. Supported by NIH grant HL-38456.

M-Pos144

EFFECT OF INTRAMOLECULAR CROSSLINKS ON THE ENTHALPY OF THE INTERMEDIATES OF OXYGENATION OF HUMAN HEMOGLOBIN.
((E.Bucci, C.Fronticelli, Z.Gryczynski, A.Razynska, and J.H. Collins.)) UMAB, Baltimore, MD (Spon. by E. Bucci)

We have reported [Bucci et al. Biochemistry 30:3195-99,1991] that in human and bovine hemoglobins the binding of the third O_2 molecule is an endothermic event. To test the hypothesis that this is due to a peculiar conformation of the system, we have measured the enthalpies of the subsequent step of oxygenation of human hemoglobin crosslinked either between the ß82 or between the α99 lysines by bis(3,5-dibromosalicyl)-fumarate. The measurements were performed at pH 9.0 in 0.1 M borate buffer to avoid thermal effects due to binding of anions and protons. The two crosslinks had opposite effects. The crosslink between the ß subunits decreased while that between the α- subunits increased the endothermic behavior of the third step of oxygenation. These data are consistent with the hypothesis that the R/T transition in hemoglobin involves novel conformations not included in the R/T system. It may be speculated that the novel conformations of the triligated specie may be similar to the Y structure of hemoglobin Ypsilanti.

M-Pos145

DOUBLE CROSSLINKED AND MULTILINKED HEMOGLOBINS AS POTENTIAL BLOOD SUBSTITUTES
((K.W. Olsen, Q.-Y. Zhang, H. Huang, L. Zhao, E.J. Fernandez, P.A. Pavlik, G.K. Sabaliauskas and M.K. Boyd)) Chemistry Dept., Loyola Univ., 6525 N. Sheridan Rd., Chicago, IL 60626

Oxy and deoxy hemoglobin crosslinked by DFDNB (difluorodinitrobenzene) gave only monomers and crosslinked dimers on SDS gels. Denaturation gave two transitions with ΔT_m's of 6 and 20°C. This crosslinker can span 3Å, locking the quaternary structure more tightly and give greater thermal stability than longer reagents. Three double crosslinked hemoglobins have been produced. The first was made by crosslinking purified β82-fumarate crosslinked Hb with dimethylpimelimidate. It had a T_m of 63°C, compared to 57°C for the singly crosslinked proteins. Thus, double crosslinking only slightly increased the stability over that of singly crosslinked hemoglobins. Double crosslinking experiments using fumarate and DFDNB crosslinking gave similar results. A more interesting double crosslinked hemoglobin has fumarate crosslinks between both the α99 lysines and the β82 lysines. The ΔT_m is 20°C, which is 4°C greater than the singly crosslinked species. The oxygen affinity and cooperativity are similar to that of α99XLHb but unaffected by IHP. The autoxidation is similar to that of HbA and, thus, is slower than that of α99XLHb. Trimesoyl tris(methyl phosphate) trilinked hemoglobin had the same thermal stability as the fumarate-crosslinked ones. Catalase and superoxide dismutase each decreased the autoxidation rate 2-fold. In combination, they decreased it 4-fold. Molecular dynamics calculations on the bis(3,5-dibromosalicyl) fumarate reaction have demonstrated the importance of electrostatic interactions in this reaction. (Supported in part by a grant from the Research Corporation.)

M-Pos146

COLLECTIVE PROPERTIES OF TRYPTOPHAN REPORTER GROUPS IN LUMBRICUS HEMOGLOBIN.
((R.E. Hirsch, G.J.A. Vidugiris, J.M. Friedman, and J.P. Harrington)) Albert Einstein Coll. Med., Bronx, NY 10461 & Univ. of S. Alabama, Mobile 36688. (Spon. by M.L. Lin)

Fluorescence analysis has been used to study dissociation of the dodecameric 3.8kDa Lumbricus terrestris hemoglobin (LbHb). Since the crystal structure of LbHb remains unsolved, it is of interest to describe the environment(s) of the >500 tryptophan (Trps) reporter groups. Shifts in the fluorescence emission maximum to longer wavelengths upon dissociation at pH 9.2 suggest that Trps buried at the subunit interface become more exposed. Acrylamide titration (to 2.5M) indicate only a fraction of the residues can be quenched at either pH. At pH 7.0 the Stern-Volmer plot has downward curvature while at pH 9.2 there is slight upward curvature, again indicating a change in environment. The intrinsic fluorescence decay requires at least 4 exponentials at both pHs. The mean fluorescence lifetime of COLbHb increases from 1.1ns at pH 7 to 3.3ns at pH 9.2. The lifetime data can be further interpreted as a decrease (~20%) in the number of residues with a ~ 30ps lifetime with a concomitant increase in the longer lifetime components. This is consistent with interface Trps becoming exposed to solvent upon dissociation, and loss of quenching by intersubunit hemes. The overall results suggest that in the dodecamer, most of the Trps are located in a hydrophobic environment, not all of which are located at the subunit interface.

M-Pos147

A RESONANCE RAMAN STUDY OF LIGAND-INDUCED TERTIARY CHANGES IN MULTIMERIC LUMBRICUS HEMOGLOBIN.
((G.J.A. Vidugiris, J.P. Harrington, J.M. Friedman, and R.E. Hirsch))Albert Einstein Coll. Med., Bronx, N.Y. 10461 & Univ. S. Alabama, Mobile, Al. 36688.

In vertebrate Hbs, changes in protein tertiary structure induced by either ligand binding or changes in quaternary state are manifested at the heme as reflected in resonance Raman (RR) spectral changes involving the Fe-proximal His stretching mode. No such changes are observed for Lumbricus hemoglobin (LbHb). The Fe-His stretching mode (Fe-His) and the porphyrin breathing motion (ν_4) in the deoxy, oxy or CO photodissociated forms of LbHb and HbA (pH 7.0 and 9.2, the latter to effect LbHb subunit dissociation) were studied using pulsed (10ns) light at 435nm. In contrast to that observed for HbA, a comparison of the RR spectra of the deoxy and photoproduct forms of LbHb reveal minimal differences in the region of the Fe-His and ν_4. The spectral frequencies are similar to that observed in R-state vertebrate Hbs. Such average behavior of the 144 hemes present in LbHb is more analagous to the RR spectral properties observed in myoglobin. These results may also serve to partially explain the inadequacy of the 2-state model to describe cooperativity in LbHb. These observations report average behavior of hemes and do not preclude the possibility that a small number of hemes are undergoing substantial ligation-induced structural changes of the proximal His pocket, or alternatively structural changes at the distal His.

M-Pos148

REFINEMENT AND STRUCTURAL EVALUATION OF MODEL CYTOCHROME P450SCC 3D STRUCTURE.
((S. Vijayakumar and J.C. Salerno)) Dept. of Biology & Center of Biophysics, Rensselaer Polytechnic Institute, Troy, NY 12180-3590.

Homology modeling and Evaluation of the model structures for misfolds are two emerging themes in Structural Biology. We used the programs developed recently by Eisenberg's group (1,2) to evaluate our model structure for Cytochrome P450scc(pdb1scc.ent) (3). We also carried out multiple alignment of major Cytochrome P450scc sequences using the GCG package (4). The results of these studies have been used in refining the model structure of Cytochrome P450scc. Our studies throw light on the active site and membrane binding domain of Cytochrome P450scc. Also our study indicates the advantages and shortcomings of using algorithms for assesing 3D structures for misfolds.

References: 1) R. Luthy, J.U. Bowie and D.Eisenberg, Nature, 356 83-85. (1992); 2) J.U. Bowie, R. Luthy and D. Eisenberg, Science, 253 164-170. (1991); 3) S. Vijayakumar and J.C. Salerno, Biochem. Biophys. acta, (in press) (1992). 4) J. Deveraux, P. Haberli and O. Smithies, Nucleic acids Research, 12(1), 387-395, (1984).

M-Pos149

^{1}H NMR Resonance Assignments of the Active Site Residues of the MetCyano form of the Component IV Monomer Hemoglobin from *Glycera dibranchiata*.

Steven L. Alam, and James D. Satterlee. Departments of Chemistry, Biochemistry and Biophysics, Washington State University, Pullman, WA 99164-4630

Glycera dibranchiata is a marine annelid that possesses monomer hemoglobins in nucleated erythrocytes. Significant interest in this protein stems from the observation that the conserved distal histidine seen in most myoglobins has been replaced by the aliphatic leucine residue. Since the remainder of the tertiary structure is nearly superimposable upon sperm whale myoglobin, differences in ligand binding kinetics observed between the two proteins has been attributed to this replacement. The use of two dimensional magnitude COSY (MCOSY), NOESY and TOCSY, along with one dimensional NOE experiments have led to a consistent set of assingnments for the protons of the heme, the proximal histidine and nearby amino acids within the heme active site. This is a first and crucial step in understanding the molecular reasons for the differing kinetics, and also serves as a basis for screening the integrity of recombinant mutants of this protein now being expressed in this lab.

M-Pos150

Expression and Characterization of Point Mutant Proteins of the Component IV Monomer Hemoglobin from *Glycera dibranchiata*.

Lauri A. Herman, Steven L. Alam, and James D. Satterlee. Departments of Chemistry, Biochemistry and Biophysics, Washington State University, Pullman, WA 99164-4630

Glycera dibranchiata is a marine annelid that possess monomer hemoglobins in nucleated erythrocytes. Significant interest in all four of the monomer component proteins stem from the observation that the conserved distal histidine seen in most myoglobins has been replaced by the aliphatic leucine residue. Differences in ligand binding kinetics observed between the two proteins has been attributed to this replacement. Significant advances have been made in the expression of two recombinant proteins where the distal residue leucine has been replaced by histidine and asparagine, in an attempt to mimic Myoglobin-like characteristics. Preliminary NMR data are presented as a part of the proteins' initial characterizations. It is anticipated that these point mutats will provide an understanding of the distal residue's influence on the heme active site environment.

M-Pos151

^{1}H NMR CHEMICAL SHIFT ANALYSIS AND STRUCTURAL STUDY OF METAQUOMYOGLOBIN.

((Y.-H. Kao and J.T.J. Lecomte)) Department of Chemistry, The Pennsylvania State University, University Park, PA 16802.

Metaquomyoglobin (metaquoMb) is a high-spin (S = 5/2) ferric hemoprotein in which the ground state of Fe(III) has ^{6}A symmetry. The presence of unpaired spins centered on the Fe(III) ion induces dipolar shifts which are directly proportional to the zero-field splitting (ZFS) constant. These shifts are highly dependent upon the position of the nucleus relative to the paramagnetic center and therefore provide sensitive probes of the metaquoMb structure in solution. We have obtained a number of ^{1}H chemical shifts for sperm whale and horse metaquoMb by applying homonuclear 2D NMR methods at various temperatures. By using carbonmonoxyMb as the reference diamagnetic complex, it was possible to evaluate a series of experimental dipolar shifts in metaquoMb and to determine the ZFS constant accurately. In this procedure, only residues whose position with respect to the heme in the solid state structures of metaquoMb and carbonmonoxyMb is insensitive to the change in complexation were considered. For residues which are affected, i.e. mostly those in the binding site, ring current shift calculations were carried out to adjust the diamagnetic value. Remaining discrepancies between the observed dipolar shift and the dipolar shift calculated with the optimized ZFS constant will be discussed in terms of the adequacy of the calculation methods and possible differences between crystal and solution structures.

M-Pos152

THE EXTRACELLULAR HEMOGLOBIN OF THE EARTHWORM, *LUMBRICUS TERRESTRIS*: DETERMINATION OF THE SUBUNIT STOICHIOMETRY.

((David W. Ownby, Hao Zhu, Klaus Schneider*. Ronald Beavis*, Brian Chiat*, and Austen F. Riggs)) Dept. of Zoology, University of Texas, Austin, TX 78712. *Dept. of Mass Spectrometry and Gas Phase Ion Chemistry, The Rockefeller University, New York, NY 10021.

The giant hemoglobin has four O_2 binding chains, *a*, *b*, *c* (forming a disulfide-linked trimer) and *d* (monomer). Additional linker chains are necessary for the assembly of the 3900+ kDa native molecule. We have determined the proportions of linker chains, trimer, and chain *d* by reverse phase HPLC, with simultaneous determination of heme content. A weight proportion of linker chains of 0.163 ± 0.033 was determined by integration of the absorbance at 220 nm and verified by amino acid analysis. This value, together with both sequence- and mass spectrometry- derived molecular masses, gives a molar ratio of *abcd* chains to linkers of 8:1 corresponding to the minimal unit, $(abcd)_2$ L. This ratio suggests that 24 $(abcd)_2$ units and 24 linker chains form the complete structure with a total calculated molecular mass of protein of ≈3970 kDa composed of 216 chains. Mass spectrometry of the chains indicates additional mass of ≈135 kDa, attributed to carbohydrate. The presence of equimolar quantities of three unique linker chains means that the one-twelfth structural units seen in electron micrographs cannot all be identical, and that each linker may have a different role in assembly. The data indicate that one linker chain has heme so that the calculated heme content is 3.11% on the basis of protein content, close to the measured value of 3.04%. Supported by NSF Grant MCB-9205764, Welch Foundation Grant F-0213, and NIH Grant GM-35847.

M-Pos153

STRUCTURAL CHARACTERIZATION OF HEMOGLOBIN OF GLOSSOSCOLEX PAULISTUS.

((Hidetake Imasato, Maria H. Tinto, Janice R. Perussi, Marcel Tabak)). Instituto de Física e Química de São Carlos-USP, C.P. 369, 13560-970, São Carlos-SP, Brasil.

Chromatography in Sephadex G-200 of giant whorm extracellular hemoglobin of G. paulistus evidentiates an unique band at pH 7.0 and several bands at pH 9.0 as a result of alkaline dissociation. SDS-PAGE of the intact protein obtained at pH 7.0 shows the existence of 6 different bands with molecular weights (M.W.) of 13 kDa, 23.2 kDa, 24.5 kDa, 31.5 kDa, 49.3 kDa and 51.1 kDa. In the presence of β-mercaptoethanol also 6 distinct bands are obtained with M.W. 13.4 kDa, 14.8 kDa, 15.5 kDa, 16.4 kDa, 34.3 kDa and 39.6 kDa. The reduction of disulfide bonds of a trimer of M.W. around 49.3 - 51.1 kDa leads to the appearance of monomeric subunits of 14.8 kDa, 15.5 kDa and 16.4 kDa. The M.W. obtained from chromatography in Sephadex G-200 at pH 9.0 are different from those from SDS-PAGE. An intense band around 100 kDa is observed together with a small amount of undissociated protein, poorly resolved trimer and monomer (M.W. 13 kDa). Fluorescence quantum yields of different fractions obtained in the chromatography as well as extinction coefficients at 280nm and 415nm were estimated and compared to human hemoglobin evidentiating the greater content of aromatic residues, exposure of tryptophan fluorescence to solvent and increase in fluorescence yields upon dissociation.

Support: FAPESP, CNPq, CAPES, FINEP.

M-Pos154

THE ROLE OF HYDROGEN BONDING TO BOUND DIOXYGEN IN OXYGEN BINDING PROPERTIES OF SOYBEAN LEGHEMOGLOBIN.

((H. Caroline Lee, Jack Peisach and Jonathan B. Wittenberg))Depts. of Molecular Pharmacology, Physiology & Biophysics, Albert Einstein College of Medicine, Bronx, NY 10461.

A histidine residue is in the distal heme pocket of leghemoglobin (Lb), a monomeric hemoprotein from root nodules. Interaction of this histidine with bound O_2 has been used to explain the pH dependency of the O_2 affinity of this protein and myoglobin (Mb). The presence of a distal histidine, and the formation of a hydrogen bond between this histidine and the bound O_2 in oxy Mb have been well established. In a previous study, we used electron spin echo envelope modulation (ESEEM) spectroscopy to study hyperfine interactions with the proximal histidine N_ϵ and with exchangeable ^{2}H on the distal histidine in oxyCo(II)-substituted Mb. Here we use a similar approach to study ^{14}N and ^{2}H hyperfine interactions in oxyCoLb and demonstrate their pH dependency. Previously, we have established that in oxyCoMb the strength of hyperfine coupling to ^{2}H increases with decreasing coupling to ^{14}N. The same relation is found in oxyCoLb.

M-Pos155

USING RECONSTITUTED HEMOPROTEINS TO EXAMINE AXIAL BASE EFFECTS ON THE EPR PROPERTIES OF LOW SPIN CO(II).

((H. Caroline Lee and Jack Peisach))Depts. of Molecular Pharmacology, Physiology & Biophysics, Albert Einstein College of Medicine, Bronx, NY 10461.

The proximal histidine, the endogenous axial ligand to heme iron, is conserved in many heme peroxidases and O_2-carrying hemoproteins, as exemplified by horseradish peroxidase (HRP) and myoglobin (Mb). The proximal histidines in these two proteins differ in their interactions with nearby amino acids and in the alignments of the imidazole with respect to the porphyrin pyrroles. By reconstituting the Fe proteins with Co(II) protoporphyrin IX, it is possible to prepare paramagnetic, five-coordinated HRP and Mb having the same electron spin (S=1/2) state, and to uniquely study outer sphere effects of the axial ligand on the electronic structure of low spin Co(II). In this investigation, we used EPR and ESEEM spectroscopy to compare the hyperfine couplings to ^{59}Co, ^{14}N(pyrroles), $^{14}N_\varepsilon$, $^{14}N_\delta$ (proximal imidazole), in CoHRP and CoMb. The differences in hyperfine couplings are explained based on current EPR theory of low spin Co(II) and the known differences in σ and π bonding to the proximal histidines in the two proteins.

SPECTROSCOPIC STUDIES (EPR, NMR)

M-Pos156

^{13}C NMR AND FLUORESCENCE STUDIES OF THE MOTIONAL BEHAVIOR OF WILD TYPE AND SINGLE-TRP MUTANTS OF THIOREDOXIN IN NATIVE AND UREA DENATURED FORMS.

((P. Yuan§, M. D. Kemple§, K. E. Nollet†, and F. G. Prendergast†)) §Department of Physics, Indiana University-Purdue University at Indianapolis, Indianapolis, IN 46205-2810, †Department of Biochemistry and Molecular Biology, Mayo Foundation, Rochester, MN 55905.

The internal motions of ^{13}C-labeled tryptophan residues of wild type *E. coli* thioredoxin (TRX) and of two single-trp mutants of TRX, *viz.* W28F and W31F in which phenylalanine replaces trp-28 and trp-31 respectively, were examined both by ^{13}C NMR relaxation measurements at 75.4 and 125.7 MHz and by fluorescence anisotropy measurements on native and urea denatured forms of the reduced proteins in solution. Values of the spin-lattice relaxation time T_1 decreased and values of the steady state nuclear Overhauser effect (NOE) increased in going from the native to the denatured forms, indicating that the trp residues have more motional freedom in the denatured form. In contrast, there was little evidence of an increase in internal mobility of the trp residues in the native proteins at elevated temperatures. In the reduced forms of the native proteins, trp-31 has more mobility than trp-28 in general, but they have nearly the same mobility in the denatured proteins. The denaturation of the proteins became noticeable at urea concentrations around 2 M through the appearance of well resolved NMR signals for the native and denatured forms, which were assigned from their T_1 and NOE values. Differential line broadening data were used to provide additional confirmation of the results. The work was supported in part by NSF DMB-9105885 (MDK) and NIH GM34847 (FGP).

M-Pos157

LOCAL CORRELATION TIMES AND ORDER PARAMETERS CALCULATED FROM FLUORESCENCE ANISOTROPY AND ^{13}C-NMR OF ISOTOPICALLY LABELLED MELITTIN IN MONOMERIC COIL AND HELICAL FORMS.

((P. Buckley, M. D. Kemple*, & F. G. Prendergast)) Department of Biochemistry and Molecular Biology, Mayo Foundation, Rochester, MN, 55905 and *Department of Physics, IUPUI, Indianapolis, IN 46205-2610.

Melittin is a naturally occurring hexacosa peptide which forms an amphiphilic helix in methanol and a poorly structured coil in water at low pH (Lauterwein, J., Brown, L.R., WOthrich, K., 1980. Biochim. Biophys. Acta, 662:219-230). We have measured T_1 and steady state NOE values at two magnetic field strengths for seven select ^{13}C labelled alpha-carbons and four sidechain atoms (W19-indole-4 and K7, K21, and K23 ^{13}C-6) along with both steady state and time dependent anisotropy and fluorescence lifetime values for W19 in the monomeric helix and aqueous coil forms. Using the form of the spectral density proposed by Lipari and Szabo we computed motional parameters for the specific sites along the peptide in the context of a single correlation time for molecular rotation. The relative values of the order parameters and local correlation times generated for the ^{13}C-H vector probes assess the extent of dynamical end fraying of the helix and indicate the presence of some residual structure in the monomeric peptide in dilute aqueous solution. These results are in agreement with the average helicity determined by circular dichroism.
Supported in part by NIH GM 34847 and NSF DMB-9105885.

M-Pos158

STUDY OF THE INDOLE TRIPLET STATE IN A P-DIBROMO-BENZENE MIXED SINGLE CRYSTAL BY ZERO- AND LOW-FIELD OPTICALLY DETECTED MAGNETIC RESONANCE.

((C.A. Smith and A.H. Maki)) Department of Chemistry, University of California, Davis, CA 95616. (Spon. by R. Nuccitelli)

The triplet state properties of indole as a guest in a mixed single crystal host of 1,4-dibromobenzene (DBB) were investigated by high resolution phosphorescence and zero- and low-field ODMR. Two origins are resolved (413.56, 414.41 nm) that are associated with differing zero field splitting (zfs), sublevel decay kinetics, and radiative character. Low-field ODMR of an oriented crystal, monitoring blue and red origin emissions allowed the location of principal zfs axes of each. The principal x-axis is found to be oriented +49±5° (red origin) and -56±10° (blue origin) relative to the long axis of DBB, with both z-axes near the DBB normal. We assume that the "red" and "blue" emissions originate from indole molecules substituted in DBB sites with normal and long axes coincident, but flipped by 180° relative to one another about the long axis. Arguments based on external heavy atom effects (HAE) then suggest that the sense of rotation places the x-axis roughly at right angles to the ethylenic double bond of the 5-membered ring. T_x is identified as the triplet sublevel with intermediate energy which is the most radiative one in the absence of an external HAE.

M-Pos159

INTERACTION OF ALPHA-LACTALBUMIN WITH SPIN-LABELED MODEL AND BIOLOGICAL MEMBRANE SMALL UNILAMELLAR VESICLES.

((Dipankar Chaudhuri and Lawrence J. Berliner)) Department of Chemistry, The Ohio State University, Columbus, OH 43210.

Alpha-lactalbumin (α-LA) is the modifier protein of the lactose synthase complex in the mammary cell. In vivo, α-LA is biosynthesized and stored on the smooth endoplasmic reticulum (ER) and then transported to the Golgi lumen after stimulation by prolactin for lactose biosynthesis and milk secretion. Since both the smooth ER surface and the environment of galactosyl transferase in the Golgi lumen are composed of membranes, it is of interest to examine the interaction of α-LA with both model and biological membrane small unilamellar vesicles (SUV).

The work to be presented in the poster uses ESR to study the binding of α-LA with model/biological membrane (DMPC, lecithin, etc.) SUV's by incorporating the 5-doxyl stearic acid spin label into the DMPC and egg lecithin SUV's. The interaction between the α-LA and spin labelled lipid vesicles is then monitored through changes in the outer hyperfine splitting $2T_{\|}$ and the order parameter S which indicated whether fluidization/immobilization of the bilayer occurs on binding to α-LA. Results of experiments to find out how this binding affects lipid order/fluidity as a function of temperature across the broad gel-liquid crystalline phase transition region of egg lecithin will also be presented along with the effect of calcium on the binding of α-LA to lipid vesicles.

This research is supported in part by a grant from the USPHS (GM40778).

M-Pos160

EPR DEPTH MEASUREMENTS OF NITROXIDES IN MEMBRANE BILAYERS USING SPIN LABELED MUTANTS OF BACTERIORHODOPSIN

((Christian Altenbach, Duncan A. Greenhalgh, H. Gobind Khorana, Wayne. L. Hubbell)) Jules Stein Eye Institute and Department of Chemistry and Biochemistry, UCLA, Los Angeles, CA. MIT, Depts. of Biology and Chemistry, Cambridge, MA.

A series of bacteriorhodopsin (bR) mutants containing single nitroxide spin-labels at the positions A103, G105, L109, G113, G116, or I117 were prepared. These residues were selected to be located on the surface of the protein, facing the lipids at different depths from the water membrane interface. The spin-labeled mutants refolded to generate chromophores identical to wild-type bR and each was completely active in proton translocation.

Room temperature EPR spectra of these mutants reconstituted into egg-phosphatidylcholine vesicles were very mobile, having correlation times on the order of a few nanoseconds. The collision frequencies of the side-chains with freely diffusing paramagnetic probes were measured with power saturation EPR spectroscopy. The rates of collision with either the neutral complex nickel-acetylacetonate (NiAA) or the charged complex chromium oxalate (CROX) decreased rapidly with distance from the membrane surface, while collisions with the apolar molecule O_2 increased. These experiments confirm that the spin labels are located on the outside surface of the protein, facing the lipids at different depths in the membrane bilayer.

Following calibration of the system with spin-labeled phospholipids, we find that $\Delta P_{1/2}(oxygen)/\Delta P_{1/2}(NiAA)$ can be used to estimate the depth of the spin labeled bR sidechains from the membrane surface. These results were found to be consistent with a transmembrane α-helix. This method provides a new and general approach for estimating the depths of nitroxide spin labels in bilayers.

M-Pos161

MAGIC-ANGLE SPINNING NMR STUDIES ON THE GALACTOSE-H$^+$ SYMPORT PROTEIN OF *ESCHERICHIA COLI*.

((Paul J.R. Spooner, Anthony Watts and Peter J. F. Henderson[1])) Departments of Biochemistry, University of Oxford, South Parks Road, Oxford OX1 3QU and [1]University of Leeds, Leeds LS2 9JT.

Preliminary investigations have been conducted to assess the ability of Magic-Angle Spinning (MAS) NMR, combined with specific isotopic labeling, to provide structural information on the substrate binding sites within the membrane proteins responsible for sugar-H$^+$ symport. Inner-membrane vesicles from *Escherichia coli* with the galactose-H$^+$ symport protein, GalP, over-expressed to levels above 50% of total protein were prepared by explosive decompression followed by sucrose density ultracentrifugation and resuspension in 20mM Tris-HCl buffer at pH 7.4. MAS NMR measurements were conducted at 2°C throughout on membrane pellets containing about 27mg (~0.5μmol) of GalP. Alequots of D-glucose(1-^{13}C) were titrated into the membrane pellet to provide up to two molar equivalents of substrate. Proton-decoupled ^{13}C MAS NMR measurements were able to detect as little as 250nmol of added substrate, when using conditions of cross-polarization that will discriminate just the bound fraction. Spectral features of the substrate were well resolved and indicate a preference for binding the β-form of the sugar. This work shows that it should even be possible to proceed with structural studies without any additional protein purification and whilst maintaining protein and membranes in a functional native state. The study also provides direct justification for the proposed strategy in which bound substrate is to be used as a 'filter' to confine observations to residues within the binding domain of the protein.

M-Pos162

SOLUTION MEASUREMENT OF THE THYMIDYLATE SYNTHASE CONFORMATIONAL CHANGE USING EPR SPECTROSCOPY

((C.W. Carreras, N. Naber, R. Cooke, and D.V. Santi)) Departments of Pharmaceutical Chemistry and of Biochemistry & Biophysics, University of California, San Francisco, CA 94143-0448

Spin labels were attached to the C-terminus of *L. casei* thymidylate synthase (TS, EC 2.1.1.45) and used to monitor ligand induced conformational changes. TS catalyzes the reductive methylation of dUMP by CH_2H_4folate to produce dTMP and H_2folate. The mechanism of TS has been extensively characterized, and crystallographic analysis of free and bound forms of the enzyme show that a major conformational change occurs at the C-terminus upon binding of dUMP and folate analogs. Prior to the conformational change, the C-terminal tetrapeptide is quite flexible (B=40-60 Å^2), but in ternary complexes these residues are quite ordered and participate in an extensive H-bond network not present in the unliganded enzyme or in binary complexes. Using the technique of site-directed mutagenesis, a mutant TS (C244T/V316C) has been constructed which has only the active-site cysteine and a new cysteine introduced at the C-terminal residue. Using the substrate dUMP to block the active site, the C-terminus was specifically labeled with maleimido-TEMPO, and this spin label was used to report the flexibility of the C-terminus in the presence of various substrates and drugs which bind to TS. Ligand-induced immobilization of the C-terminus was observed, and increased as the following series: free enzyme < E•dUMP = E•FdUMP <E•FdUMP•CH_2H_4folate. In all of these cases there are populations of both flexible and immobilized forms, demonstrating the dynamic role of the C-terminus in the binding of ligands.

M-Pos163

ELECTRON SPIN ECHO ENVELOPE MODULATION SPECTROSCOPY OF ^{1}H and ^{2}H HYPERFINE INTERACTIONS IN ORGANIC RADICALS.

((K. Warncke, G.T. Babcock and J.L. McCracken)) Department of Chemistry, Michigan State University, East Lansing, MI 48824

The range of application of the electron spin echo envelope modulation (ESEEM) technique of pulsed-EPR spectroscopy to obtain detailed descriptions of the nuclear and electronic structures of organic radicals is systematically investigated. The ESEEM spectroscopic features of hyperfine (hf) couplings with a wide range of anisotropies and isotropic coupling strengths are provided by tyrosine radicals that incorporate all ^{1}H nuclei, or are ^{2}H-labelled specifically in the β-methylene-, and α-ring 2,6- and 3,5- positions. The radicals are formed in aqueous glasses by UV photolysis. We find that the microwave pulse-swapping technique (Fauth, Schweiger, Ernst, 1989, *J. Mag. Res.* 81: 262) is practically useful for revealing the extent of anisotropically-broadened lines due to ^{2}H hf interactions, provided that the envelope modulation for the ^{2}H-labelled compound is divided by that of the per-^{1}H compound. This eliminates phase memory- *vs.* T_1- relaxation-induced time domain discontinuities that distort the frequency spectrum. The scaled ^{1}H hf parameters obtained from these data are consistent with spectral simulations based on principal values determined in previous cw-ENDOR studies. Features from the corresponding ^{1}H nuclei are also observed in 3-pulse (2,6- and β-methylene- ^{1}H) and 2-pulse (3,5-^{1}H splitting of the ^{1}H combination line). Hyperfine interactions of the phenolic oxygen atom with exchangeable hydroxyl- and hydrogen bonded- ^{2}H nuclei are examined using a strategy based on the pulse-swapping technique and division of envelopes for the radical in different labelled solvents: $^2H_2SO_4$ *vs.* $^1H_2SO_4$ (protonated cation) and saturated NaO^2H *vs.* NaO^1H (deprotonated neutral radical) glasses. Features due to exchangeable ^{2}H interactions observed in the $^2H_2SO_4$ *vs.* $^1H_2SO_4$, but not in NaO^2H *vs.* NaO^1H, ESEEM frequency spectra suggest an axially symmetric hyperfine tensor for ^{2}H in the ^{2}H-O hydroxyl bond, with principal components of |2.8| and |4.4| MHz. The results show the conditions for using ESEEM methods to successfully characterize ^{2}H and ^{1}H couplings in organic radicals, and establish a foundation for interpretation of ESEEM studies of hf interactions in enzyme catalytic amino acid and dissociable organic cofactor radicals. Supported by: NIH GM37300 (G.T.B.) and GM45795 (J.L.M.)

M-Pos164

Determination of the Positions of Magnetic Ligand Atoms in Spin Coupled Multi-Spin Systems from ENDOR Hyperfine Constants

S. Khangulov and G. C. Dismukes
Princeton University, Dept. of Chemistry, Hoyt Laboratory, Princeton, NJ

It has been difficult to determine the location of magnetic atoms surrounding a paramagnetic site in cases where the spin density is distributed over two or more centers. We have developed a theoretical model which enables extraction of metrical coordinates from the hyperfine couplings between ligand nuclei and two spins, such as occurs for spin-coupled dimetalloproteins. This is applied to determine the positions of protons surrounding the active sites of several enzymes and complexes, including dimanganese(III,IV) catalase, the diiron(II,III) site of uteroferrin and the tetramanganese cluster of the water oxidizing enzyme from Photosystem II. The model treats the two spins as point dipoles which are coupled by the Heisenberg exchange interaction and separated by a known distance. This is called the "spin-coupled point pair model".[1] The locations of the protons are determined from the dipolar part of the ligand hyperfine tensors, obtained by simulation of the ENDOR powder lineshape. The model reveals that the individual spins of the coupled paramagnetic centers will be smaller or larger or even reversed in sign, depending on the total electronic spin in the state being observed. This requires a scaling of the dipolar interaction in order to properly extract the nuclear positions. Analysis of the angle selected ^{1}H ENDOR spectrum of MnCat(III,IV) revealed that one proton is located at distances of 4.6 and 2.9 Å to Mn(III) and Mn(IV), respectively. A second proton exists at a greater distance.
These coordinates are compatible with a water or hydroxide molecule H-bonded to a terminal ligand on Mn(IV). NIH GM39932.

[1]Khangulov, Sivaraja, Barynin and Dismukes *Biochem.* submitted.

M-Pos165

CONTROL OF OXIDATIVE PHOSPHORYLATION BY ADP IN TRANSGENIC MOUSE LIVERS EXPRESSING CREATINE KINASE

((J.M. Halow, K.R. Miller and A.P. Koretsky)) Dept of Biological Sciences, Carnegie Mellon University, Pittsburgh, Pa. 15213

The mechanisms of control of oxidative phosphorylation are not yet completely understood. Several factors have been implicated such as cytosolic levels of Pi and ADP, mitochondrial [NAD$^+$]/[NADH], local [O_2], and mitochondrial membrane potential. The creatine kinase equilibrium has routinely been used, along with ^{31}P NMR, to determine free ADP levels in muscle and brain. A transgenic mouse expressing creatine kinase in its liver, a tissue where it is not normally found, enables one to measure the cytosolic free ADP levels in liver. Experiments have been done to vary the levels of ADP using fructose doses (3mM, 5mM and 7mM). ^{31}P and ^{1}H NMR (to calculate free [ADP]) and O_2 consumption were monitored. With perfusate Pi at 0.4 mM, fructose caused a rise in ADP without any changes in Pi or ATP. Using Lineweaver-Burke analysis, with O_2 consumption as a measure of velocity, ADP was shown to regulate oxidative phosphorylation with a K_m of 18.4±4.1 μM (95% confidence limit), at 0.4 mM perfusate Pi. This is the first time that it has been possible to vary [ADP] in a tissue without changing [Pi], clearly quantitating the role of ADP in regulating oxidative phosphorylation.

M-Pos166

TRANSGENIC LIVERS EXPRESSING CREATINE KINASE ARE PROTECTED DURING LOW OXYGEN: A ^{31}P NMR STUDY.

((K.R. Miller, J.M. Halow, and A.P. Koretsky)) Dept. of Biological Sciences, Carnegie Mellon University, Pittsburgh, PA 15213

Creatine kinase (CK), which is found in muscle and brain, catalyzes the reaction: phosphocreatine (PCr) + MgADP + H^+ ⇌ Cr + MgATP. This reaction predicts that PCr buffers the level of ATP and that the CK reaction is involved in the regulation of intracellular pH. Transgenic mice that express the BB-dimer of CK in liver, where it is not normally expressed, have allowed us to assess the role of CK during periods of low oxygen. During ischemia of the perfused liver at 25 deg C, ATP decreases with a half time of 4 min. and pH decreases from 7.4 to 6.6 in control livers. PCr decreases with a half time of 16 min., while ATP levels begin to fall after 32 min. of ischemia in transgenic livers. pH remains at a pre-ischemic level for 16 min., a time when intracellular pH has dropped to 6.9 in control livers. During hypoxia of the perfused liver at 37 deg C, ATP decreases in control livers with a half time of 30 min. and there is a large increase in the release of lactate dehydrogenase (LDH) after 30 min. In transgenic livers, ATP is buffered at a pre-hypoxic level and no increase in LDH release is observed for up to 90 min. These results prove the role of CK in buffering ATP levels and regulating intracellular pH during periods of low oxygen.

M-Pos167

ETYA, STABLE IN D6-DMSO UNDER AMBIENT CONDITIONS, AS JUDGED BY H1-NMR, DIFFERENTIALLY INDUCES MALONDIALDEHYDE AND MORPHOLOGIC CHANGES IN U937 AND PC3 CELLS.

Anderson,KM[1,2],Kleps, RA[3], Dudeja, PK[4], Harris, JE[1], Depts. Med[1] and Biochem[2], Rush Med Col, NMR Lab[3] and Dept Biochem, U of Ill Chicago, Il 60612.

ETYA(5,8,11,14 eicosatetraynoic acid, 0.04M) in DMSO turned yellow at RT and -20°, but not -80° and was "chemiluminescent" by LSC. ETYA in D6-DMSO at ambient light and temp remained colorless. H1-NMR spectra were unchanged except for absorption of water during 4 months. Spectra in methanol altered in ways difficult to interpret. ETYA (40uM) cultured with PC3 cells did not increase malondialdehyde(MDA,nmol/mgP); arachidonic acid(AA) doubled it. U937 MDA was doubled by ETYA and increased 20-fold with AA. ETYA-induced ultrastructural changes consistent with "oxidative stress" occurred only in PC3 cells. In summary: D6-NMR studies of ETYA provided no evidence for spontaneous generation of free radicals, which may be revealed by current ESR studies, and could contribute to the apparent chemiluminescence by LSC.Lack of correlation between MDA and ultrastructure of cultured cells, which may be related to differences in lipid, phospho lipid, cholesterol or free radical metabolism, remains unexplained.

M-Pos168

AN ON-LINE NMR VIEW OF HUMAN T LYMPHOCYTE ACTIVATION.

((M. Bental and C. Deutsch)) Univ. of Penn., Philadelphia, PA 19104 (Spon. by DF Wilson)

A system optimized for NMR studies of T lymphocytes in a defined, serum-free growth medium (Bental and Deutsch, Magn. Reson. Med., in press), has been used to characterize metabolic changes and evaluate the role of ion homeostasis and membrane potential in mitogenesis. Using ^{1}H- and ^{13}C-NMR, we found that glycolysis was enhanced 6-fold within the first 2 hrs of stimulation (early G_1), and 15-fold by 48-96 hrs (late G_1 to S phase). Aerobic lactate production was increased 3-fold by 48 hrs, with only a minor increase during the first 12 hrs of stimulation. Our results indicate a shift of cellular metabolism from mostly aerobic to mostly anaerobic lactate production in T cells within the first 90 min of the G_0-G_1 transition during cell cycle progression. Phosphorus metabolites remained constant during this period.

Having identified early metabolic events that define a discrete G_0-G_1 transition, we can investigate the effect of membrane potential and pH on these events. Depolarization to -38mV affected neither the cellular ATP level, nor the rates of glucose utilization or lactate production in quiescent or stimulated cells. This indicates that the inhibition of mitogenesis by depolarization (Freedman et al., J.I., 1992) is specific, and not due to generalized metabolic limitations. To investigate intracellular pH, we use a new probe, vicinal difluoro-α-methyl alanine and its methyl ester. The acid pK is 7.05 at 140mM K^+, and its sensitivity is 0.83ppm/pH unit. The non-toxic ester crosses the cell membrane, and is hydrolyzed. The acid generated is retained by the cells at mM concentrations. Upon removal of the ester, the intracellular acid pool can be observed with good S/N for at least 3 hrs. Due to the two equivalent fluorines, this molecule provides a greater sensitivity at physiological temperature and pH than ^{19}F pH probes previously studied in this laboratory. Supp. by GM 36433.

M-Pos169

PLATELET FACTOR-4 LYSINE MUTANTS AND HEPARIN BINDING

Sharon Barker[1], Michael Kuranda[2] and Kevin H. Mayo[1], Jefferson Cancer Institute[1], Thomas Jefferson University, Philadelphia, PA 19107, and Repligen Corporation[2], Cambridge, MA 02139.

Human platelet factor 4 is a 70 residue protein known to form dimers and tetramers in slow exchange on a 600MHz ^{1}H-NMR time scale. Under physiological conditions, PF4 exists in the tetrameric state which functions in heparin binding. X-ray diffraction analysis of the bovine PF4 tetramer has shown that the molecule is composed of four solvent exposed helices folded onto a β-sheet scaffolding. The α-helices contain two pairs of lysine residues (IIKKLLKKES) which have been proposed as being important in heparin binding. In this present study, PF4 mutants have been genetically engineered and expressed with singly- and doubly- substituted alanines in place of the lysines. Nitrocellulose filter binding assays (PF4-heparin) indicate that differences exist in binding profiles and affinities. NMR analyses of all mutants indicate conservation of overall structural features. Dimer and tetramer aggregation properties, however, do vary from mutant to mutant. The K61A mutant, in particular, shows significant differences from native protein behavior.

This work was supported by an NIH research grant, HL-43194 (to K.M.)

SPECTROSCOPIC STUDIES (FLUORESCENCE I)

M-Pos170

SIMULATION OF SOLVENT DYNAMICS EFFECTS ON THE FLUORESCENCE OF 3-METHYLINDOLE IN POLAR SOLVENTS.

((Pedro L. Muiño and Patrik R. Callis)). Department of Chemistry. Montana State University. Bozeman, MT 59717.

The UV absorption and fluorescence of 3-methylindole in water and butanol at 300K have been simulated over periods of 4 to 30 ps, using a combination of classical molecular dynamics simulations and spectroscopically calibrated semiempirical molecular orbital methods, (INDO/S-CI). Several types of simulations have been done, involving different solvent models and geometries, (drops or periodic boundary conditions). Solute polarization is also included in several simulations. The solvent causes a stabilization of both ground and excited states, but larger in the latter. The polarity and size of the solvent are key factors in the amount and time scale of this stabilization. Relaxation of the solvent after absorption is very fast: It is about 50% complete within ~20 fs, in water, while the remaining relaxation occurs during the next 200 fs. The values for butanol are larger, (200fs and 1ps, respectively). The values obtained for the fluorescence redshift are ~5000cm^{-1} for water and ~3000cm^{-1} for butanol, in reasonable agreement with the experimental values of 3800cm^{-1} and 2700cm^{-1}. Correlation of the redshift with oscillator strength and dipole of the excited states was found. The ^1L_a dipole values were found to vary between 8 and 14 Debyes, in response to fluctuations in the water environment. The temporal behavior of the fluorescence redshift can be roughly fitted to a double exponential decay.

M-Pos171

^1L_a TRANSITIONS OF JET-COOLED INDOLES AND COMPLEXES FROM TWO-PHOTON FLUORESCENCE EXCITATION.

((David M. Sammeth, Pedro L. Muiño, and Patrik R. Callis)) Dept. of Chemistry, Montana State University, Bozeman, MT 59717.

We have observed the polarization resolved two-photon fluorescence excitation spectra of jet cooled (~2K) indole, 3-methylindole (3MI), and 5-methlyindole (5MI). ^1L_a lines are distinguished from ^1L_b lines by their distinctive low intensity under excitation with circularly polarized light and by their sharp Q branch using linear polarization. For 3MI, ^1L_a lines are seen at 409, 420, 468, 609, 617, 739, 820, and 918 cm^{-1} above the ^1L_b origin --in contrast to indole, where the only ^1L_a lines below 783 cm^{-1} were at 455 and 480 cm^{-1}, and 5MI, where the lowest ^1L_a line observed was at 1424 cm^{-1}. The piling up of ^1L_a lines a few hundred cm^{-1} above the ^1L_b origin and the fact that we find more ^1L_a character in the ^1L_b origin of 3MI together suggest an avoided crossing of the ^1L_a and ^1L_b potential surfaces. Preliminary two-photon spectra of the 3MI-water complex suggest even more ^1L_a character in its strong origin peak. Extensive one-photon excitation spectra of complexes of indole with water, D_2O, and methanol indicate surprisingly small (~10 cm^{-1}) differential shifts of ^1L_a lines relative to ^1L_b lines. The two-photon spectra of these complexes are being investigated.

M-Pos172

EVIDENCE FOR EXPONENTIAL DISTANCE-DEPENDENT RATE OF QUENCHING FROM FREQUENCY-DOMAIN FLUOROMETRY.

((J. Kuśba, B. Zelent, I. Gryczynski, H. Szmacinski, M.L. Johnson*, and J.R. Lakowicz)) University of Maryland, School of Medicine, Center for Fluorescence Spectroscopy, Dept of Biological Chemistry, Baltimore, MD 21201; *University of Virginia, Dept of Pharmacology, Charlottesville, VA 22908. (Sponsored by H. Malak)

We report results of frequency-domain and steady-state measurements of the fluorescence quenching of p-bis[2-(5-phenyloxazolyl)]benzene (POPOP) when quenched by carbon tetrabromide (CBr_4), bromoform ($CHBr_3$), methyl iodide (CH_3I), N,N-diethylaniline (DEA) or 1,2,4-trimethoxybenzene (TMB). The quenching efficiency of the compounds appeared to decrease in the order: DEA, TMB, CBr_4, CH_3I, $CHBr_3$. In the case of DEA, TMB and CBr_4 the measurements clearly confirm the applicability of the experimental distance-dependent quenching model (EDQ), in which the bimolecular quenching rate k(r) exponentially depends on the fluorophore-quencher separation r, $k(r) = k_e exp[-(r-a)/r_e]$. Simultaneous analysis of the frequency-domain and steady-state data significantly improves resolution of the recovered molecular parameters k_e and r_e. The data cannot be satisfactorily fit using either the Smoluchowski or Collins-Kimball (RBC) model. The quenching behavior of the less efficient quenchers CH_3I and $CHBr_3$ can be adequately described with both the EDQ and RBC models. In this case the values of parameters k_e and r_e are highly correlated, which makes their separate evaluation from the data nearly impossible. The efficiency of quenching is discussed based on the mechanisms of interaction between fluorophore and quencher molecules, which involves electron transfer and/or heavy atom effects.

M-Pos173

MEASUREMENTS OF FLUORESCENCE LIFETIMES AND ANISOTROPIES BY ONE-PHOTON AND TWO-PHOTON EXCITATION.

((Chen Dong, Peter T. C. So, and Enrico Gratton)) University of Illinois at Urbana-Champaign, Laboratory for Fluorescence Dynamics, Department of Physics, 1110 W. Green St., Urbana, IL 61801.

We studied the lifetimes and anisotropies of indole derivatives using one-photon and two-photon excitation. The measurements are performed on a MHz frequency-domain lifetime fluorometer supplemented with an optical multichannel analyzer (OMA). Our OMA permits simultaneous measurements of lifetimes across the emission spectrum with a wavelength range of 256 nm and a maximum resolution of 1 nm. OMA measurements showed the advantages of using two-photon excitation in investigating blue region of emission previously obscured by Raman scattering in one-photon excitation. The anisotropy data are analyzed and compared to theoretical prediction. This work was performed at the Laboratory for Fluorescence Dynamics (LFD) at the University of Illinois at Urbana-Champaign (UIUC). The LFD is supported jointly by the National Institute of Health (RR03155) and by UIUC.

M-Pos174

SOLVENT DIPOLAR RELAXATION OF THE TRYPTOPHAN RESIDUE IN HUMAN SUPEROXIDE DISMUTASE IN 80% GLYCEROL.

((Norberto D. Silva Jr. and Enrico Gratton)) University of Illinois at Urbana-Champaign, Laboratory for Fluorescence Dynamics, Department of Physics, 1110 W. Green St., Urbana, IL 61801.

Solvent dipolar relaxation results in the increase in apparent fluorescence lifetime with increasing emission wavelength. Systems displaying dipolar relaxation are typically placed in viscous environments. We are studying the possibility of dipolar relaxation from the time-resolved fluorescence of the single tryptophan (Trp) residue of human superoxide dismutase (HSOD). Measurements of HSOD are done in 80% glycerol (GlOH) at various temperatures and excitation wavelengths. Our study is aided by the use of a time-resolved optical multichannel analyzer that can attain a 1.0 nm resolution and lifetime resolution on the order of 50 psec. Preliminary results for HSOD in 80% GlOH show that 1) tau modulation, τ_m, increases linearly with increasing wavelength, 2) the slope of τ_m increases with decreasing excitation wavelength and 3) the slope of τ_m increases as temperature is decreased. Such results suggest that the Trp residue of HSOD in 80% GlOH displays dipolar relaxation. Control experiments of NATA in 80% GlOH were also performed. Supported by National Institutes of Health (RR03155) and UIUC.

M-Pos175

SOME EFFECTS OF CHARGE ON THE EMISSION OF TRYPTOPHAN

((D. B. Bivin[1] , S. Kubota[2] , R. Pearlstein3 and M.F. Morales[1]))
1. UOP, San Francisco 2. Peninsula Labs Bellmont 3. DCRT, NIH

Motivated by the need to explain why the emission of a tryptophan residue of myosin S-1 is enhanced moderately by the binding of ADP, and strongly by the binding of ATP, we have undertaken to study environmental factors such as charge on the emission from the indole ring. For this purpose we have synthesized diketopiperazines in which Trp is teamed with a negatively (e.g., Asp, Glu) or positively (e.g., His) residue, which may be in either the L- or the D-configuration. The molecular geometry in each case has been assessed using the Sybyl Program, and the corresponding potential field using the Delphi Program of Insight II. In the experimental measurements aqueous 50uM solutions of a compound were excited at 280nm, and the steady state emission at 355nm was measured in an SLM Model 8000 Spectrofluorometer. By varying the pH in 2mM buffer, charge (positive or negative, depending on the "second" amino acid) could be generated, in a prescribed relation to the indole ring. In every case the charge had a strong influence on the emission intensity. Positive charge inhibiting, and negative charge enhancing, the intensity. As the pH decreased below 3 there was an increasing inhibition of the intensity which appears to arise from the increasing proton concentration. If this effect was subtracted, the resulting data could be adequately represented by least squares fits to simple titration curves. An attempt was made to understand the observed effects in terms of a model in which the field of the generated charge superimposes on a dipole field. Research supported by R37 HL-44200, NSF DMB-9003692, and assisted by a Fogarty Scholarship-in-Residence to M.F.M.

M-Pos176

STEADY-STATE AND DYNAMIC FLUORESCENCE OF NADH IN SOLUTION AND BOUND TO LIVER ALCOHOL DEHYDROGENASE.

((A.S. Ladokhin and L. Brand)) Biology Dept. and McCollum-Pratt Inst., The Johns Hopkins Univ., Baltimore, MD 21218.

Despite the fact that fluorescence properties of NADH have been extensively studied there is no consensus whether fluorescence decay is mono- or multiexponential, or on possible origins of heterogeneity of lifetimes. In this study the temperature dependence of fluorescence of NADH in different solvents and when bound to liver alcohol dehydrogenase (LADH) was studied by frequency-domain and steady-state fluorometry. In liquid solutions (aqueous buffer, ethanol, glycerol at 50°C) and in LADH complexes biexponential decay was observed, while for glycerol at lower temperatures a more complicated decay law was required. In the later solvent a significant dependence of position of the emission spectra on excitation (red-edge shift) was observed. Moreover, a slight dependance on excitation was present in all cases producing 3-10% increase in average lifetime with an excitation change from 325 to 365 nm. For NADH bound to LADH this is attributed to the difference in initial amplitudes while lifetimes appear to remain the same. Possible mechanisms causing complex decay of NADH (ground state conformational heterogeneity, dipolar solvent relaxation, excited state reaction yielding either fluorescent or quenched species) will be discussed. (Supported by NIH grant GM11632, NSF Biological Research Centers Award, DIR-8721059 and W.M. Keck Foundation Award.)

M-Pos177

DYNAMIC ASPECTS OF L7/L12, FREE AND RECONSTITUTED INTO THE 50S RIBOSOMAL SUBUNIT: STEADY-STATE AND TIME-RESOLVED FLUORESCENCE STUDIES.

((B.D. Hamman[1] and D.M. Jameson[1], A. Oleinikov[2] and R.R. Traut[2])) [1]Dept. of Biochemistry and Biophysics, University of Hawaii at Manoa, Honolulu, HI 96822; [2]Dept. of Biological Chemistry, University of California, Davis, CA 95616

L7/L12 is a 24kD dimeric protein in the large (50S) subunit of the *E. coli* ribosome. The wild-type L7/L12 has no cysteine residues; using site-directed mutagenesis single cysteines were incorporated into the protein at residues 33, 63, or 89. These cysteine residues were specifically labeled with iodoacetamidofluorescein and steady-state and time-resolved methods were utilized to study the motional properties of the probes. In all cases global rotational relaxation times of ~24 nsec were found with varying extents of local probe motion. The C63 derivative (in the C-terminal region) displayed the most local mobility. The fluorescein labeled L7/L12 proteins were reconstituted into 50S ribosomal subunits. In all cases the global motion decreased (rotational relaxation times >50 nsec), although local motion was not affected. These results demonstrate that both the globular C-terminal domain (C63 and C89) and C33 near the alpha helical N-terminal domain have significant mobilities on the ribosome. Gu-HCl unfolding studies on these L7/L12 adducts and a hinge-deleted (Δ35-52) C89 variant were carried out. The results indicate that the local unfolding of the C-terminal domain precedes subunit dissociation and that the hinge deletion still permitted formation of the C-terminal domain but destabilized it with respect to Gu-HCl induced folding.

M-Pos178

FLUORESCENCE STUDIES OF THE E.COLI GALACTOSE REPRESSOR PROTEINS' CARBOHYDRATE BINDING EVENTS.((Martha P.Brown, M.Brenowitz, and L.Brand.)) Dept. of Biology,The Johns Hopkins University,Baltimore MD. 21218,Dept. of Biochemistry,Albert Einstein College of Medicine,Bronx NY 10461.

The sequence-specific binding of the galactose repressor protein (GalR) to the gal operon is regulated by galactose and fucose (Majumdar,A. et al. J.Biol.Chem.(1987) 262,2326). Each GalR monomer contains a single tryptophan, which has a KI quenching rate constant, k_q, of $1.8E+09M^{-1}sec^{-1}$. The fluorescence of this solvent-exposed tryptophan is enhanced when galactose and fucose bind to GalR. Analysis of this enhancement reveals that both bind cooperatively at pH 8.0. When GalR is saturated with galactose, neither the k_q nor the steady-state anisotropy change. Increasing the pH of the environment of GalR from 7.5 to 9.5 decreases the association constant that describes galactose binding. The steady-state anisotropy of GalR remains constant over this range. The fluorescence decay of GalR is triexponential. The pre-exponential factors change in a manner which is dependent on both galactose concentration and pH. Glucose produces no change in the steady-state fluorescence, anisotropy, or time-resolved fluorescence of GalR. Competitive binding experiments with galactose and glucose have been performed. Supported by NIH grant No. GM11632, GM077231-17, and GM39939 (M.Brenowitz).

M-Pos179

FLUORESCENCE OF *B. SUBTILIS* TRYPTOPHANYL TRNA SYNTHETASE AND TRNA AMINOACYLATION INTERMEDIATES WITH 4-FLUOROTRYPTOPHAN.

((C.W.V. Hogue[1,2], H. Xue[3], J.T. Wong[3] and A. G. Szabo[1])). 1. Institute for Biological Sciences, National Research Council, Bldg. M54 Montreal Rd. Ottawa, Ont. Canada. K1A 0R6. 2. Graduate student, Biochemistry, University of Ottawa. 3. Dept. of Biochem. U. of Toronto, Toronto, Ont. Canada M5S 1A8.

Tryptophanyl tRNA synthetase (TrpRS) of *B. subtilis* has a single Trp-92 which can be used as an intrinsic fluorescent probe of conformation, structure and function. This Trp is also highly conserved and essential for tRNA aminoacylation. Several Trp analogs can be incorporated into bacterial proteins, including 4-fluorotryptophan (4FW). TrpRS represents the sole enzymatic recognition step involved in such in-vivo incorporation. 4FW is a nonfluorescent substrate, hence changes in the fluorescence of the intrinsic Trp-92 can be studied. Herein we demonstrate the capacity of *B. subtilis* TrpRS to form the stable, enzyme-bound 4-fluorotryptophanyl-adenylate. A decrease in the fluorescence of Trp-92 accompanies the filling of the active site with 4FW-adenylate. Titrations of ATP added in the presence of 4FW while monitoring Trp-92 fluorescence show 1:1 stoichiometry. Equilibrium binding of excesses of 4FW, ATP or $tRNA^{Trp}$ do not alone affect the fluorescence of Trp-92. However equilibrium binding of 4FW causes an increase in Tyr fluorescence. A large fluorescence change arises in the enzyme when the 4-fluorotryptophanyl-adenylate intermediate is present in the enzyme's active site. This change suggests that Trp-92 becomes more exposed. This conformational change precludes tRNA binding, and indicates that Trp-92 may be involved in tRNA binding. Fluorescence decay parameters of Trp-92 also differ in the presence of a combination of ATP and $tRNA^{Trp}$, indicating the presence of a ternary TrpRS:ATP:$tRNA^{Trp}$ complex. The fluorescence parameters of trp-$tRNA^{Trp}$ are also presented, and reflect a highly quenched Trp.

M-Pos180

FLUORESCENCE INTENSITY DECAY OF RIBONUCLEASE-T1 TRYPTOPHAN-59: MINIMUM PERTURBATION MAPPING STUDY OF NEIGHBOR SIDE CHAIN ISOMERIZATION((Christopher Haydock and Franklyn G. Prendergast)) Department of Biochemistry and Molecular Biology, Mayo Foundation, Rochester, Minnesota 55905.

It is well known that the fluorescence intensity decay of ribonuclease-T1 is monoexponential at slightly acidic pH and biexponential at neutral pH. Since ribonuclease-T1 has a single tryptophan at position 59 and three histidine residues that are not close neighbors, long range electrostatic effects from multiple histidine protonation states might account for the observed fluorescence lifetime heterogeneity. An alternative hypothesis ascribes the heterogeneity to multiple side chain isomers of neighboring lysine-25. The tryptophan fluorescence lifetime for each lysine isomer depends on the collision rate between lysine and tryptophan and the pH effect results from shifts in the lysine isomer populations. The fluorescence intensity decays of the site-specific mutants K25H, K25N, and K25R have lifetimes and preexponential factors that are very similar to wild type ribonuclease-T1. The insensitivity of fluorescence spectra to mutations at position 25 suggests that another critical residue remains unidentified. Here we report results of minimum perturbation mapping simulations at positions 25 and 33. These results suggest why fluorescent spectra may be insensitive to mutations at certain positions and suggest other promising positions for site-specific mutations. This work is supported in part by the W. M. Keck Foundation and GM 34847.

M-Pos181

FLUORIMETRIC CHARACTERIZATION OF TRP RESIDUES IN E. COLI SINGLE-STRANDED DNA-BINDING (SSB) PROTEIN AND ITS POLY(DT) COMPLEX((J.R. Casas-Finet)) Struct. Biochem. Prog., PRI/DynCorp, NCI-FCRDC, Frederick, MD 21702 (Spon. by J.R. Casas-Finet)

The steady-state contribution of the 4 Trp residues (at positions 40, 54, 88, and 135) of *E. coli* SSB to its fluorescence emission was elucidated by deconvolution of the spectral envelope of wild type (wt), singly (-W40F; -W54F; -W88F; -W135F) and doubly (-W88F+W135F) point mutated SSBs. Upon excitation at 297 nm, Trp 40, 54, 88 and 135 peaked at 342, 347, 344, and 352 nm, resp., and accounted for 22, 43, 24, and 11%, of the SSB integrated emission. Extensive Tyr to Trp energy transfer at the singlet level was detected.

Upon binding poly(dT), the fluorescence peak of all SSBs containing Trp 135 was red-shifted by 3 nm and their emission linewidth broadened by *ca.* 4% whereas for SSBs lacking Trp 135 no spectral shift was observed but broadening was *ca.* 9%. In poly(dT) complexes, the limiting quenching (Q_{max}) at saturation (relative to the free protein) for the various SSB mutants was 93, 90, 89, 88, 85 and 79% for -W88F+W135F, -W135F, wt, -W88F, -W40F, and -W54F, resp. From these Q_{max} values, and the steady state contribution of individual Trp to the fluorescence emission of free SSB, the calculated individual fluorophore Q_{max} were 92, 95, 81, and 59% for Trp residues 40, 54, 88 and 135, resp. Note that Trp 40 and 54, which were shown by ODMR spectroscopy to be the only two Trp residues involved in stacking interactions with nucleic acid bases in SSB/polynucleotide complexes, exhibited the largest quenching. Trp 40, 54, 88 and 135 account for 14, 18, 33 and 36% of the total emission in wt SSB/poly(dT) complex. The dominance of the red-emitting Trp 135 in the fluorescence emission of SSB/poly(dT) complexes accounts for the observed red-shift in systems containing this residue.

Global analysis of fluorescence lifetime experiments in the frequency domain showed that Trp 54 has the longest average lifetime (8.0 ns). The long lifetime of Trp 54 appears to be due to its particular microenvironment, since the average lifetime for all individual Trp were in the 2-4 nm range in 8 M urea.

M-Pos182

SPECTROSCOPIC STUDIES OF THE INTERACTION OF NEVIRAPINE WITH HIV-1 REVERSE TRANSCRIPTASE.((C.A. Grygon, R.C. Cousins, D.J. Greenwood, R. H. Ingraham, T.C. Warren, P. McGoff, and J. Stevenson)) Boehringer Ingelheim Pharmaceuticals Inc., Ridgefield, CT 06877-0368. (Spon. by C.A. Grygon)

Binding of a series of non-nucleoside dipyridodiazepinone inhibitors (including nevirapine) to recombinant HIV-1 reverse transcriptase (RT) has been found to affect the interaction between the enzyme and synthetic template-primer nucleic acids. The emission intensity of a fluorescently labelled RT-poly(rA)-$pd(T)_{12-18}$ complex was altered in the presence of nevirapine. These spectroscopic changes were used to calculate dissociation constants for several of these inhibitors which correlated well with IC_{50} determinations. Some of these compounds also produced changes in the intrinsic tryptophan fluorescence of the protein upon binding, providing evidence that the non-nucleoside inhibitors induce a conformational change on the enzyme. Similar spectroscopic changes were not observed for nevirapine binding to a site-directed mutant of HIV-1 RT (amino acid change at position 181). The secondary stucture content of RT has been evaluated by circular dichroism spectroscopy using the variable selection algorithm of Johnson (P. Manavalan and W.C. Johnson, 1987, *Anal. Biochem.* **167**, 76). The calculated secondary structure elements are 37% α-helix, 26% β-sheet, 15% β-turn, and 22% other. Binding of nevirapine does not alter the secondary structure of the protein. These results will be presented in terms of a mechanism of action of this class of potential therapeutic agents for AIDS.

M-Pos183

FLUORESCENCE SPECTROSCOPIC AND KINETIC STUDIES OF TRYPTOPHAN MUTANT LUCIFERASES.

((Zhi Li and Edward A. Meighen)). Department of Biochemistry, McGill University, 3655 Drummond Street, Montreal, PQ H3G 1Y6 Canada.

Purified tryptophan-mutant luciferases from luminescent bacterium *Xenorhabus luminescens* are investigated for the role of the individual tryptophan residues in the interactions with substrates, flavin and long-chain aldehydes. While all the Trp mutants are functionally active, mutations of Tryptophans 40, 194 or 250 in the α subunit significantly alter the kinetic properties, indicating the possible involvements of these residues in the binding of substrates. Preliminary steady-state fluorescence and low-temperature phosphorescence studies show that mutations of the individual tryptophan residues cause unique changes in the emission spectra. Differing interactions with flavin mononucleotide, fatty acid and fluorescence dyes found with each mutant also provide useful structural information in terms of location of each tryptophan residues. Tryptophan mutations in the β subunit result in a considerable increase of the tyrosine phosphorescence intensity, suggesting that the two subunits have rather independent electronic processes which are not affected by the those occurring in the α subunit. Supported by a grant from the Medical Research Council of Canada.

M-Pos184

PROBING METAL-INDUCED CONFORMATIONAL CHANGES IN CALBINDIN D9K: TIME-RESOLVED FLUORESCENCE STUDIES. ((T.E.S. Dahms[1,2], S. Linse[3], H. Thulin[3], S. Forsen[3], and A.G. Szabo[1])) [1]Institute of Biological Sciences, National Research Council, Ottawa, Ontario, Canada, K1A 0R6. [2]Graduate Student, University of Ottawa. [3]Physical Chemistry 2, University of Lund P.O.B. 124, S-221 00 Lund, Sweden.

Calbindin D9k (bovine) belongs to the highly homologous superfamily of calcium regulatory proteins, which are characterized by an EF-hand calcium binding site (helix-loop-helix motif). This calcium binding protein contains a single tyrosine but no tryptophyl residues. NMR studies suggest that the hydroxyl proton of the Tyr13 and the carboxylate of Glu35 are hydrogen bonded.

The recombinant protein was purified by HPLC. The tyrosyl fluorescence decay of the calcium-loaded (holo) Calbindin D9k is best described by three decay times. This suggests that Tyr13 exists in at least three different conformational states. Treatment with EDTA has only a small effect on the decay time values but the relative proportions change significantly. Apo protein, prepared by an alternate method involving TCA precipitation, resulted in a large change in the longest decay time. However, the pre-exponential terms were essentially identical to those of the holo form.

Decay-associated excitation spectra, giving information on the hydrogen bonding of the phenolic hydroxyl group, will be presented.

M-Pos185

FLUORESCENCE DECAY KINETICS OF A TRYPTOPHYL RESIDUE IN A PROTEIN CRYSTAL

T.E.S. Dahms[1,2], K.J. Willis[1], and A.G. Szabo[1].
[1]Institute for Biological Sciences, National Research Council, Ottawa, Ont., Canada, K1A 0R6.
[2]Graduate Student, University of Ottawa.

Erabutoxin b, a short chain neurotoxin from *Lacticauda semifaciata* contains a single tryptophan residue and the crystal structure has been determined to 1.4A. The protein was purified by HPLC and its identity and purity were confirmed by electro-spray ionization mass spectrometry. Single crystals of the purified protein were grown and were shown to diffract X-rays well. In this paper we present the first time-resolved fluorescence measurements of a (non-heme) single protein crystal. Multi-exponential fluorescence decay kinetics were observed in which the decay times were distinct from the solution values. The proportion of each decay time was found to be dependent on the orientation of the crystal with respect to the laser beam. This provides direct evidence for the rotomer model of tryptophan photophysics.

M-Pos186

INFLUENCE OF HYDRODYNAMIC SHEAR ON THE TRYPTOPHAN TRIPLET LIFETIMES OF PROTEINS IN SOLUTION. **((Li Sun, Chong Yi and William C. Galley)) Department of Chemistry, McGill University, Montreal, PQ H3A 2K6 Canada.**

The long-lived phosphorescence observed with many globular proteins in solution at room temperature derives from tryptophan residues buried within relatively inflexible structural domains. Even in the absence of the diffusional quenching due to dissolved O_2, the triplet lifetimes vary with the local viscosity over orders of magnitude; as has been observed for the triplet lifetimes of aromatic chromophores in solution. It has been proposed (Galley, 1988) that a direct effect of local dynamics on the chromophore occurs through fluctuating perturbations to the Franck-Condon factors involved in the non-radiative decay. These perturbations are considered to result from "diffusional-type" motions of the chromophore relative to its local environment. We have sought to test this hypotheses from the influence on the tryptophan phosphorescence of fluctuating structural perturbations induced in proteins at a constant temperature. In a preliminary study the effect of hydrodynamic shear is utilized to produce the dynamic structural perturbation. In the absence of dissolved O_2 a shear rate dependent decrease in the triplet lifetime of the single tryptophan in HSA in viscous solution is described.

Galley, W.C., 3rd Chemical Congress of North America, Toronto, June 1988.

M-Pos187

Metal Binding Studies of E. coli Glutamine Synthetase as Followed by Lanthanide Luminescence Spectroscopy

L. P. Reynaldo, Wm. DeW. Horrocks Jr., J. J. Villafranca.
Department of Chemistry, Penn State University, University Park, PA 16802

E. coli glutamine synthetase (GS) catalyzes the ATP dependent conversion of glutamate to glutamine. The two metal binding sites were studied as a function of the enzyme's regulatory state induced by post-translational adenylylation of Y397. Curve fitting of the asymmetric Eu^{3+} $^7F_0 \rightarrow {}^5D_0$ excitation spectra of fully adenylylated (E_{12}) and de-adenylylated (E_0) Eu-GS at 2.0 eq can be resolved into two peaks, 579.13nm, 579.20nm for E_0 and 579.11nm, 579.18nm for E_{12}. Analysis of the emission decay of Eu-GS at 2.0 eq in D_2O reveals the presence of two lifetimes for both E_0 (1.5ms, 2.2ms) and E_{12} (1.7ms, 2.3ms). The time-resolved emission spectra of E_0 also produces a 1.5ms (red-shifted) and 2.2ms (blue-shifted) component. Using the individual peak intensities and emission decay component intensities at t=0, the individual binding site isotherms were produced. Fitting these isotherms to a simple 2-site metal binding model, equilibrium binding constants were determined for E_0 (7.7μM and 5μM) and E_{12} (7.5μM and 12μM). Previous substrate binding studies and correlation of the peak transition energies to the relative ligand charges allow us to conclude that the weaker metal ion binding site, responsible for ATP binding and activation is markedly affected by this regulatory change.

This work is supported by NIH grant GM23599 and GM23529.

M-Pos188

EVIDENCE FOR TWO TRIPLET STATES OF TRYPTOPHAN IN PROTEINS. ((K. Sudhakar[1], W.W. Wright[1], J.M. Vanderkooi[1], S.A. Williams[2] and C.M. Phillips[2])), [1]Dept. of Biochem. & Biophys., School of Medicine, [2]Regional Laser & Biotech. Lab, Dept. of Chem., Univ. of Pennsylvania, Philadelphia, PA 19104.(Spon. by J.M. Vanderkooi).

The quantum yield of fluorescence and phosphorescence of trp in proteins is not unity. In order to examine this excited singlet and triplet states of the single trp in cod parvalbumin type III were examined in the time scale of subnanosecond to millisecond at 25° C, pH 7.00 in 0.01 M tris and 0.1 M NaCl. The fluorescence decay of trp is biexponential in both Ca(II) bound and Ca(II) depleted parvalbumin. The decay of anisotropy for Ca(II) bound and depleted forms could be approximated with a single exponential but the decay of the Ca(II) depleted form was faster, this, along with a red shift in fluorescence maximum indicates that buried trp in the Ca bound parvalbumin becomes exposed upon Ca removal. Triplet absorption and emission spectra revealed one short lived (T_1) and one long lived (T_2) species. Both species showed approximately the same transient absorption and emission spectrum and the kinetics reveal that T_1 is not the precursor of T_2. This is the first time that a short lived triplet state species of trp has been identified in a protein. The T_1 species both in Ca bound and Ca-free parvalbumin decay with a lifetime of ~30 nsec. Where as the T_2 species decays exponentially with a lifetime of 5 msec with Ca and a fast non-exponential decay is seen for Ca free parvalbumin. (Supported by NIH GM34448).

M-Pos189

PH DEPENDENCE OF TIME-RESOLVED ROOM-TEMPERATURE PHOSPHORESCENCE OF APO AND METALLOAZURINS

((John E. Hansen, Duncan G. Steel, and Ari Gafni)) Institue of Gerontology, University of Michigan, Ann Arbor, Michigan 48109 (Spon. by Robert Zand)

The blue copper protein azurin from the bacterial species Pseudomonas aeruginosa (azurin Pae), contains a single tryptophanyl residue buried and constrained in a β-barrel structure. The fluorescence spectrum of the apo-protein is strongly blue shifted (maximum at 308 nm) and the corresponding fluorescence decay is well fit by a single-exponential function. In contrast, azurin shows a typical phosphorescence spectrum though the decay can not be fit by a monoexponential function. Rather, the decay is fit to a sum of three exponentials - two major components with 417 and 592 ms lifetimes and a minor component with a 98 ms lifetime. The weights of the two major components, α_1 and α_2, vary with pH. Decays collected as a function of pH were fit simultaneously by linking together the lifetimes. The global fit had a χ^2 of 1.28. Plotting $\alpha_2 / (\alpha_1 + \alpha_2)$ against pH generates a titration curve with a pK of 5.7 ± 0.1. This pK corresponds closely to that of his-35, which has previously been proposed to act as a pH induced switch between active and inactive conformations of the native protein. Similar pH-dependent phosphorescence decays were obtained for several metalloazurins (Zn(II), Cd(II), Hg(II)) but not for Ag(I). In Ag(I) azurin the metal cation may bind too tightly to one of the ligands so that the pH induced conformational change is inhibited. This study demonstrates that new information is obtained from time-resolved phosphorescence and complements fluorescence studies. Funded by ONR and NIA Grant # AG09761

M-Pos190

EVIDENCE FOR A PHOSPHORESCENCE LIFETIME DISTRIBUTION IN ALCOHOL DEHYDROGENASE

((Joseph A. Schauerte, Bruce D. Schlyer, Duncan G. Steel & Ari Gafni))
Institute of Gerontology, University of Michigan, Ann Arbor, Michigan

The single phosphorescent tryptophan-314 residue of apo-horse liver alcohol dehydrogenase (LADH) shows non-monoexponential phosphorescence decay behavior with a mean lifetime of approximately 650msec. This phosphorescence decay was fit either to discrete components, or to a distribution of decays. The results show that the decay was best described by a phosphorescence lifetime distribution. LADH from Boehringer-Mannheim was shown to be pure EE isozyme with no significant subfractions (<5%) by the criteria of PolyAcrylamide Gel Electrophoresis and Isoelectric Focusing. Since the phosphorescence lifetime of a tryptophan residue is related to the local viscosity around this residue (Strambini & Gonnelli, Chem. Phys. Lett. 115,196. 1985), the non-monoexponential decay behavior implies that the tryptophan residue of apo LADH is best described as existing in at least two states of different local viscosity, which are not equilibrated in the time frame of the phosphorescence decay. The existence of a ground state distribution is suggested by the observation that the phosphorescence lifetime is excitation wavelength dependent. Additionally, the binding of the coenzyme analogue adenosine diphosphoribose (ADPR) increases the phosphorescence lifetime to 1.2 seconds and reduces the relative width of the lifetime distribution, suggesting that the apo- to holo-LADH conformation change is associated with structural tightening and either a reduction in the number of states, their distribution, or the equilibration kinetics between the states of the LADH/ADPR complex.

Supported by NIA grant #AG09761 and by ONR.

M-Pos191

TRIPLET STATE ENERGY TRANSFER FROM TRP109 TO BOUND TERBIUM IN E. COLI ALKALINE PHOSPHATASE.

((Bruce D. Schlyer, Duncan G. Steel, Ari Gafni)) Institute of Gerontology, University of Michigan, Ann Arbor, MI 48109.

The addition of one or more equivalents of Tb^{+3} to metal-depleted *E. coli* alkaline phosphatase (AP) results in Tb^{+3} luminescence (488, 544 nm) with a Trp-like excitation profile. This emission is not observed in control experiments performed under similar conditions (280 nm excitation) using either Tb^{+3} alone or Tb^{+3} plus holo-AP and therefore arises form enzyme-bound Tb^{+3}. The complexed Tb^{+3} luminescence increases 3- to 4-fold with sample deoxygenation. A sub-millisecond component exhibiting a negative prefactor was observed at 544 nm using near-UV excitation, with or without dissolved oxygen. The decay kinetics of bound Tb^{+3} directly excited at 488 nm shows that the sub-millisecond component is the Tb^{+3} radiative decay time. The results of the steady-state and time-resolved experiments suggest that the time evolution of Tb^{+3} (bound to AP) emission is determined by energy transfer from the triplet state of Trp to Tb^{+3} and Tb^{+3} decay. This model is based on the observations that 1) the Trp phosphorescence lifetime (previously determined to be due to Trp109) corresponds to the longer component of the Tb^{+3} emission and 2) the long time emission is enhanced as is the Trp109 phosphorescence by deoxygenation. (Supported by NIA grant AG09761 and by ONR).

M-Pos192

LUMINESCENCE STUDIES WITH *trp* REPRESSOR AND ITS SINGLE TRYPTOPHAN MUTANTS.

((M.R. Eftink, G.D. Ramsay)) University of Mississippi, University, MS 38677, ((L. Burns and A.H Maki)) University of California, Davis, CA 95616, and ((C.A. Ghiron)) Univeristy of Missouri, Columbia, MO 65201.

Time-resolved and steady-state fluorescence, low temperature phosphorescence, and optically detected magnetic resonance (ODMR) measurements have been made to resolve the luminescence contributions of the two intrinsic tryptophan residues in the subunits of *trp* repressor from *E. coli*. Phosphorescence studies show a clear resolution of 0-0 vibronic transitions for each type of trp residue, with maxima at 407 nm and 415 nm. Measurements with the single tryptophan mutants, W19F and W99F, enable the assignment of the 407 and 415 nm transitions to Trp-19 and Trp-99, respectively. Solute fluorescence quenching of the mutants with acrylamide and iodide show Trp-99 to be more solvent exposed, a result that is consistent with the crystal structure. The fluorescence decay of both individual trp residues is non-exponential, with the bluer emitting Trp-19 having a larger average decay time. Anisotropy decay measurements show a significant degree of rotational freedom of Trp-99, but show Trp-19 to depolarize primarily by global rotation of the protein. The existence of resonance energy transfer from Trp-19 to Trp-99 is indicated by three types of data: comparison of the fluorescence quantum yield of the wild type and mutant proteins; comparison of the long-lived decay time (attributed to Trp-19) in the absence (mutant) and presence (wild type) of the acceptor (Trp-99); and observation of unequal intensities of the 407 and 415 nm phosphorescence peaks. Additionally we will present studies of intramolecular quenching of the intrinsic trp residues by energy (or electron exchange) transfer to ligands bound to the tryptophan binding site. This research is supported by NSF grant DMB 91-06377.

NEW PROTEIN STRUCTURES

M-Pos193

CRYSTALLIZATION AND PRELIMINARY X-RAY DIFFRACTION ANALYSIS OF RED CELL FERRITIN L SUBUNIT

((J. Trikha*, G. Waldo , E. C. Theil P. C. Weber# & N. M. Allewell*)) *Department of Biochem., University of Minnesota, St Paul, MN 55108; Department of Biochem., North Carolina State University, Raleigh, NC 27695; #Dupont-Merck Pharmaceutical Company, Dupont Experimental Station, Wilmington, DE 19880.

Expression of red cell specific ferritin L-subunit is regulated in a developmentally specific fashion. Native bullfrog red cell ferritin and a genetically engineered mutant with altered iron transport properties have been cloned and overexpressed in *E. coli* . The sequence of bullfrog L-subunit combines features common to both H- and L-subunits of mammalian ferritins; the rate of iron uptake is similiar to that of mammalian L-subunits. The determination of the three-dimensional structure will make it possible to investigate the relationship between structure and mineralization rate.

Crystals that diffract to atleast 1.9 Å, have been obtained in the presence of both $MnCl_2$ and $MgCl_2$. Both wild type and mutant proteins form body-centered tetragonal crystals. The wild type and mutant have unit cell dimensions of a=b=128.4Å and c=181.0Å and a=b=128.6Å and c=181.7Å respectively in the presence of $MnCl_2$. Unit cell dimensions of wild type in $MgCl_2$ are a=b=129.1Å and c=182.3Å. The R factor between wild type and mutant protein in the presence of $MnCl_2$ is 31% and for wild type protein in the presence of $MnCl_2$ and $MgCl_2$ 10%.

The three subunits in the asymmetric unit, are related by a non-crystallographic 3-fold symmetry (as determined by the self rotation function) indicating that the ferritin molecule has 432 symmetry.

M-Pos194

CRYSTALLIZATION AND PRELIMINARY CHARACTERIZATION OF HUMAN ENDOTHELIN.

((Diane H. Peapus[1,2], Robert W. Janes[1], and B. A. Wallace[1]))[1]Dept. of Crystallography, Birkbeck College, University of London, London, UK and [2]Dept. of Chemistry and Center for Biophysics, Rensselaer Polytechnic Institute, Troy, NY, USA.

Endothelin is a highly potent, ubiquitous, endogenous 21 amino acid polypeptide which is secreted from the endothelium into the blood vessels as a pre-pro form; it interacts with receptors throughout the vascular, cardiac, renal and respiratory systems to cause vaso- and bronchoconstriction. Crystals of the active, uncomplexed form of human endothelin (h-ET), which are of a suitable size for X-ray diffraction analysis, have been grown from aqueous solutions. These crystals are long hexagonal prisms, and are apparently of space group $P222_1$ with cell dimensions a=33.45A, b=59.89A, c=59.61A.

Small crystals, grown in microbatch, appear after 2-3 days and reach maximum growth of 0.75 x 0.05 x 0.05mm by 2 weeks. After this time, secondary nucleation on the crystal surface occurs. A 2.9 A data set consisting of 8336 independent observations of 2567 unique reflections in 91 degrees of data (97% complete) was collected with an image plate using CuK_α radiation. The unit cell is consistent with precession photographs. Strong pseudo 6-fold symmetry is observed in the data, as suggested by the crystal morphology, as is strong pseudo-centering, and this is being investigated. (Supported by British Heart Foundation Grant 91/86, and a gift from Bristol-Myers Squibb)

M-Pos195

CRYSTALLIZATION AND PRELIMINARY STRUCTURAL ANALYSIS OF THE REPLICATION TERMINATOR PROTEIN OF *BACILLUS SUBTILIS*.

((Dirksen Eli Bussiere§*, Prashant P. Mehta§, David W. Hoffman§, Deepak Bastia§*, and Stephen W. White§*)) §Department of Microbiology and *The Program in Cell and Molecular Biology, Duke University Medical Center, Durham, North Carolina 27710. (Spon. by D.E. Bussiere)

DNA replication can be separated biochemically and physiologically into three distinct steps: initiation, elongation, and termination. While in some chromosomes, such as those of SV40 and phage λ, there is no defined replication terminus, most prokaryotic chromosomes have fixed terminus sites. In several systems, it has been shown that termination is mediated by site-specific DNA-binding proteins known as terminator proteins. Such a protein has been identified in *Bacillus subtilis* and is known as the Replication Terminator Protein (RTP). RTP is a dimeric molecule that binds specific sequences within the replication terminus of the *Bacillus subtilis* chromosome and prevents the passage of replication forks; an RTP monomer contains 122 amino acids and has a molecular mass of 14,500 daltons. The gene for RTP has been expressed in *Escherichia coli* and the protein has been purified in amounts sufficient for structural studies by Nuclear Magnetic Resonance (NMR) and X-ray crystallography. One-dimensional NMR experiments show that the protein has a well-folded, compact tertiary structure, as well as a high α-helical content. Circular dichroism (CD) studies confirm this finding and show that approximately 32% of the protein is α-helical. RTP has been crystallized as monoclinic plates that diffract to better than 2.6 Å. Precession photographs show the space group to be C2 with unit cell dimensions a=76.7 Å, b=52.7 Å, c=70.4 Å, and β=89.8°, with two molecules occupying the asymmetric unit. Several native data sets have been collected and merged to give a native data set 100% complete to 2.6 Å. Three potential heavy atom derivatives have been identified for use in the multiple isomorphous replacement strategy, and derivative data sets have been collected. To facilitate producing co-crystals of an RTP-DNA complex, gel-shift assays were performed to establish the shortest sequence of DNA required for tight binding of DNA to RTP. These show that two turns (approximately 18 to 20 base pairs) of DNA are required, centered on an 8-base pair consensus sequence, to elicit relatively stable binding.

M-Pos196

NON-BONDED INTERACTIONS IN ALCOHOL DEHYDROGENASE-BOUND β-METHYLENE SELENAZOLE-4-CARBOXAMIDE ADENINE DINUCLEOTIDE. ((H. Li, W. H. Hallows, J. S. Punzi, V. E. Marquez and B. M. Goldstein)) Dept. of Biophysics, University of Rochester Medical Center, Rochester, NY 14642 and LNC, NCI, NIH, Bethesda MD 20892.

The crystal structure of a binary complex between horse liver alcohol dehydrogenase and the NAD analogue β-methylene selenazole-4-carboxamide adenine dinucleotide (β-SAD, below) has been determined from a 2.7Å data set. The orthorhombic structure has been refined to 18%. β-SAD is the phosphodiesterase-resistant analogue of SAD. SAD is the active anabolite of the antitumor agent selenazofurin. Crystal structures, computational studies and database surveys of selenazofurin and its analogues indicate the presence of an attractive non-bonded intramolecular selenium-oxygen interaction of sufficient magnitude to constrain rotation about the C-glycosidic bond. The conformation of the bound ligand in the complex appears to maintain this interaction. The implications of this constraint will be discussed. (Supported by NIH grant CA45145.)

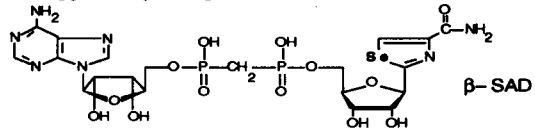

M-Pos197

STRUCTURAL STUDIES ON ISOLATED COMPONENTS OF THE PROKARYOTIC RIBOSOME: RIBOSOMAL PROTEINS S17 AND L6. ((Barbara L. Golden[1], David W. Hoffman[1], Venkatraman Ramakrishnan[2] and Stephen W. White[1]))
[1]Duke University Medical Center, Durham, NC 27710 and
[2]Brookhaven National Laboratories, Upton, NY 11973

The universal site of protein biosynthesis, or translation, is the ribosome, a large particle made up of many small proteins and several large RNA molecules. A fundamental understanding of the process of translation will ultimately require a model of the ribosome at atomic resolution. To this end, our laboratory is currently investigating the structure of isolated components of the prokaryotic ribosome. In order to facilitate structural studies, we have recently cloned and over-expressed the genes for several ribosomal proteins from the thermostable bacterium *Bacillus stearothermophilus*. The structures of two proteins, S17 and L6 will be presented.

Ribosomal protein S17 is a 16S RNA-binding protein which plays a role in ribosome assembly in *Escherichia coli*. The secondary structure of S17 is being determined using two-dimensional NMR spectroscopy. Assignments of the protein are mostly complete and these suggest that the majority of the secondary structure is β-sheet. Ribosomal protein L6 is protein of the large subunit that is thought to play a role in translational fidelity.The crystal structure of L6 has been solved at 2.8Å . The structure of this protein, like the other ribosomal proteins solved to date, contains an exposed, antiparallel β-sheet. The structures of these two protein will be discussed in the context of the evolution of ribonucleoprotein particles and their RNA binding properties.

M-Pos198

STRUCTURAL STUDIES OF *B. STEAROTHERMOPHILUS* TRYPTOPHANYL-tRNA SYNTHETASE. ((S.Doublié, C.W.Carter, Jr.)) Dept. of Biochemistry and Biophysics, CB 7260 University of North Carolina at Chapel Hill 27599-7260.

Tryptophanyl-tRNA synthetase (TrpRS; 327 residues) is the smallest of the twenty aminoacyl-tRNA synthetases responsible for translating the genetic code. Like GlnRS, TyrRS, and MetRS, TrpRS is a type I enzyme. Crystals of TrpRS complexed with product analog tryptophanyl-ATP diffract to 1.7Å. Two separate 3.0 Å phase sets are in hand, one involving non-isomorphous double derivatives, the other making use of engineered TrpRS for which all 10 methionines were substituted by selenomethionine. Initial phases came from non-isomorphous gold and gold+mercury derivatives. Non-isomorphism was partially overcome by maximum entropy solvent flattening, phase permutation, and likelihood ranking (MICE; Xiang, et al., *Acta Cryst.* D:1 (1993) in press), permitting 9 Selenium positions to be found in a difference Fourier calculated using these improved phases. These sites were later confirmed using SIR phases from a trimethyllead acetate derivative, which is the only heavy metal for which binding to the protein did not induce loss of isomorphism. Phases were calculated using the selenomethionyl, lead and gold-mercury derivatives with the program MLPHARE. Because of its true isomorphism and the 9 fully substituted sites, selenomethionyl TrpRS turned out to be a very good derivative. The resultant electron density map shows very clear definition of the solvent boundary and extensive secondary structures, both helices and β-sheets. Interpretation is facilitated by the known methionine positions. MICE is currently being used to improve and extend both phase sets, providing the first successful use of maximum entropy methods in phasing an unknown protein structure. Supported by NIGMS RO1-26203

M-Pos199

ANTIBODY STRUCTURE STUDIES WITH MELANOMA-ASSOCIATED GD2 GANGLIOSIDE. **((S. L. Pichla, R. Murali, M. Kordowicz and R. M. Burnett)) The Wistar Institute, Philadelphia, PA 19104, and E. Merck, Darmstadt, Germany.**

Malignant Melanoma cells differ from normal melanocytes in the abundance of the gangliosides on their cell surfaces. GD2 ganglioside is highly expressed on melanoma cells (J. Thurin *et al.*, Cancer Res. 47, 1229-1233, 1987) and is involved in cell-cell signaling or cell-substrate interactions regulating cell growth. Monoclonal antibody ME36.1 binds to GD2 and shows potential for immunotherapy (D. Ollopoulos *et al.*, J. Natl. Cancer Inst. 81, 440-441, 1989). Tumor cell-surface carbohydrates have been used as markers for disease and targets for immunotherapy but more effective treatments will depend on a complete understanding of antibody-carbohydrate interactions.

Highly purified Fab fragments from MAb ME36.1 crystallize in space group $P2_1$ (a=37.9, b=94.0, c=67.6, β=101.0). The crystals diffract to 2.5 Å resolution and a complete data set has been collected to 2.8 Å. Structure determination is proceeding using an initial set of phases determined with XPLOR (Brunger A. T., 1992, Version 3.0) using Fluorescein-Fab (4-4-20) as the starting model (J. N. Herron *et al.*, Proteins 5, 271-280, 1989).

Crystallization attempts with the Fab-GD2 complex depended on obtaining a soluble antigen from the scarce glycolipid. GD1b ganglioside was digested with β-galactosidase to give 1 mg of GD2 (M. K.), which was digested with ceramide glycanase to cleave the ceramide group from the sugar and give a soluble carbohydrate form (Li *et al.*, Meth. Enzym. 179, 479-487, 1989). Small co-crystals of the complex have been obtained. Progress on the structure determinations of the native Fab and the Fab-GD2 complex will be reported.

M-Pos200

STRUCTURE OF FIBRINOGEN BY COORDINATED X-RAY CRYSTALLOGRAPHY AND CRYO-ELECTRON MICROSCOPY. ((P. Walian, S. Rao and C. Cohen)) Rosenstiel Research Center, Brandeis University, Waltham, MA 02254.

The centric projection of the $P2_1$ crystal form of a protease-modified fibrinogen has been determined to 18 Å resolution (Rao et al. (1991) J. Mol. Biol. 222, 89-98). This density map was obtained by combining X-ray amplitudes with phases from ice-embedded specimens. Using simulation methods, the general run of the molecular filaments and the possible disposition of domains were established. In order to extend this approach to three dimensions and to higher resolution, a number of views of the crystal are being collected and processed. Phases are being refined and extended using an iterative solvent leveling method. The use of solvent leveling in this case is especially powerful since the unit cell contains about 70% solvent. At a sterting resolution of 40 Å, about 60% of the reflections have been phased; most of these are centric. After extension to 18 Å, where 25% of the reflections are image-based, about 60% of the data sets have been phased with a figure of merit of 80 or better. Our immediate goal is a map at 10 Å. In certain directions the X-ray data extend to about 3.5 Å, and images of several views show diffraction to almost this resolution. This approach therefore has the potential to provide a 6 Å map of the molecular filaments where elements of secondary structure can be identified. Supported by a grant from the NIH. P.W. is the Howard Sprague Fellow of the AHA, Massachusetts Affiliate.

M-Pos201

PHOSPHOLIPID COMPOSITION DEPENDENT IMMISCIBILITIES IN THE CRITICAL ACTIVATION OF EXTRACELLULAR PHOSPHOLIPASE A_2.

((W.R.Burack, Qiang Yuan, and R.L.Biltonen)) Department of Pharmacology, Univ. of Virginia, Charlottesville,VA 22908. (Spon. by C. Creutz)

PLA_2 activity on large unilamellar zwitterionic vesicles is characterized by a long lag phase followed by rapid hydrolysis. The rapid activation has been hypothesized to depend on membrane structure which changes abruptly at some critical mole fraction of reaction products. The structural transition may be compositionally driven gel/gel or gel/liquid immiscibilities. The relationship between the rapid activation of PLA_2 and critical changes in membrane structure was investigated by simultaneously measuring product accumulation and the fluorescence of membrane probes which are sensitive to phospholipid structure and dynamics. The fluorescence of trans-parinaric acid, a fatty acid, is sensitive to the phase of the lipid. In the liquid state, the fluorescence increases abruptly prior to, or concomitant with, the onset of rapid hydrolysis. Using t-parinaric acid fluorescence, a liquidus line on a partial phase diagram for ternary codispersions of substrate and products (dipalmitoyl-phosphatidylcholine and 1:1 mono-palmitoyl-phosphatidylcholine:palmitic acid) was confirmed. These data imply that the rapid activation of PLA_2 on liquid state vesicles is coupled to the formation of gel domains enriched in reaction products. In the gel state, pyrenyl-dodecanoate was used to monitor membrane structure. This probe's emission properties also changed prior to the rapid activation. The fluorescence change is further correlated with a gel/gel immiscibility of reaction products and substrate. (Supported by NIH and NSF).

M-Pos202

THE EFFECT OF THE LOCAL ANESTHETIC DIBUCAINE ON PHOSPHOLIPASE A_2-CATALYZED HYDROLYSIS OF MONODISPERSE AND VESICULAR PHOSPHATIDYLCHOLINES

((Brian K. Lathrop, Deborah L. Stokes, and Rodney L. Biltonen)) Department of Pharmacology, University of Virginia, Charlottesville, VA 22908.

PLA_2-catalyzed hydrolysis of large unilamellar vesicles of dipalmitoylphosphatidylcholine (DPPC LUV) is characterized by an initial lag of duration τ preceding maximal hydrolysis. The lag phase has been interpreted to be a reflection of a slow activation process on the membrane surface. The local anesthetic dibucaine (DBC) can alter τ but not the rate of hydrolysis of monodisperse dibutryoyl-phosphatidylcholine nor the maximal rate of hydrolysis of DPPC LUV. τ decreases then increases as a function of DBC concentration at 37°. Above the substrate T_m (42°), τ increases monotonically with DBC concentration, even at 47° where melting is almost complete. A minimum in τ as a function of temperature occurs near the T_m of the lipid. Under conditions where DBC lowers the T_m 1°, the minimum in τ as a function of temperature is lowered 3°. These results indicate that the effect of DBC on PLA_2 is a reflection of the anesthetic effect on the membrane substrate structure, but is not solely a reflection of DBC altering the fractional degree of melting. (Supported by a grant from the NIH.)

M-Pos203

HYDROLYSIS OF LYSOPHOSPHATIDYLCHOLINE BY PHOSPHOLIPASE A_2

((J.D. Bell, B.L. Baker, B.C. Blaxall, D.A. Reese and G.R. Smith)) Department of Zoology, Brigham Young University, Provo, UT 84602.

The rate of hydrolysis of phosphatidylcholine bilayers by phospholipase A_2 (PLA_2) is greatly enhanced by the presence of lysophosphatidylcholine (lyso) in the bilayer. To further understand the relationship of lyso to PLA_2 activity, the binding of lyso to PLA_2 from the venom of Agkistrodon piscivorus was examined by fluorescence spectroscopy. The tryptophan emission intensity of the enzyme was enhanced by about 50% upon addition of lyso. This increase in fluorescence intensity, however, was transient and the decay of such was accompanied by the formation of a precipitate (at 10 mM $CaCl_2$) and by the release of protons suggesting that the lyso was being hydrolyzed. The apparent hydrolysis required the presence of enzyme and calcium, and it was observed with several other PLA_2 purified from a variety of snake venom sources. The binding isotherm for lyso to the PLA_2 estimated from the initial fluorescence change was biphasic with a clear break in the curve occurring at the critical micelle concentration of the lyso. The apparent dissociation constant estimated from the isotherm was about 10^{-6} M. The value of K_m estimated from the rate of proton release was greater than 10^{-3} M suggesting that either the rate of catalysis is much greater than the rate of dissociation of the lyso from the PLA_2 or that multiple interactions of lyso with PLA_2 are occurring. The quantitative relationship between the hydrolysis of lyso and the interactions of PLA_2 with phospholipid bilayers is currently under investigation.

M-Pos204

ANNEXIN II AND LIPOCORTIN 85 BIND A LARGE NUMBER OF CALCIUM IONS UPON MEMBRANE ASSOCIATION.

((Tom Evans and Gary Nelsestuen)) Department of Biochemistry University of Minnesota, St. Paul, MN 55108

Annexin II and Lipocortin 85 show calcium-dependent binding to vesicles containing acidic phospholipids. The free proteins bind little calcium but are reported to bind 2-4 ions when phospholipid is present (reviewed in Klee, C. (1988) *Biochem* 27, 6645-6653). However, these proteins also aggregate vesicles which greatly complicates the determination of bound calcium ions by standard techniques such as the Hummel-Dreyer method and equilibrium dialysis. A new method was developed in which phenyl-Sepharose was coated with phospholipids. Protein was bound to this affinity gel in the presence of $^{45}Ca^{++}$. The gel prevented secondary aggregation. Unbound protein was washed from the column with buffer containing $^{45}Ca^{++}$. Bound protein was then eluted with the same buffer that contained excess EGTA. The Bradford assay was used to determine the amount of protein eluted from the column and bound $^{45}Ca^{++}$ was determined by the peak of excess $^{45}Ca^{++}$. A control determined the amount of calcium bound to the column with no protein present and was subtracted from the calcium bound in the presence of protein. The resulting calcium binding stoichiometry determined for Annexin II was 10 ± 2 at 50 μM Ca^{++} and 11 ± 1 at 12.5 μM Ca^{++}. Lipocortin 85 bound 12 ± 1 Ca^{++} at 12.5 μM Ca^{++} and 15 ± 1 Ca^{++} at 50 μM Ca^{++}. These large calcium stoichiometries are similar to those obtained for annexins V and VI (Bazzi, M., & Nelsestuen, G., (1991) *Biochem* 30, 971-979) and suggest a common feature of annexin-membrane-calcium interaction (supported by grant GM 38819 from NIH).

M-Pos205

CYTOCHROME B_5 BINDING AND INSERTION INTO POPC LUVS CONTAINING CHOLESTEROL.

((Kenneth M. P. Taylor and Mark A. Roseman)) Dept. of Biochemistry, USUHS, Bethesda, MD 20814.

We have previously shown that cholesterol inhibits cyt b_5 binding to 1-palmitoyl-2-oleoyl PC LUVs[1]. To further characterize this phenomenon, we have systematically studied cyt b_5 binding and insertion into POPC LUVs over the 0-50 mole percent range of cholesterol compositions. In direct binding mixtures containing saturating cyt b_5 levels and POPC LUVs, cholesterol reduces cyt b_5 binding by up to 60 fold. However, the reduction in binding is a complex function of cholesterol composition: The saturation binding curve appears triphasic, with a sharp decrease between 0-20% cholesterol, a plateau between 20-33%, and finally a linear decrease from 33-50%. Perhaps more significant is the finding that, while inhibiting cyt b_5 binding, cholesterol accelerates the rate at which bound cyt b_5 is converted from the "loose" to the "tight" configuration. The rate constant for tight insertion sharply rises from $k \approx 3 \times 10^{-3}$ hr^{-1} at 0% cholesterol, to a maximum of $k \approx 1 \times 10^{-1}$ hr^{-1} at 20-25%; further increase in cholesterol content causes a decrease in the tight insertion rate, which falls to near baseline at 50%. Our results can be explained in terms of the physico-chemical model for cholesterol-phospholipid interactions proposed by Presti *et al.*[2]. [Supported by USUHS Protocols C071AH and T071AO]

[1]Taylor, K. M. P. and Roseman, M. A. (1990) *Biophys. J.* 57, 476a.
[2]Presti, F. T. *et al.*, (1982) *Biochemistry*, 21, 3831-3835.

M-Pos206

THE EFFECT OF NATIVE AND MUTANT FORMS OF CYTOCHROME B5 ON THE ACYL CHAIN ORDER OF LIPID VESICLES AS QUANTITATED BY FTIR.

((Robert Doebler, A. W. Steggles* and Peter W. Holloway)) Dept. of Biochemistry, Univ. of Virginia Sch. Med., Charlottesville, VA. *Dept. of Biochemistry, North-eastern Ohio Univ. Coll. Med., Rootstown, OH.

Cytochrome b_5 binds spontaneously to lipid vesicles via a 43 amino acid membrane-binding domain and our previous studies have shown that each protein molecule removes 14 molecules of lipid from the co-operative phase transition. Fourier transform infrared spectroscopy (FTIR) has been used to quantitate the various acyl chain conformers in lipid bilayers (Casal and McElhaney, Biochemistry 29, 5423 (1990)) and here we apply this technique to native cytochrome b_5 and a mutant form where Trp residues at positions 108 and 112 have been replaced by Leu. Small unilamellar vesicles (SUV) and large unilamellar vesicles (LUV) were prepared in aqueous buffer from dimyristoyl-phosphatidylcholine by sonication and extrusion, respectively. The FTIR spectra between 1400-1300 cm^{-1} were curve fitted with four Lorentzian bands at 1378, 1367, 1353, and 1341 cm^{-1} and the last three bands, due to wagging modes of CH_2 in gauche-trans-gauche', double gauche ('gg'), and end gauche, were normalized to the 1378 band. The largest changes seen were in the 'gg' conformers. With SUV the native protein caused a small increase in 'gg' and the mutant a larger increase. With LUV the native caused a large decrease and the mutant a small decrease. These different responses are consistent with the known geometry of the vesicles and the larger bulk of the Trp in the native protein versus the Leu in the mutant. Supported by GM23858.

M-Pos207

A FLUORESCENCE STUDY OF A TEMPERATURE INDUCED CONVERSION FROM THE "LOOSE" TO THE "TIGHT" BINDING FORM OF MEMBRANE-BOUND CYTOCHROME B5. ((Alexey S. Ladokhin, A. W. Steggles* and Peter W. Holloway)) Dept. of Biochemistry, Univ. of Virginia Sch. Med., Charlottesville, VA. *Dept. of Biochemistry, Northeastern Ohio Univ. Coll. Med., Rootstown, OH. (Spon. R. P. Taylor)

Cytochrome b_5 is a liver integral membrane protein which has now been expressed in, and isolated from, E. coli. The structure-function relationships of the 43 amino acid membrane-binding domain (nonpolar peptide) have been examined in both native and mutant forms of the protein; in the latter, Trp residues at positions 106 and 112 were replaced by Leu. The temperature dependence of the fluorescence quantum yield of the Trp residues in the isolated membrane-binding domain was examined and showed an irreversible transition above 50°C when these domains, of either the native or the mutant protein, were bound to lipid vesicles. This transition leads to the conversion of the meta-stable, intermembrane-exchangeable ("loosely" bound), conformation to a final, virtually un-exchangeable ("tightly" bound) conformation. There was little change in either the degree of quenching of Trp fluorescence by brominated lipids or in the secondary structure, as evaluated by FTIR spectroscopy. Changes in the steady-state fluorescence observed with this transition and the formation of the "tightly" bound form are consistent with the transition being associated with a conversion from a looped back conformation to a bilayer-penetrating conformation, as the C-terminal segment of the nonpolar peptide passes across the bilayer, while Trp-109 remains in its original position. Supported by GM23858.

M-Pos208

^{2}H NMR STUDIES OF THE EFFECT OF PULMONARY SURFACTANT SP-C ON THE DPPC HEADGROUP. ((S. Taneva, G.A. Simatos, M. R. Morrow, K.M.W. Keough)) Depts. of Physics and Biochemistry and Discipline of Pediatrics, Memorial University of Newfoundland, St. John's, Newfoundland, CANADA A1B 3X7.

Pulmonary surfactant protein (SP-C) was isolated from porcine lung surfactant. Bilayers were prepared with 0, 8, 12, 17 and about 25% SP-C (w/w) in DPPC deuterated at the α and β positions of the choline (DPPC-d_4). ^{2}H NMR was used to examine the effect of SP-C on the lipid headgroup between 55°C and 15°C. In the liquid crystalline phase, the α splitting decreased with increasing protein concentration but was insensitive to temperature. The β splitting increased slightly with protein concentration and decreased with increasing temperature. Given the effect of protein concentration on the gel to liquid crystal transition temperature, and thus on bilayer fluidity at a given temperature, this observation is qualitatively consistent with an electrostatic interaction [MacDonald, Leisen & Marassi (1991) Biochemistry 30, 3558–3566] between the headgroup dipole and positive charges associated with the protein near the bilayer surface. The effect of the protein on the headgroup deuteron transverse relaxation time T_{2e} is qualitatively similar to that seen in the acyl chain region. (Supported by NSERC and MRC Canada. The authors thank Deneen Spracklin for assistance in data analysis.)

M-Pos209

ROLE OF THE DOUBLE-LAYER POTENTIAL IN Ca^{2+}-DEPENDENT BINDING OF PROTEIN KINASE C (PKC) TO THE MEMBRANE. ((Mosior, M. & Epand, R.M.)) Department of Biochemistry, McMaster University, Hamilton, Ontario, Canada L8N 3Z5

Binding of PKC to a phospholipid bilayer was measured by the sucrose loaded vesicle method. The measurements were conducted at high lipid/protein ratio with <1 protein per vesicle. When the surface potential of the membrane, produced by the anionic lipid PS, was kept constant, the bound/free protein ratio changed linearly with the Ca^{2+} concentration in the solution. This indicates that there is only one Ca^{2+} binding site on PKC which affects its binding to the membrane. The electrostatic potential was then changed by membrane-adsorbed metallic cations as well as by cationic drugs and lipids. The extent of the PKC binding to the membrane was correlated with the Ca^{2+} concentration at the interface, which in turn was determined by the exponential function of the electrostatic potential of the membrane. The Ca^{2+} concentration at the interface changed exponentially by two orders of magnitude when the mole% PS is raised from 0 to 40. Hence the accumulation of Ca^{2+} in the layer immediately adjacent to membrane accounts partially for the sigmoidal dependence of PKC binding to membrane on the mole% PS. The binding of PKC to the membrane in the absence of Ca^{2+} was not affected by the double-layer potential. The diacylglycerol-induced increase in PKC affinity toward the membrane was Ca^{2+} independent.

M-Pos210

INTERACTION OF α-LACTALBUMIN (α-LA) WITH NEUTRAL AND ANIONIC PHOSPHOLIPIDS. AN ELECTRON SPIN RESONANCE STUDY. ((Guillermo G. Montich and Derek Marsh)) Max-Planck-Institute für biophysicalische Chemie, Abteilung Spektroskopie, D 3400, Göttingen, Germany.

We have measured the ESR spectra of phospholipids spin-labelled at carbon 5 (5-SL) or at carbon 14 (14-SL) of the *sn*-2 chain in multilamellar vesicles of dioleoylphosphatidylcholine (DOPC), dioleoylphosphatidylglycerol (DOPG), dimyristoylphosphatidylcholine (DMPC), and dimyristoylphosphatidylglycerol (DMPG) in the presence of α-LA at 20 mM ionic strength and at different pHs. At pHs below the isoelectric point of the protein, the spectra from 5-SL showed a larger outer splitting in α-LA/DOPG and α-LA/DMPG complexes than in the pure lipid indicating a reduction in the chain mobility; the spectra from 14-SL in these complexes showed two components, one of them with reduction in the chain mobility. In the α-LA/DOPG complexes, a selective interaction of the protein with 5-PCSL, 5-PESL, 5-PGSL, 5-PASL or 5-PSSL was not observed at pH 4, but at pH 2 less selectivity of interaction with 5-PCSL was observed compared with the other 5-SLs. A reduction in the mobility of the 5-SL lipids was not observed in the presence of α-LA at pHs between 5 and 7 in DOPG dispersions, nor in DOPC between pH 2 and pH 7. The results indicate that α-LA penetrates the membrane in the partially denatured state at low pH, and this interaction is stronger with anionic phospholipids.

M-Pos211

EFFECT OF MONOLAYER SURFACE PRESSURE ON THE BINDING OF ANTI-N-ETHYL LYSINE IGG ANTIBODIES TO N-ETHYL PHOSPHATIDYLETHANOLAMINE. ((James R. Trudell and A. Seelig)) Stanford School of Medicine, Stanford, CA 94305-5123 and Biocenter of the University of Basel, CH-4056 Basel, Switzerland

Binding of anti-N-ethyl-RSA IgG antibodies to monolayers of 25% N-ethyl-1,2-dioleoyl-sn-glycero-3-phosphoethanolamine (N-ethyl-DOPE) and 75% 1-palmitoyl-2-oleoyl-sn-glycero-3-phosphocholine (POPC) was measured as a function of the initial surface pressure of the monolayer. The IgGs were injected into the subphase of monolayers with initial surface pressures ranging from 10 to 32 mN/m and binding was detected by an increase in surface pressure as the antibody bound to the N-ethyl-DOPE. In addition, fluorescence was measured in monolayers that were transported over successive compartments of a special annular ring Teflon trough so that the monolayer containing N-ethyl-DOPE was exposed to anti-N-ethyl-RSA IgGs, washed, exposed to a fluorescein-conjugated second antibody, washed, and then bound fluorescein was determined. Extrapolation to zero effect yielded cutoff pressures of 25 and 22 mN/m, respectively, much less than the bilayer equivalence pressure of 32 mN/m.

M-Pos212

PHOSPHORYLATION BY PROTEIN KINASE C REVERSES THE MEMBRANE ASSOCIATION OF PEPTIDES THAT MIMIC THE CALMODULIN-BINDING DOMAINS OF MARCKS AND NEUROMODULIN. ((J. Kim[1], P.J. Blackshear[2], J.D. Johnson[3], and S. McLaughlin[1])) 1. HSC, SUNY, Stony Brook NY 11794; 2. Howard Hughes Medical Institute, Duke University, Durham, NC 27710; 3. Ohio State University Medical Center, Columbus, OH 43210.

Neuromodulin and the MARCKS protein, which are probably tethered to the plasma membrane by their acyl chains, bind calmodulin (CaM) with high affinities ($K = 10^8$ and 10^9 M^{-1}) and could act as effective buffers to sequester much of the CaM in cells. Phosphorylation by protein kinase C (PKC) decreases the affinities of these proteins for CaM; thus they could produce spatially and temporally restricted increases in the free [CaM] in the cell and be important components of the calcium/phospholipid signalling pathway. The short calmodulin-binding domains of these proteins contain both clusters of basic residues and the serines that are phosphorylated by PKC. We measured the binding of peptides that mimic these domains to phospholipid vesicles containing acidic lipids such as PS or PG. Binding increases sigmoidally with the % acidic lipid in the membrane, as predicted from a Gouy-Chapman/mass action theory. The affinities of these peptides for phospholipid vesicles containing 20% acidic lipids are comparable to their affinities for CaM; phosphorylation of the MARCKS peptide by PKC rapidly reduces the membrane binding 100-fold. These experiments support the hypothesis that the CaM-binding domains of the native neuromodulin and MARCKS proteins can interact with the plasma membrane through a PKC-reversible electrostatic association of basic residues with acidic lipids.

M-Pos213

BINDING OF SMALL ACYLATED PEPTIDES AND FATTY ACIDS TO PHOSPHOLIPID VESICLES ((R.M. Peitzsch, H. Wu, and S. McLaughlin)) Dept. of Physiology and Biophysics, HSC, SUNY Stony Brook, Stony Brook, N.Y. 11794.

Myristoylation of an N-terminal glycine facilitates the binding of many intracellular proteins to the plasma membrane. To determine the myristoyl (Myr) chain's contribution to the binding energy, we measured the adsorption of saturated fatty acids (C_{10} - C_{16}) and small acylated peptides to phospholipid vesicles using zeta potential and equilibrium dialysis techniques. The anionic form of the fatty acids and the acylated glycines have identical binding energies. The binding energy changes by 0.86 kcal/mol per CH_2 group, in agreement with the hypothesis that the adsorption is driven by the hydrophobic effect (Tanford, C. *The Hydrophobic Effect*, 1973). The anionic forms of myristic acid, Myr-G, Myr-GA, and Myr-GAA all have dimensionless partition coefficients of 10^4, assuming they bind to a monolayer 20 Å thick. The binding energy is essentially independent of membrane composition (phosphatidylcholine in combination with phosphatidylethanolamine, sphingomyelin, or cholesterol,). If the results we obtained with these acylated peptides can be extrapolated to proteins, a myristoyl chain provides barely enough energy to bind the protein to the plasma membrane of a cell with a typical surface area/volume ratio.

M-Pos214

CALCULATIONS OF ELECTROSTATIC POTENTIALS ADJACENT TO MEMBRANES AND PEPTIDES THAT MIMIC THE CALMODULIN-BINDING DOMAINS OF NEUROMODULIN AND THE MARCKS PROTEIN. ((C. Coburn, J. Eisenberg, M. Eisenberg, S. McLaughlin and L. Runnels)) HSC, SUNY, Stony Brook NY 11794

Several groups have shown that neuromodulin and the MARCKS protein bind calmodulin (CaM) with high affinity ($K = 10^8$ and 10^9 M^{-1}) and release it when phosphorylated by protein kinase C (PKC). Peptides with sequences identical to the CaM-binding domains of these proteins contain both clusters of basic residues and all the serine residues that are PKC phosphorylation sites. These peptides bind to CaM and to membranes containing 20% acidic lipids with equal affinity; binding is reduced following phosphorylation by PKC. The peptides do not bind to membranes formed from zwitterionic lipids such as PC and exhibit no specificity between the monovalent acidic lipids PS and PG, which suggests the membrane binding is due mainly to electrostatic interactions. We are attempting to calculate the magnitude of this electrostatic binding energy by constructing molecular models of phospholipid membranes and peptides in different conformations (α, β, random coil). We are using the nonlinear Poisson-Boltzmann equation to calculate potentials adjacent to the membrane, the free peptides, and the peptide-membrane complexes, but detailed calculations will require structural information. Circular dichroism measurements indicate the peptides are random coils in solution, but have different structures when bound to membranes or SDS micelles.

M-Pos215

ENERGETICS OF BINDING OF A HIGHLY AMPHIPATHIC PEPTIDE TO MEMBRANES; LIPID DOMAIN FORMATION AND PEPTIDE STRUCTURE ((K. Gawrisch, K.-H. Han, J.-S Yang, L.D. Bergelson, J.A. Ferretti)) NHLBI, NIH, Bethesda, MD 20892

The fragment 828-848 of the envelope glycoprotein gp160 of HIV-I (N-Arg-Val-Ile-Glu-Val-Val-Gln-Gly-Ala-Cys-Arg-Ala-Ile-Arg-His-Ile-Pro-Arg-Arg-Ile-Arg-COOH) forms a highly amphipathic α-helix upon interaction with a negatively charged lipid membrane as measured by circular dichroism. In solution the peptide is not structured. Currently 2D NMR investigations of the structure of the bound peptide are in progress. The lipid peptide interaction was studied on model membranes composed of DOPC and DOPG using microelectrophoretic mobility of lipids, fluorescence polarization of labelled lipids and energy transfer between them, NMR and DSC. The peptide attaches electrostatically to the lipid surface with a free energy of binding of 8.3 kcal/mol (pure DOPG membrane, 0.1 M NaCl, 20 C). Hydrophobic interactions between the peptide and the membrane are weak or absent. In DOPC/DOPG lipid mixtures the peptide preferentially interacts with the negatively charged lipid component. Peptide binding causes the formation of lipid domains enriched in DOPG. The binding energy of the peptide to the mixed DOPC/DOPG bilayer is significantly decreased (4.5 kcal/mol, 0.1 M NaCl, 20 C). We ascribe the difference in comparison with pure DOPG membranes to the loss of free energy caused by domain formation. The binding results in an increased conductivity of membranes for ions, very similar to the conductivity changes observed after binding of magainins. These observations could be related to the well known cytopathogenicity of gp160.

M-Pos216

NMR STUDIES OF THE HIV FUSION PEPTIDE ((Frances Separovic[#],Bruce A Cornell[#],Alan Kirkpatrick[+]and Cyril C Curtain[+])) [#]CSIRO Division of Food Processing, PO Box 52 North Ryde NSW 2113 [+]CSIRO Division of Biomolecular Engineering, Parkville Vic 3052.

The 23-residue sequence of the gp41 envelope of the human immunodeficiency virus (HIV) has been implicated in the fusion of the viral envelope with the membrane of the target cell. The fusion appears to be an essential step in HIV infection. We have specifically ^{13}C labelled a 23-residue N-terminal sequence of gp41, a fusogenic polypeptide from HIV and incorporated the peptide into phospholipid membranes. The membrane dynamics and lipid phases have been determined by ^{13}C, ^{31}P and ^{14}N solid state NMR spectroscopy. At 50% w/w water the lipid remains lamellar in both oriented and powder samples at 1:30, 1:20 and 1:10 peptide to phosphatidylcholine (PC) lipid ratio. A non-lamellar phase was observed at higher water content in pure PC multilayers. With 10 mole % phosphatidylserine to PC, a non-lamellar phase was detected at 50% w/w water in the presence of the charged lipid and polypeptide. The fusogenic peptide, which acts as a lytic agent, was membrane perturbing and formed aggregates in the lipid samples. The implications of these results on viral fusion will be discussed.

M-Pos217

INTERACTIONS BETWEEN MAGAININ 2 AND LIPID BILAYERS: A REDOR NMR AND FT-IR STUDY. ((Jack Blazyk*, Melody Ferguson*, Jin Hua*, Andrew W. Hing† and Jacob Schaefer†)) *Chemistry Department, Molecular and Cellular Biology Program, and College of Osteopathic Medicine, Ohio University, Athens, Ohio 45701, and †Chemistry Department, Washington University, St. Louis, MO 63130.

Magainin 2, a naturally occurring 23-amino acid cationic peptide isolated from the skin of the African clawed frog, is lethal to a wide variety of microorganisms and enveloped viruses. The bactericidal activity of the peptide is believed to be associated with the disruption of the integrity of the membrane system of the target organism. Magainins have the potential to adopt a highly amphiphilic α-helical secondary structure, which is typical for many membrane-active peptides. Unlike other cationic peptides, such as melittin, which are cytotoxic, magainins are nonhemolytic at antimicrobial concentrations. Thus, magainins and related peptides may have therapeutic potential as antibiotics. The molecular nature of the interaction between magainin 2 and the cell surface has yet to be determined. Does magainin act similarly to detergents to disrupt membrane structure, or do oligomeric clusters of magainins form well-defined ion channels through the membrane? Recent evidence suggests that magainins may form cation channels and that the helical axis of magainins lies parallel to the plane of the bilayer. We have applied the new solid-state NMR technique, REDOR (rotational-echo double-resonance), to define the proximity of ^{15}N-labeled magainin and ^{31}P in the polar headgroups of DPPG bilayers. By measuring ^{15}N-^{31}P dipolar coupling in the REDOR experiment, it is possible to determine approximate distances between these nuclei. Lipid and peptide structure also is evaluated by FT-IR spectroscopy to monitor effects on lipid fluidity and peptide secondary structure using C–H stretching and amide I bands, respectively. Future REDOR and TEDOR (transferred-echo double-resonance) experiments to explore oligomer formation and other lipid-peptide interactions will be discussed.

M-Pos218

CYTOLYTIC MECHANISM OF MAGAININ. ((S.J. Ludtke, K. He, Y. Wu, and H.W. Huang)) Rice University, Houston, TX 77251-1892.

We present evidence that magainin undergoes a concentration dependent conformation change in synthetic lipid multilayers. Since vesicle cytolysis exhibits a similar concentration dependence, we believe the conformational change is responsible for the cytolytic action of magainin. Using oriented circular dichroism (OCD) we have shown that in low concentrations, magainin forms α-helices lying parallel to the membrane surface. When the concentration becomes greater than a lipid specific value, the magainin undergoes a conformational change to a yet unidentified state. The OCD spectra of this state is not a superposition of any known protein conformations (α-helix, β-sheet, random coil, or turn). Since magainin returns to an α-helical conformation when the multilayer sample is dissolved in trifluroethanol (TFE), the change is reversible. Linear superpositions of the α-helical and high concentration OCD spectra have been observed at concentrations above the threshold value, and the intensity of the high concentration spectra varies directly with concentration. For these reasons we are confident that the high concentration OCD spectra are caused by an unknown state of the protein. For diphytanoyl phosphatidylcholine multilayers, the critical peptide:lipid molar ratio is roughly 1:80.

M-Pos219

Effect of cholesterol on the lytic properties of melittin.

M. Lafleur, M. Monette (Département de chimie, Université de Montréal, Montréal, Québec, H3C 3J7) and M.-R. Van Calsteren (Agriculture Canada, St-Hyacinthe, Québec, J2S 8E3). (Spon. by F. Lamarche)

^{2}H and ^{31}P NMR spectroscopy was used to study the polymorphism of 1,2-dipalmitoyl-sn-glycero-3-phosphocholine (DPPC)/cholesterol mixtures in the presence of melittin, a peptide known to cause micellization of DPPC vesicles. It is known that DPPC/melittin complexes (incubation molar ratio 20/1) show a reversible thermal behavior from small particles resulting from the lysis at $T<T_m$ to large assemblies formed by the fusion of the small particles above T_m. The present study reveals that cholesterol affects this behavior, and that the modulation of the lytic power of melittin induced by cholesterol is a consequence of the original effect of the sterol on the thermotropism of pure lipid bilayers. For moderate concentrations, cholesterol leads to the coexistence of small complexes and large assemblies over a wider range of temperatures, while no cooperative transition between these two species is observed when cholesterol content reaches 30(mol)%; this is likely related to the effects of cholesterol on the transition from gel to fluid phase. When melittin interacts with cholesterol-rich bilayers (30(mol)%), the subsequent lysis is partial, and the resulting small particles are enriched in DPPC compared to the initial lipid mixture. Concentrations of cholesterol ≥ 35(mol)% severely limit the lysis induced by melittin, suggesting that the tight lipid packing due to high cholesterol concentrations leads to high resistance to the lytic power of melittin.

M-Pos220

INTERACTION OF AN AMPHIPATHIC HELICAL PEPTIDE, ALAMETHICIN, WITH MEMBRANES.

((Y. Wu, K. He, S.J. Ludtke and H.W. Huang)) Rice Univ., Houston, TX 77251-1892.

Alamethicin associates with a membrane in two ways: at low concentrations it adsorbs parallel to the membrane surface; at high concentrations it inserts perpendicularly in the bilayer; the transition between these two states occurs over a small range of concentrations, indicating that it is a cooperative phenomenon (Huang and Wu, 1991, Biophys. J. 60, 1097). To understand the structure of peptide-lipid interactions, we performed x-ray lamellar diffraction of alamethicin-diphytanoyl phosphatidylcholine multilayers. In all cases, we don't expect to see the peptide in the electron density profile, since the peptide to lipid molar ratio (P:L) is small (<1:20). But the structure of the bilayer changes significantly even with a small amount of peptide. In pure lipid multilayers, the phosphocholine group is oriented parallel to the plane of the membrane. In the presence of the peptide at low P:L, the head group is partially pointed outward, indicating, perhaps, alamethicin in the surface state is in contact with the lipid glycerol backbone and the underside of the head group. This head group interaction also greatly increases disorder in the hydrocarbon chains. At high P:L (>1:50), the peptide is inserted perpendicularly in the bilayer. The x-ray diffraction shows very disordered bilayer structures.

M-Pos221

THE SPONTANEOUS INSERTION OF MODEL HYDROPHOBIC PEPTIDES INTO LARGE UNILAMELLAR VESICLES

((Thomas S. Moll and Thomas E. Thompson.)) University of Virginia, Dept. of Biochemistry, Charlottesville, Virginia, 22908

Models of protein translocation and secretion will not be complete without details into the mechanism of lipid bilayer insertion. The study of spontaneous peptide insertion into model membrane systems has been hindered by the low solubility of hydrophobic peptides in aqueous solutions. A novel protocol has been developed that enables the site-specific (N-terminus) attachment of hydrophobic peptides to a water-soluble carrier protein (bovine pancreatic trypsin inhibitor) using a heterobifunctional crosslinker (SPDP). As a reference state, H-$(Ala)_{20}$-Tyr-Cys-$CONH_2$ and H-$(Ala)_{10}$-Tyr-Cys-$CONH_2$ were synthesized, since (1) alanine is the simplest of all a-helix-forming amino acids, and (2) the lengths would be just long enough to span the lipid bilayer and monolayer, respectively. The procedure involves the cleavage of the synthetic peptides in the presence of detergents to prevent peptide-peptide aggregation, the removal of detergent, after crosslinking, by propionic/formic acid-based gel filtration techniques, followed by purification of conjugates using RP-HPLC. The binding parameters of the two semi-synthetic proteins were measured by ultracentrifugation of vesicle-protein mixtures. As a control, the proteins were reconstituted into DMPC liposomes using octylglucoside-dilution techniques. $(Ala)_{20}$-BPTI is able to spontaneously insert into LUVs and reconstituted liposomes forming a stable complex, whereas $(Ala)_{10}$-BPTI remained in the aqueous phase in both experiments. Further studies utilizing leucine peptides will help elucidate the length and hydrophobicity requirements for spontaneous insertion and membrane stability. Supported by NIH grant GM-14628.

M-Pos222

SOLVENT HISTORY DEPENDENCE OF GRAMICIDIN-LIPID INTERACTIONS: A RAMAN AND FTIR SPECTROSCOPIC STUDY.

((Mario Bouchard and Michèle Auger)), CERSIM, Département de chimie, Université Laval, Québec, CANADA, G1K 7P4

Gramicidin has been widely used as a model for the hydrophobic part of intrinsic membrane proteins. Recently, it has been shown by circular dichroism, NMR spectroscopy and HPLC that gramicidin can adopt various conformational states in hydrated phospholipid bilayers. A number of factors may determine the conformation that gramicidin molecules ultimately adopt in a phospholipid dispersion, such as the peptide/lipid ratio, the solvent used to cosolubilize the phospholipid and gramicidin, the incubation time and the temperature. Therefore, we have investigated the interactions between gramicidin and a model membrane composed of one phospholipid, dimyristoylphosphatidylcholine (DMPC), as a function of the cosolubilization solvent and incubation time. Three organic solvents have been used: trifluoroethanol (TFE), a mixture of methanol/chloroform (1:1 v/v) and ethanol. By used of Fourier Transform Infrared (FTIR) spectroscopy, we are able to demonstrate that the conformation adopted by gramicidin in the membrane is dependent upon the cosolubilization solvent used and only with TFE it is possible to incorporate gramicidin entirely as a $\beta^{6.3}$ helix. The effect of the incorporation of gramicidin on the thermotropism of the lipid bilayer, as well as the orientation of the peptide in the membrane determined by attenuated total reflectance (ATR) were also found to be dependent on the cosolubilization solvent and the incubation time. On the other hand, we have used Raman spectroscopy to obtain information on the environnement of the tryptophan side chains in gramicidin and their interactions with the hydrocarbon chains of the lipids.

M-Pos223

INTERACTIONS BETWEEN HUMAN DEFENSINS AND PHOSPHOLIPID BILAYERS. ((William C. Wimley, Michael C. Wiener and Stephen H. White)). Department of Physiology and Biophysics, University of California, Irvine CA. 92717.

As part of a complex system of host defense, mammalian neutrophils contain granules of small (29-34 amino acid) peptides called defensins. Defensins are cationic, compact, disulfide-linked globular peptides that exhibit a broad range of antibiotic specificity, and act by permeablizing cell membranes (Lehrer et al (1991) *Cell*, 64,229). We have purified three of the defensins found in human neutrophils, HNP-1, HNP-2 and HNP-3, and have examined their interactions with phospholipid bilayers by equilibrium binding methods and by X-ray diffraction. Oriented multilayers were prepared for X-ray diffraction by a novel method of rapid solvent evaporation. Lamellar diffraction patterns (66% relative humidity) were obtained for all the samples which contained Dioleoylphosphatidylcholine (DOPC) and between 0 and 20 mol% HNP-2. The repeat spacing decreased from 49.5 ± 0.3 Å for 100% DOPC to 44.9 ± 0.8 Å for 10:1 DOPC:HNP-2. These results indicate that the peptide is probably incorporated into the bilayers under the conditions of the diffraction experiments. In contrast, HNP-2 in solution binds only to phospholipid vesicles containing the anionic lipid phosphatidylglycerol (PG). The fraction of peptide bound is a sigmoidal function of the mole fraction of PG, as expected for multivalent peptide-bilayer interactions (Kim et al (1991) Biophysical. J., 60,135,). About half of the peptide is bound (in 50 mM KCl) at 20 mol% PG and 10 mM total lipid. Supported by NIH grant GM 46823. W.W. is supported by NIH fellowship GM14178.

M-Pos224

PHOSPHOLIPID BINDING AND INFERRED MECHANISM OF TOXICITY OF THIONINS. COMBINED X-RAY, NMR, AND MODELING STUDIES. ((B. Stec, U. Rao, O. Markman, G. Heffron, K.A. Lewis, M.M. Teeter)) Department of Chemistry, Boston College, Chestnut Hill, MA 02167

We present a detailed molecular model for binding of phospholipids to a family of small plant toxins, the thionins. In highly refined X-ray structures of α1- and β-purothionins (R=14.0% at 2.8Å, and R=17.8% at 2.2Å) a bound phosphate ion and MPD molecule were detected thus suggesting a possible phospholipid binding site. ^{31}P NMR experiments on these and other toxins show the presence of phosphate ion in solution as well. We have carried out 1-D and 2-D NMR solution binding studies of organic phosphates and phospholipids to the different members of the family. The existence of a specific binding site for the organic phosphates and phospholipids, as suggested by crystallographic studies, has been confirmed by these NMR experiments. On the basis of the experimental data, a phospholipid has been docked into the X-ray determined crystal structure. The model presented here suggests an explanation for the mechanism of toxicity of the peptides including the role of oligomerization. It also provides insight into the structural principles of protein-membrane interactions.

M-Pos225

A DOPAMINE RECEPTOR TRANSMEMBRANE CONSENSUS PEPTIDE; PURIFICATION AND CONFORMATIONAL STUDIES

(V.L. WILLIAMS AND R.B. MURPHY) Department of Chemistry and Center for Neural Studies, New York University, NY, NY 10003

We have prepared model peptides whose primary sequences correspond to the putative transmembrane domains of the dopamine D_2 receptor family. Site-specific mutagenesis and other studies have suggested that ligand binding determinants of the receptor are contained within these transmembrane domains. As example, we prepared the sequence DYAIFVLYASAWLSFNCPFIVTLNIK. Purification of this highly hydrophobic peptide necessitated the use of a novel, ternary gradient HPLC system using a C_4 column heated to 55 ° C. The purified peptide was incorporated into small unilamellar vesicles of DMPC, as verified by electron microscopy. Circular dichroism studies in these and other model membrane systems suggest that the secondary structure is only partially helical. Tryptophan fluorescence quenching and lifetime anisotropy studies indicate multiple conformational states in these lipid systems. The present peptide/lipid system is therefore a useful model for critical structural aspects of the dopamine D_2 receptor.

M-Pos226

CD AND NMR STUDIES OF THE CONFORMATION OF A 20-AMINO ACID PIP2-BINDING DOMAIN OF GELSOLIN IN MIXED SOLVENT.

((Wujing Xian, William H. Braunlin)), Department of Chemistry, University of Nebraska-Lincoln, Lincoln, NE 68588-0304. ((Paul A. Janmey)), Experimental Medicine Division, Brigham and Women's Hospital and Harvard Medical School, 221 Longwood Avenue, Boston, MA 02115

The interaction of the actin binding protein gelsolin with phosphotidylinositol 4, 5-bisphosphate (PIP2) is a crucial step in biological signal transduction that leads to modification of the cytoskeleton. A 20 amino acid PIP2 and actin-binding domain is found in gelsolin, and a peptide with the same sequence has been synthesized. CD studies of this peptide in mixed solvent solutions show that it adopts a random coil conformation in H2O, but a predominantly α-helical conformation in PIP2 micelle solution and in >20% Trifluoroethanol (TFE). In 25% TFE, 2D NMR DQF-COSY and HOHAHA/TOCSY experiments are performed for spin system assignments, and NOESY is used for sequential assignments. The results suggest that a relatively hydrophobic central region of the peptide is helical. The NOE data provide constraints that are used in molecular modelling studies.

M-Pos227

MEMBRANE-BOUND CONFORMATIONS OF SIGNAL PEPTIDES BY trNOE

((Z. L. Wang, J. D. Jones, J. Rizo and L. M. Gierasch)) Department of Pharmacology, University of Texas Southwestern Medical Center, Dallas, TX 75235-9041.

The propensities of signal peptides to adopt an α-helical conformation in interfacial environments and to insert spontaneously into the hydrophobic acyl chain region of lipid bilayers have been shown to correlate well with *in vivo* activity in protein export. However, little detailed structural information has been reported for signal peptides in the membrane-bound state. In the present study, a LamB signal peptide analogue with enhanced water solubility (KRR-LamB) was designed by inserting three charged residues (KRR) between Arg6 and Lys7 in the sequence, which is likely to correspond to a non-perturbing mutation *in vivo*. We carried out a detailed structural analysis of the signal peptide KRR-LamB when bound to large unilamellar vesicles (LUVs) mainly by using the transferred nuclear Overhauser effect (trNOE) NMR technique. To observe the trNOE phenomenon, which relies on rapid chemical exchange between the free and bound states, the binding affinity of the KRR-LamB peptide for LUVs was tuned by changing the proportion of the acidic lipid POPG in the LUVs. By incorporating a paramagnetic nitroxide label into the lipid acyl chain at different depths, the positions of specific residues in the bilayer could be located by resonance linewidth broadening effects. We found that the KRR-LamB signal peptide inserted into the lipid bilayer with an α-helical secondary structure which extends from approximately residue Pro9 to the C-terminus.

M-Pos228

The Conformation of Membrane-Active Peptides in Dry Lipid

W. D. Braddock[a], F. J. Puga II, and P. H. Axelsen[b]
Department of Biochemistry and Molecular Biology
Mayo Foundation, Rochester MN. 55905

A 20-residue peptide representing the fusogenic segment of the influenza hemagglutinin was synthesized with and without an amidated C-terminus. Circular dichroism measurements had indicated that the amidated peptide has a random conformation in pH 5.5 buffer, whereas it forms a helix when associated with POPC liposomes[1]. With a free C-terminus, we find that the peptide does not associate with liposomes and maintains a random conformation. When the peptides are mixed with POPC in CCl_4 and dried onto the surface of a germanium crystal[2], infrared absorption spectra clearly indicate that the amidated peptide forms a β-sheet, whereas the peptide with a free terminus is probably helical (but may be random). These results are preliminary to a study of water-solvated systems, but they add to earlier reports in which dramatically different conclusions were obtained in dry versus solvated lipid systems[3].

1. Lear & DeGrado, J Biol Chem 1987;262:6500-6505
2. Brauner et al, Biochemistry 1987;26:8151-8158
3. Frey & Tamm, Biophys J 1991;60:922-930

Supported by (a) a training grant from the Keck Foundation, and (b) the L. P. Markey Charitable Trust.

M-Pos229

THE INTERACTION OF THE TACHYKININ SUBSTANCE P WITH PC AND PG MODEL MEMBRANES.

((MARK W. TRUMBORE AND KYUNG YU))Biomolecular Structure Analysis Center, UNIV. OF CT HEALTH CENTER, FARMINGTON, CT 06030-2017.

Substance P (SP) is a member of the tachykinin family of neuropeptides and is involved in the transmission of pain. In order to better understand the mechanism by which the amphipathic SP interacts with membranes, we have studied the interaction of SP with dimyristoyl-phosphatidylcholine and phosphatidylglycerol membranes by means of differential scanning calorimetry. Consistent with findings by Seelig and Macdonald (Biochemistry 28:2490-2496, 1989), we observed no perturbation of membrane thermal properties when SP was mixed with PC vesicles. When SP was mixed with PG vesicles there was a dramatic effect on membrane thermal properties. SP decreased the cooperative unit size of the main phase transition and induced the formation of a small lower melting domain. When incorporated into PG/PC mixtures, SP interacted preferentially with the PG domains and did not perturb the PC domains. We interpret these results to be consistent with a model in which SP is inserting into the PG membranes with its positively charged domain in electrostatic contact with the lipid headgroups and its hydrophobic domain inserted into the glycerol backbone upper acyl chain region of the membrane. We are currently performing x-ray diffraction and Fourier-transform infrared spectroscopy to confirm this interpretation of the DSC results. This work was supported by a grant from Miles Pharmaceutical Div., Miles Inc.

M-Pos230

HELICAL STRUCTURE VARIATION IN SICKLE HEMOGLOBIN FIBERS.

((M. R. Lewis, L. J. Gross, and R. Josephs)), Lab for Image Analysis and Electron Microscopy, Dept. Molec. Genetics/Cell Biol., U. of Chicago, Chicago IL 60637

Cryo-electron micrographs of sickle hemoglobin (HbS) fibers show that these helical particles have variable pitch†. The pitch of HbS fibers varies not only from one particle to the next but also locally along the length of any given fiber. One result of variable pitch is that there are substantial changes in the structure of the fiber unit cell. Consequently, in order to reconstruct fibers both the local pitch and the angle of view must be determined.

Previous work in our laboratory used cross-correlation analysis to determine local pitch in negatively stained fibers. In this work we have developed a new cross-correlation procedure to exploit the data present in cryo-electron micrographs. In particular we have taken advantage of the internal structure which is visible in micrographs of frozen hydrated HbS fibers but not in negatively stained fibers. In the new procedure we determine the local pitch and angle of view of fiber segments by cross-correlating each to a gallery of model images. This gallery was created from 33 uniform pitch electron density models calculated for every 0.5° rotation/unit cell over the experimentally observed range (0° - 16°). Projections of these models were calculated for angles of view from 0° to 360° in 1° increments, thus producing a gallery of model images covering *ca.* 12,000 pitch and angle of view combinations.

This cross-correlation procedure is optimized by minimizing misalignment and magnification differences between fibers and model images. We align a fiber by finding the rotation which minimizes the difference between the left and right side of its Fourier amplitudes. We determine a fiber's magnification by the one dimensional Fourier transformation of the meridional projection of its Fourier amplitudes.

† Lewis, M. R., Gross, L. J., and Josephs, R. (submitted) J. Electron Micr. Tech.

* Supported by NIH grants HL30121 (RJ) and training grant GM08282 (MRL)

M-Pos231

OSMOTIC PRESSURE OF 3-DIMENSIONAL ORDERED COLLOIDAL SUSPENSIONS. ((Joel A. Cohen, V. Adrian Parsegian and Donald C. Rau)) Univ. of the Pacific, San Francisco, CA 94115 and NIH, Bethesda, MD 20892.

Osmotic stress has been used to measure interactions between lamellae of multilamellar phospholipid vesicles (planar geometry) and between DNA double helices, polysaccharides, or collagen triple helices in condensed arrays (cylindrical geometry). We now are extending this technique to 3-dimensional suspensions of charged phospholipid and microsomal vesicles (spherical geometry). An excellent control system for such studies is that of charged 0.1 μm latex spheres that interact electrostatically to form crystalline arrays in deionized water. The osmotic pressures expected for such systems at particle volume fractions .01-.1 are 10^{-4} to 10^{-3} atm (1-10 mm H_2O). A simple osmometer capable of measuring 1 mm H_2O osmotic pressure difference between two chambers was built from a dialysis cell and 500,000 MWCO dialysis membrane. Osmotic pressure differences were measured between suspensions of latex colloidal crystals and deionized water. Plots of osmotic pressure vs. particle concentration yield force vs. distance relations. The results are compared to those calculated in the Wigner-Seitz cell approximation assuming electrostatic and entropic interactions.

M-Pos232

STRUCTURAL STUDIES OF LUMBRICUS ERYTHROCRUORIN BY ELECTRON MICROSCOPY AND X-RAY CRYSTALLOGRAPHY ((K. Strand, R.W. Craig and W.E. Royer)) U. Mass. Medical Center, Worcester, MA 01605. (spon. by W.E. Royer)

Erythrocruorin, a 3.9x 10^6 D oxygen transport protein, is found freely dissolved in the blood of numerous annelids. Crystallographic investigations from the high salt orthorhombic form continue in order to learn the molecular basis of cooperative oxygen binding and self assembly of this macromolecular complex. Crystals show the symmetry of the space group $C222_1$ with unit cell constants of a=502.1, b=297.8 and c=350.1Å. Self-rotation calculations indicated D_6 symmetry oriented 15° from the c axis with a molecular diad axis coincident with the a axis. The position of the molecular center with respect to a is unknown but restricted by crystal packing considerations. To determine the position of the molecule in the crystal lattice, we have begun an analysis by electron microscopy. Crystals were cross-linked with 0.3% gluteraldehyde, fixed, embedded and sectioned perpendicular to the b axis. Thus, the ac plane was imaged in projection. Images were processed using lattice filtering techniques and analysis of these images suggest the molecular center is close to 1/4 a. To refine the position of the molecular center, accurate low angle diffraction patterns were obtained on a Rigaku rotating anode x-ray generator with an RAXIS system imaging plate. Resolution of the low angle pattern was enhanced by a crude helium path from the sample to the imaging plate. Using this procedure, diffraction data corresponding to Bragg spacings less than 150 Å were measured whereas previous data sets contained data no lower than 70 Å. The inclusion of these data has improved phasing statistics for model based symmetry averaging at low resolution.

M-Pos233

NONRANDOM DISTRIBUTION OF INTERPHASE CHROMOSOMES IN HUMAN LYMPHOCYTES. ((S. Lesko, D. Callahan, C. N. Chen and P. O. P. Ts'o)) Biochem. Dept., Johns Hopkins SHPH, Baltimore, MD, 21205. (Spon. L.-S. Kan)

We have obtained evidence, utilizing three color fluorescence in situ hybridization and computer imaging microscopy, for the non-random spatial arrangement of chromosomes 7, 11 and 17 in interphase nuclei of human lymphocytes. Three alpha-satellite DNA probes were labeled with three different haptens and detected with three distinquishable fluorophores. Individual nuclei (21) were optically sectioned in 0.23 micron increments leading to a total 3-D spatial analysis of about 131,000 pixels. Three stacks of 32 images were collected for each nucleus using filter combinations for red, blue and green fluorescence. Image stacks were registered and combined into one pseudocolored composite image stack that provided the 3-D information on the spatial arrangement of the six hybridization signals. Establishment of an internal reference frame and transformation of the coordinates allowed us to compare the spatial arrangement of centromeres in 21 different nuclei. The data showed that each homolog appeared to be restricted to a limited and specific region of the nucleus.

Supported by DOE grant DE-FG02-88ER60636.

VIRUS STRUCTURE

M-Pos234

THREE-DIMENSIONAL STRUCTURES OF REOVIRUS VIRIONS, ISVPs AND CORES BY CRYO-ELECTRON MICROSCOPY AND IMAGE ANALYSIS: IMPLICATIONS FOR VIRUS-CELL INTERACTIONS AND MORPHOGENESIS.

((K. A. Dryden[*], M. Yeager[*], G. Wang[*], K. M. Coombs[#], M. L. Nibert,[@] D. B. Furlong,[@] B. N. Fields[#] and T. S. Baker[*].))

[*]The Scripps Research Institute, La Jolla, CA 92037, USA; [#]Purdue University, West Lafayette, IN 47907, USA; [@]Harvard Medical School, Boston, MA 02115, USA.

Three structural forms of mammalian reovirus (virions, infectious subvirion particles [ISVPs], and cores) have been examined by cryo-electron microscopy and image reconstruction at 27-32Å resolution. Alterations in supramolecular organization and protein conformation during defined stages of reovirus infection can be inferred from the analysis of the three-dimensional structures and inspection of difference maps. The intact virion (~850Å diameter) is designed for environmental stability in which the dsRNA genome is protected not only by tight σ3-μ1, λ2-σ3, and λ2-μ1 interactions in the outer capsid but also by a densely packed core shell formed primarily by λ1 and σ2. Depending on viral growth conditions, virions undergo cleavage by enteric or endosomal/lysosomal proteases, to generate the activated ISVP (~800Å diameter). In this transition the outer capsid layer formed by tetrameric and hexameric clusters of ellipsoidal σ3 subunits is released. In addition, the vertex-associated hemagglutinin, σ1, undergoes a striking change from a compact form to an extended, flexible fiber, which appears designed to maximize interactions with cell surface receptors. Transcription of viral mRNAs is thought to be mediated by the core particle (~600Å diameter), generated from the ISVP after penetration and uncoating. The transition from ISVP to core involves release of the σ1 fibers and an outer capsid layer formed by trimeric clusters of rod-shaped μ1 subunits. In addition, λ2 subunits, which form a tightly packed flower-shaped pentamer in the virion and ISVP, rotate and swing upward and outward to open a large solvent channel at each vertex. This novel conformational change may be required to permit the exit of newly synthesized mRNAs. The essence of these orchestrated events is that reovirus is superbly designed to undergo stages of controlled degradation in which the release of structural proteins in the outer capsid is coordinated with large protein conformational changes at the icosahedral vertices, the sites for virus-cell interactions and viral transcription.

M-Pos235

INHIBITION OF PROCAPSID ASSEMBLY IN VITRO BY BIS-ANS

((P.E.Prevelige Jr*, C. Teschke, J.King)) *Boston Biomedical Res. Instit, Boston MA. & Mass. Inst. of Tech., Cambridge, MA).

The assembly of Salmonella bacteriophage P22 procapsids requires the copolymerization of approximately 300 molecules of scaffolding protein with 420 molecules of coat protein. The resultant structure has the 420 coat protein subunits arranged in a T=7 lattice, with an inner core of scaffolding protein. Although coat protein alone will polymerize at high concentration the scaffolding protein is critical in controlling form determination. Studies on the dissociation of the procapsid under conditions of high pressure have demonstrated that hydrophobic interactions provided the stabilizing forces. The hydrophobic fluorophores ANS and bis-ANS were examined for their binding to both coat and scaffolding protein monomers, and the procapsid. Bis-ANS bound to both the coat and scaffolding proteins. No binding of ANS was found to either protein.The coat protein has a single binding site for bis-ANS with a Kd of 5 uM, while the scaffolding protein has multiple sites . The presence of bound bis-ANS blocked the assembly reaction. Coat protein alone in the presence of bound bis-ANS was unable to polymerize suggesting that the free energy of coat/coat protein interactions required for assembly is less than -7 kcal/mol. This low value suggests that bis-ANS acts by blocking nucleation of assembly. Further evidence for coat protein oligomerization being the first step in assembly was obtained by sedimentation equilibrium studies of coat protein and coat/scaffolding mixtures at sub-critical concentrations. Binding of bis-ANS to coat protein does not seem to induce any substantial conformational changes as determined by circular dichroism and limited proteolysis. Similar studies on scaffolding protein demonstrated a conformational change induced upon bis-ANS binding.

M-Pos236

LOCATION OF VP26 IN THE HERPES SIMPLEX VIRUS CAPSID

((B.L. Trus, F.P. Booy, W.W. Newcomb, J.C. Brown and A.C. Steven)) LSBR-NIAMS and CSL-DCRT, NIH, Bethesda, MD 20892, and Dept. of Microbiology and Cancer Center, Univ. of Virginia Health Sciences Center, Charlottesville, VA 22908 ((Spon. by M. Eden)

VP26 is a small protein (MW = 12,095) present in high copy number (~ 1000 molecules) in the surface shell of herpes simplex virus type 1 (HSV-1). With a view to inferring its possible role in capsid assembly, we have attempted to localize VP26 by quantitative difference imaging based on three-dimensional reconstructions calculated from cryo-electron micrographs. The capsids compared were G-capsids, i.e. native B-capsids treated with 2.0M guanidine-HCl which quantitatively removes VP26 as well as certain other structural components (Newcomb & Brown, J. Virol. 65:613 (1991)), and G26-capsids, which are G-capsids to which VP26 has been rebound. The only biochemical difference between G-capsids and G26-capsids was the presence in the latter of the original amount of VP26 (as confirmed by SDS-PAGE). Reconstructions were calculated and compared after careful matching of their radial scaling. The maps differ only in that the G-capsid shows a small but clear shortening of the hexon protrusions compared with the G26-capsid, which matches native capsids in this respect. This result suggests that, providing that strong allosteric effects do not accompany binding of VP26, six copies of this molecule are distributed around the tip of each hexon.

M-Pos237

EFFECTS OF RADIATION DAMAGE ON STRUCTURE OF FROZEN HYDRATED HSV-1 CAPSIDS

((J.F. Conway, B.L. Trus, F.P. Booy, W.W. Newcomb, J.C. Brown and A.C. Steven)) Lab. of Structural Biology Research, NIAMS, and Computer Systems Lab., DCRT, NIH, Bethesda, MD 20892; and Dept. of Microbiology and Cancer Center, University of Virginia Health Sciences Center, Charlottesville, VA 22908, USA.

Radiation damage imposes severe limitations on the information content of electron micrographs of biological specimens. In this context we are investigating the effects of moderate electron radiation damage on capsids of herpes simplex virus type-1 (HSV-1) by examining three-dimensional density maps calculated from cryo-electron micrographs. Highly purified B-capsids (DNA-free precursor capsids) were imaged at 100 kV. Multiple exposures were recorded of the same field, each corresponding to a dose of ~6$\bar{e}$/Å^2. The first and fifth images were analyzed further. Orientations of 39 particles were determined from the first image and these data were then used to generate a 3-D reconstruction according to Fourier-Bessel techniques. The same set of particles from the fifth exposure was also reconstructed using the same orientation angles corrected for a uniform (small) relative rotation introduced during digitization. The effects of the higher cumulative dose are visible in both the micrographs and the reconstructions as a smearing out of fine detail. This trend was analyzed further by calculating Fourier Ring Correlation (FRC) functions between the particle images and the corresponding reprojections from the reconstructions. Preliminary results indicate that although the nominal resolution of both reconstructions is approximately 31Å, the loss in information content at the higher dose is evident and is expressed as a systematic attenuation of the higher spatial frequencies (primarily between (1/80Å)$^{-1}$ and (1/31Å)$^{-1}$).

M-Pos238

MOLECULAR STRUCTURE AND CONFORMATIONAL SWITCHING OF A VIRAL ADHESIN

((A.M. Makhov, B.L. Trus, J.F. Conway, M.N. Simon, T.G. Zurabishvili, V.V. Mesyanzhinov, and A.C. Steven)) LSBR-NIAMS and CSL-DCRT, NIH, Bethesda, MD 20892; Ivanovsky Inst., Moscow 123098, Russia; Brookhaven National Lab., Upton, NY 10973. (Spon. by H. Pant)

The short tail-fiber of bacteriophage T4, an oligomer of gp12 (526 residues), binds the virion irreversibly to the bacterial surface during infection. We have used electron microscopy, image processing, and computational sequence analysis to investigate its structure, after purifying functionally active protein from mutant-infected cells. Visualized in negative stain, these filamentous molecules are 38nm in total length, with an arrowhead-shaped head (10nm by 6nm), a 24nm shaft of uniform width (3.8nm), and a relatively small, flexible, tail. The primary sequence contains a domain consisting of tandem quasi-repeats, each about 40 residues long, between residues ~ 50 and 320. Mass determinations and mapping by scanning transmission electron microscopy confirm that the molecule is a trimer, and yield masses for the head, shaft, and tail domains that are consistent with their representing (trimers of) the carboxy terminus, the repeat region, and the amino terminus, respectively. When short tail-fibers extend from baseplates, their heads are distal, implying that the tail that remains in contact with the baseplate and the head contains the receptor binding sites. Analysis of the molecules' curvature properties detects three hinge-sites: these suggest how the short tail-fiber may be initially accommodated in a compact conformation in the 'hexagon' state of the baseplate, from which it converts to an extended conformation when the baseplate switches into its 'star' state.

M-Pos239

DO INTERMEDIATES INVOLVED IN VIRUS UNCOATING AND/OR ASSEMBLY SHARE PROPERTIES WITH THE MOLTEN GLOBULAR STATE?

((A. K. Dunker)) Dept. of Biochemistry & Biophysics, Washington State University, Pullman, WA 99164-4660

The fd filamentous phage can be converted to short rods called I-forms and into spheroidal particles called S-forms, out of which the DNA is largely extruded [1]. These conformational changes serve as a model for virus and phage uncoating. The assembly of the fd phage very likely involves similar conformational changes for the coat protein, but in reverse order, and so the morphological changes may also provide information about virus and phage assembly. The I-form and S-form particles have the following properties: i. native-like secondary structure; ii. non-native tertiary structure; iii. regions of nonrigid side chain packing as evidenced by abnormally high fluorescence quenching using hydrophobic molecules, by avid binding of the fluorescent probe 1-anilino-naphthalene-8-sulfonate, and by easy deformability during preparation for electron microscopy [2, 3]. The three listed properties are shared by the molten globular state [4]. Here it is proposed that non-rigid side chain packing, which is the key characteristic of the molten globular state, provides a possible mechanism for the large scale morphological changes that frequently occur during virus or phage uncoating and assembly.

1. Griffith, J., Manning, M., and Dunn, K., (1981) *Cell* **23**: 747-753.
2. Dunker, A. K., Ensign, L. D., Arnold, G. E. and Roberts, L. M. (1991) *FEBS Lett.* **292**: 271-275.
3. Dunker, A. K., Ensign, L. D., Arnold, G. E. and Roberts, L. M. (1991) *FEBS Lett.* **292**: 275-278.
4. Ohgushi, M and Wada, A. (1983) *FEBS Lett.* **164**: 21-24.

M-Pos240

ICOSAHEDRAL VIRUS LATTICES VIA UNIFORM PACKING DYNAMICS

((C.J. Marzec and L.A. Day)) Public Health Research Institute, New York, NY, 10016

The Caspar-Klug quasi-equivalence theory posited that, of all ways to enclose a volume with nearly identical subunits, trigonal coordination lattices of the icosahedron, with three subunits per facet, show the least perturbation of chemical bonds from subunit to subunit. But polyoma, with pentamers at all 72 of its lattice points, afforded a counterexample to quasi-equivalence, which requires that polyoma contain 12 pentamers and 60 hexamers. The questions we address are why the coordination lattices are still found empirically, and how might the capsid morphological unit (MU) enter into determining capsid architecture.

We represent the MU as $\sigma_{MU}(\Omega)$, a mass density written via spherical harmonics. The icosahedrally symmetrical capsid surface density, $\sigma_C(\Omega)$, is constructed by rotating σ_{MU} into the MU positions on the 20 faces. The net capsid self-interaction E_{INT} is given by a double surface integral, wherein all mass elements interact via an arbitrary function of distance. The MUs wander on the sphere, dynamically finding local minima of E_{INT}. The, simplest global measure of interaction is the variance of σ_C; a smooth or regular capsid has small variance. The variance also follows from a Poisson-Boltzmann calculation of the electrostatic free energy, taking σ_{MU} as a charge distribution. In the best patterns, round MUs position themselves on the vertices of the coordination lattices; pentameric MUs behave similarly. But patterns made by trimeric MUs do not always relate to coordination lattices. If non-round MU's rotate about the local axis as well as move on the sphere, they form patterns like those observed in papilloma (star-like and pentagonal MUs) and $N\beta V$ (trefoil MUs).

Quasi-equivalence uses local subunit bonding patterns to form MUs; uniform packing invokes global packing of MUs, which are input with a given shape. Round MUs and most interaction functions generate the coordination lattices; but non-round MUs need a more general class of lattices.

M-Pos241

DETERMINATION OF ROTATIONAL SYMMETRY IN MACROMOLECULES.

((E. Kocsis, M.E. Cerritelli, B.L. Trus and A.C. Steven)) LSBR-NIAMS and CSL-DCRT, NIH, Bethesda, MD 20892 (Spon. by S. Yoshikami)

Many biological macromolecules possess rotational symmetry. However, when such symmetry is not strongly expressed, it is necessary to have an objective quantitative method to detect it, and to establish its statistical significance. Hitherto, the rotational power spectra of individual particles have been mainly used for this purpose. However, if the symmetry is not conspicuous, this analysis can be indeterminate because the spectral peaks may not be much higher than background levels, since the number of repeating elements contributing to each spectral component is relatively small. To address this problem, we have devised statistical tests that combine the information content of populations of particles. One test involves calculating the quantity $P(n,r,N) = \Pi\,(I_n^{(i)}(r)/I_n^{*}(r))$, where $I_n^{(i)}(r)$ and $I_n^{*}(r)$ are, respectively, the intensities of the n-th components of the rotational spectra of the i-th particle, and of appropriately normalized background images, in radial sector r. The product applies to a total of N particles. $P_n(r)$ gradually diverges if n-fold symmetry is consistently observed within the population, and otherwise converges. In a second test, the means of $I_n^{(i)}(r)$ and $I_n^{*}(r)$ are compared on the basis of the well-known t-distribution which gives an estimate of whether these two populations are different at a given significance level. These formulas were tested using micrographs of negatively stained HSV-2 hexons, which were confirmed to have 6-fold symmetry, and on sets of unit cells from 2-D crystals of the gp8 connector protein of phage T7, which was found to observe 12-fold symmetry. Currently, the tests are being applied to micrographs of free-standing connectors.

M-Pos242

MAXIMUM AND MINIMUM CHANGES IN THE STABILITY OF GLOBULAR PROTEINS UPON MUTATION THAT ALTERS THE HYDROPHOBIC EFFECT. ((BK Lee)) NCI, NIH, Bethesda, MD 20892.

One of the most direct methods of measuring the magnitude of the hydrophobic effect on protein stability is to observe the change in stability when an internal hydrophobic residue is mutated to another of smaller size. Results of such measurements have, however, been confusing because they vary greatly and are generally considerably larger than expected from the tansfer free energies of corresponding small molecules. Here I present a thermodynamic argument to suggest (1) that the variation is mainly due to that in the flexibility of the protein molecule at the site of mutation, (2) that the transfer free energies approximately give the minimum of the range of variations, and (3) that the maximum is approximately given by the work of cavity formation in water. The best numerical agreement betwen the small molecule and the protein systems is obtained when the data from the small molecule system is expressed as the molarity-based standard free energies without other corrections.

M-Pos243

A RAPID AND ACCURATE ROUTE TO CALCULATING SOLVATION ENERGY USING A CONTINUUM MODEL WHICH INCLUDES SOLUTE POLARIZABILITY. ((D. Sitkoff, K. A. Sharp and B. Honig)) University of Pennsylvania, Phila., PA; Columbia University, NY, NY.

The solvent is critical to molecular conformation and binding processes. We present a method of calculating solvation free energies which is simple and rapid, yet relies on basic physical principles. The method computes the electrostatic contributions to solvation through finite difference solutions of the Poisson-Boltzmann equation, with the solute represented in molecular detail and water represented as a dielectric continuum. Cavity/vanderwaals energies are added as a surface area dependent term, with surface tension coefficients derived from hydrocarbon transfer experiments, to obtain the full solvation free energy. The method is tested for a set of small molecules representing the amino acid side chains and backbone, and is found to accurately reproduce experimental vacuum to water transfer free energies using OPLS-derived atomic charge and radius parameters. New parameters are developed for calculations in which effects of electronic polarization are included; the completed method allows solvation free energy calculations to be performed on a wide range of biomolecular systems. The method is faster than molecular simulation approaches, and, as will be discussed, is more accurate than approaches based on simple burial of surface area.

M-Pos244

MONTE CARLO SIMULATIONS OF THE ION DISTRIBUTIONS AND FIELD GRADIENTS NEAR $d(AT)_5$-$d(AT)_5$. ((M. Braskett and P.A. Mills)) Dept. of Chem., Hunter College, 695 Park Avenue, New York, NY 10021.

We have computed the ion distributions near the oligonucleotide d(AT)5-d(AT)5 using two models of the oligoanion, the solvent and the solute. In our first model, the partial charges of all the atoms of oligoanion are included, the solvent is a uniform dielectric constant and the mobile electrolyte is composed of hard sphere univalent charges. In our second model, the charges of the oligoion are located at the phosphate residues, dielectric saturation is included using a distance dependent dielectric constant and a soft potential is assumed among the oligoion charged residues and the electrolyte ions. The ion distributions near the two models of the oligoanion are significantly different at comparable oligomer and salt concentrations. In order to determine the accuracy of the various models, we attempt to fit our data to recent ^{23}Na NMR relaxation data near the oligonucleotide $d(GATATATC)_2$ obtained from another laboratory[1]. We assume a two-state model for the counterion relaxation and compute the "bound" counterions by defining a volume containing these counterions. This volume is obtained by computing the field gradient experienced by the counterions throughout the solution during the simulations. From these field gradients we define two regions of space: near and far from the oligoion. We compute the number of counterions falling into the near volume as a function of salt concentration and for different oligonucleotide models. This number is compared with existing oligoelectrolyte theories[2-4] and the NMR data in order to determine the best model for simulating the oligonucleotide and its surrounding solution. [1]Obtained from Prof. William Braunlin, Univ. of Nebraska, Lincoln, NE. [2]M.O. Fenley, et.al., (1990) Biopolymers, 30, 1191-1203. [3]T.G. Dewey (1990) Biopolymers, 29, 1793-1799. [4]M. Satoh, et. al. (1988) Biophysical Chemistry, 31, 209-215.

M-Pos245

SIMULATIONS OF LINEAR POLYELECTROLYTES. ((C. E. Reed, and W. F. Reed)) Physics Department, Tulane University, New Orleans LA 70118 (Spon. by W. F. Reed)

We simulate isolated linear polyelectrolyte molecules using a 3-fold rotational isomeric state model with charged units and Debye-Hückel repulsion, hoping to test theories of the shape of these molecules, or failing that, find empirical rules for predicting observables such as radius of gyration Rg and light scattering function $P(\theta)$ from important parameters such as intrinsic persistence length, charge per unit contour length ρ, and Debye length $1/\kappa$. We can use pH - pKa controlled ionization, making ρ an observable. We especially want to test the ideas of electrostatic persistence length Le and electrostatic excluded volume (EEV). EEV seems confirmed for long flexible polymers. Le is hard to isolate and thus hard to confirm. Le is not sufficient by itself, but when combined with EEV, reproduces power laws for Rg as a function of $1/\kappa$ or ρ. An expression of Noda et al. fits the $P(\theta)$ of flexible charged chains well. We compare these ideas to light scattering by a charged polysaccharide, hyaluronate. These simulations were originally done using Metropolis Monte Carlo with reptation. We present a new method, "biased reptation Monte Carlo", which simulates long chains more efficiently, letting us sharpen previous conclusions. Supported by NSF grant MCB9116605.

M-Pos246

COMPLEX VECTOR REPRESENTATION OF NUCLEOTIDE SEQUENCES Y. Magarshak and C. J. Benham, Department of Biomathematical Sciences, Mount Sinai School of Medicine, New York, N.Y. 10029

Mathematical methods have been developed for describing RNA secondary structures. These provide a rigorous yet efficient way to treat transitions from one secondary structure to another, which we have proposed can occur as motions of loops within RNAs having appropriate sequences. An RNA sequence is described as a complex vector. The 48 possible different types of symmetries between nucleic acid sequences are described. Each possible secondary structure determines a symmetric, signed permutation matrix. The collection of all secondary structures, possible for a particular nucleotide sequence, is comprised of all matrices of this type whose left multiplication with the sequence vector leaves that vector unchanged. Transitions between secondary structures are given as the product of the two corresponding structure matrices. This formalism efficiently describes nucleic acid sequences, allowing questions relating to secondary structures and transitions to be addressed using the powerful methods of abstract algebra. In particular, it provides a conceptually simple description of all secondary structures, specifically including pseudoknots. A second method for describing secondary structures also is presented, which uses diagrammatic techniques that permit clear visualization of the structures involved.

M-Pos247

GANGLIOSIDE G_{M1} PREFERENCE FOR $P_{\beta'}$ GEL PHASES DEPENDS UPON THE ACYL CHAIN LENGTH AND DEGREE OF UNSATURATION. ((*P. Palestini, †M. Allietta, *G. Tettamanti, ††T.E. Thompson and †T.W. Tillack)) Department of †Pathology and ††Biochemistry, University of Virginia, Charlottesville, VA 22908, USA, and *Department of Medical Chemistry and Biochemistry, the Medical School, University of Milan, 20133 Milano, Italy.

In two-component phosphatidylcholine bilayers with coexisting fluid and $P_{\beta'}$ gel phases, the distribution between phases of low concentrations of glycosphingolipids can be determined by freeze-etch electron microscopy after labeling the glycolipid with a suitable protein. We have found that the glycolipid distribution depends upon the lipid species. (P. Rock et al., Biochemistry 30:19-25,1991). Using this technique with cholera toxin as the protein label and bilayers formed from dipalmitoyl- and dielaidoylphosphatidylcholine (1:1) containing < 1 mol % G_{M1}, we have studied the distribution of a family of G_{M1} homologues differing in the acyl chain and sphingoid base moieties. The G_{M1} preference for the $P_{\beta'}$ ripple phase decreases with decreasing acyl chain length and increasing unsaturation. G_{M1} with either a C18:1 or C20:1 sphingoid base showed similar distributions in fluid and gel phases. When the molecules are preferentially found in the $P_{\beta'}$ phase, they are positioned along the same unique locus in both ∧ and ∧/2 forms of the ripple structure. This localization and acyl chain dependence probably reflect molecular packing defects in the $P_{\beta'}$ phase. Supported by NIH grants GM-23573 and GM26234.

M-Pos248

COMPUTER SIMULATIONS OF CHOLINE HEAD GROUP DYNAMICS. ((P.H. Konstant[1], L.L. Pearce[2] and S.C. Harvey[1,2])) [1]Dept. of Physiology and Biophysics, [2]Dept. of Biochemistry, University of Alabama at Birmingham, Birmingham, AL 35294-0005. (Spon. by J. Schafer)

Membrane properties are determined by the dynamics of both the acyl chains and head groups of their constituent phospholipids. Previous work has focused on the dynamics of the acyl chains though both ^{2}H-NMR and computer simulation. In the current study, we have investigated the dynamics of the choline head group in dipalmitoylphosphatidylcholine (DPPC) by computer simulation using Langevin dynamics and a Marcelja-type mean field. We calculated phosphorus-carbon dipolar couplings (D_{P-C}) and compared them to those obtained by ^{13}C-NMR. Simulations varying the harmonic constraint on the choline nitrogen with an average N position in the plane of the phosphorus and perpendicular to the acyl chains all show close agreement with experiment in the time-averaged orientation of the glycerol carbon positions and systematic variation in the choline group carbons. Attempts to reduce this discrepancy by changing the average position of the choline nitrogen above the plane have been carried out with some success. These results suggest that an anharmonic constraint or a more accurate treatment of solvation and electrostatics may be required for accurate simulations of head group dynamics.

M-Pos249

DYNAMICAL PROPERTIES OF PHOSPHOLIPID MEMBRANES EXPLORED WITH DEUTERIUM NMR RELAXATION. ((Todd M. Alam, Theodore P. Trouard, Constantin Job, and Michael F. Brown)) Department of Chemistry, University of Arizona, Tucson, Arizona 85721.

Studies were designed to test the hypothesis that the dynamics of membranes include collective fluctuations of the assembly in additional to molecular and segmental motions. An additional objective was development of ^{2}H NMR methods for investigating membrane constituents at the molecular and atomic levels in the biologically relevant liquid-crystalline phase. ^{2}H NMR lineshapes yield knowledge of equilibrium properties in terms of motionally averaged components of the quadrupolar coupling tensor; whereas relaxation rates depend on dynamical properties through mean-squared amplitudes and reduced spectral densities of the fluctuations. Spin-lattice (R_{1Z}) and quadrupolar-order (R_{1Q}) rates were measured for bilayers of DMPC-d_{54} ± cholesterol aligned on glass substrates.[1] Director-frame spectral densities $J_1^{dir}(\omega)$ and $J_2^{dir}(\omega)$, where $\omega = \omega_0$ and $2\omega_0$, were calculated from angularly dependent relaxation rates for the first time, and analyzed theoretically in terms of models for the molecular and collective dynamics of lipids. The results show clearly that the bilayer interior is essentially liquid hydrocarbon and point to the role of the membrane lipid-water interface in governing physicochemical properties of biological membranes. [1]T.P. Trouard et al. (1992) *Chem. Phys. Lett.* 189: 67. Supported by NIH grants GM41413, EY03754, RR03529, and NIH postdoctoral fellowship EY06346 (TMA).

M-Pos250

Physico-chemical Properties of a membrane lipid from *Acholeplasma laidlawii* forming reversed micelles.

Göran Lindblom, Jón B. Haukson, Leif Rilfors, Björn Bergenståhl, Åke Wieslander and Per-Olof Eriksson. University of Umeå, S-90187 Umeå, SWEDEN

Monoglucosyldiacylglycerol (MGlcDAG) and diglucosyldiacylglycerol (DGlcDAG) are the most abundant lipids in the *A. laidlawii* membrane. A third glucolipid, 3-O-acyl-monoglucosyldiacylglycerol (MAMGlcDAG) is synthesised by strain A-EF22 when the membrane lipids contain large amounts of long, saturated acyl chains. The physical chemistry of membrane lipids, in particular their ability to form different aggregate structures, constitutes the basis for the regulation of the lipid composition in the membrane, and therefore an understanding of the phase equilibria of membrane lipids is crucial. MGlcDAG and MAMGlcDAG, isolated from *A. laidlawii* strain A-EF22 membranes, were studied by ^{2}H NMR, ^{1}H NMR, ^{1}H NMR diffusion measurements, calorimetry and X-ray diffraction. MAMGlcDAG, containing 96 mol % saturated acyl chains formed a gel or crystalline phase up to about 80 °C, where a transition occurred to a *reversed micellar (L_2) phase*. This is an unexpected finding for a membrane lipid. Despite the high melting temperature of this lipid it homogeneously mixes with other membrane lipids at physiological temperatures. MGlcDAG formed lamellar, reversed hexagonal and cubic liquid crystalline phases. MAMGlcDAG is synthesised under conditions when the phase equilibria of MGlcDAG are shifted from a non-lamellar towards a lamellar phase. Apart from MAMGlcDAG, MGlcDAG is the only major lipid in *A. laidlawii* strain A-EF22 that is able to form reversed aggregate structures. It is concluded that MAMGlcDAG assists MGlcDAG in maintaining an optimal molecular packing, or negative curvature, of the lipids in the membrane.

M-Pos251

EFFECT OF DIACYLGLYCEROLS AND CA^{2+} ON THE STRUCTURE OF PHOSPHATIDYLCHOLINE/PHOSPHATIDYLSERINE BILAYERS. ((E.M. Goldberg[1], D.B. Borchardt[2] and R. Zidovetzki[1])) Departments of Biology[1] and Chemistry[2], University of California, Riverside, CA 92521.

Interactions of five diacylglycerols (DAGs), diolein (DO), 1-stearoyl,2-arachidonoylglycerol (SAG), 1-oleoyl,2-acetylglycerol (OAG), dioctanoylglycerol (diC$_8$), and dipalmitin (DP), with lipid bilayers composed of mixture of phosphatidylcholine (PC) and phosphatidylserine (PS) was studied using ^{2}H-NMR measurements. Incorporation of either acyl chain perdeuterated PC or PS as an ^{2}H-NMR probe allowed us to discern the effects of DAGs on either PC or PS bilayer component. Addition of 25 mol% DP effected lateral phase separation of the lipids into fluid-like and gel-like domains; the effects were similar for either PC or PS components. A different effect was exhibited by SAG: 25 mol% of this DAG induced a presence of a non-bilayer phase in PC, but not in the PS lipid component. Addition of 25 mol% of DO, OAG or diC$_8$ produced relatively minor effects on the bilayer structure. However, addition of Ca^{2+} (1:2 mole/mole to PS) to PC/PS bilayers containing these DAGs resulted in formation of non-bilayer lipid phases. The observed effects may be relevant to the mechanism of activation of protein kinase C by PS, Ca^{2+} and DAG co-factors.

M-Pos252

NMR STUDIES OF THE EFFECT OF ELECTRICAL FIELDS ON LIPID-WATER AND LIPID-GLYCEROL BILAYERS.

((P.D. Osman[#] and B.A.C. Cornell[*])) [#]CSIRO Division of Applied Physics, PO Box 218 Lindfield NSW 2070, and [*]CSIRO Division of Food Processing, PO Box 52 North Ryde NSW 2113 Australia.

We have shown that glycerol/lipid samples form aligned fluid bilayers with a very high electrical impedance, making them well suited to studies of the effect of intense electric field on lipid bilayers. A comparative study has been carried out, using NMR and impedance spectroscopy, of samples prepared from phospholipids and water and the same phospholipids with dry and slightly wet glycerol. Examples of the effect of electric field on lipid bilayers will be presented. ^{2}H NMR spectra obtained in the presence of electric fields up to 16 MV/m show partial alignment of the glycerol/lipid samples with the electrical field. An electric field induced transition from the L_α to hex II phases has been observed in DOPE/water samples using ^{13}C NMR. The possible mechanisms for such a transition will be described in particular the effect of adiabatic ohmic heating has been evaluated using the temperature dependence of the quadrupole splitting of the terminal methyl of a perdeuterated DMPC/glycerol/water sample. Preliminary results will also be given of conformational changes in the choline region of EYPC/glycerol bilayers subjected to an electrical field.

M-Pos253

PHOSPHATIDYLETHANOL IS A POTENT PROMOTER OF HIGHLY CURVED NONBILAYER STRUCTURES ((Y.-C. Lee, G. Moehren, N. Janes*, Z. Gatalica, J. Krupnick, E. Rubin, J.B. Hoek*, and T.F. Taraschi*)) Department of Pathology and Cell Biology, Thomas Jefferson University, Philadelphia, PA 19107.

Ethanol is metabolized by phospholipase D (PLD) through transphosphatidylation to form an unusual anionic phospholipid, phosphatidylethanol (PtdEth), which possesses a small, nonpolar headgroup ($-CH_2-CH_3$). This unusual feature raises the possibility that PtdEth may impart unique properties to membranes. To investigate this possibility, dilute levels (5 mole%) of the dioleoyl species of PtdEth, PtdCho, phosphatidic acid (PtdOH), phosphatidylethanolamine (PtdEtn), and phosphatidylglycerol (PtdGro) were introduced into a liposomal matrix consisting of 1-palmitoyl-2-oleoyl-PtdEtn and studied by ^{31}P NMR. PtdEtn membranes undergo a lamellar to inverted hexagonal transition ($L_\alpha \rightarrow H_{II}$) in response to increasing temperature. Lipids that depress this temperature promote curved structures, while those that raise it stabilize the bilayer structure. The ability to promote curved structures is shown to correlate with headgroup size as predicted by shape theories of lipid structure (PtdCho < PtdGro < PtdEtn < PtdOH < PtdEth), except for PtdEth, which enhances curvature with a potency far in excess of any other phospholipid. Thus, PtdEth may assume an unusual conformation in the membrane that minimizes the effective size of the headgroup. Additional support for such an unusual conformation is inferred from a unique and potent depression of the main transition that is induced by PtdEth, but none of the other phospholipids. PHS AA07215, AA07463, AA07186, AA00088.

M-Pos254

ALCOHOL PARTITIONING IN MICROSOMAL LIPOSOMES: EFFECTS OF PHOSPHATIDYLINOSITOL ((L. Ma, T.F. Taraschi, E. Rubin, and N. Janes*)) Pathology and Cell Biology, Thomas Jefferson University, Philadelphia, PA 19107.

The nonspecific binding of benzyl alcohol to model and liver microsomal liposomes is studied with a newly developed NMR method. Shown in Fig. 1A is the partitioning trace (and its derivative, offset below) of benzyl alcohol in dipalmitoyl lecithin, showing the sensitivity of partitioning to the organization of the membrane. The gel, ripple, and liquid-crystalline states exhibit characteristic receptivity to alcohol partitioning. Partitioning traces showing the effects of phosphatidylinositol (PtdIns) in microsomal phospholipid membranes are shown in Figure 1B. Microsomal PtdIns was isolated by HPLC and titrated into liposomes composed of the remaining microsomal phospholipids in their natural ratios. Increasing the level of PtdIns, as shown, increases the receptivity of the membrane to alcohol partitioning. At natural PtdIns levels (8.5%), a discontinuity in partitioning near 37°C evidences a change in membrane organization. PHS AA07215, AA07463, AA07186, AA00088.

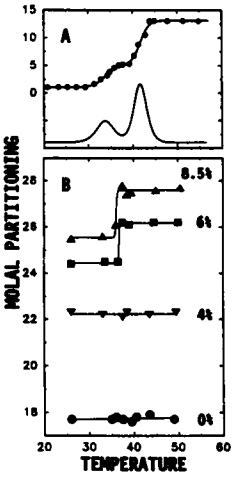

M-Pos255

PHYSICOCHEMICAL CHARACTERIZATION OF AQUEOUS LIPID PHASES OF RELEVANCE TO INTESTINAL FAT DIGESTION AND ABSORPTION: A ^2H NMR AND X-RAY DIFFRACTION STUDY. ((Philip W. Westerman and Li Chen)) Dept. of Biochemistry, Northeastern Ohio Universities College of Medicine, Rootstown, OH 44272 and Liquid Crystal Institute, Kent State University, Kent, OH 44242.

The phase behavior of several model monoglyceride/fatty acid/H_2O systems at 37°C has been characterized by ^2H NMR. The time-averaged quadrupole splitting of a $-C^2H_3$ group, synthetically incorporated into either monoglyceride or fatty acid, varies according to whether it exists in a micellar, multi-lamellar (MLV) or solid phase. From the relative intensities of powder patterns in the wide-line ^2H NMR spectra, we have identified one-, two-, and three-, phase regions in the equilibrium phase diagram and determined the chemical composition of each phase. Incorporation of cholesterol into monoglyceride/fatty acid mixtures tends to stabilize the multi-lamellar phase. Addition of dimyristoylphosphatidylcholine further increases the proportion of lipids in the MLV phase. Introduction of unsaturation into either the fatty acid or monoglyceride tends to produce cubic and hexagonal phases which are readily identified by x-ray diffraction. (Supported by the Ohio Affiliate of the American Heart Association).

M-Pos256

SPONTANEOUS VESICLE FORMATION BY EQUIMOLAR MIXTURES OF LYSO PHOSPHATIDYLCHOLINE AND FATTY ACIDS

((Shastri P. Bhamidipati and James A. Hamilton)) Biophysics Department, Boston Univ. School of Medicine, 80 E. Concord St., Boston MA 02118

Aqueous dispersions of lyso 1-acyl phosphatidylcholine (lyso-PC) and fatty acids (FA) in equimolar ratio have earlier been shown to form multilamellar structures by ^{31}P NMR and electron microscopy [M.K. Jain et al., Nature 284, 486-487 (1980)]. We have found that small unilamellar vesicles (SUVs) can be formed spontaneously from equimolar mixtures of lyso-PC ($C_{16:0}$) and oleic acid ($C_{18:1}$). A dried lipid film is hydrated in 50mM Tris buffer at pH 7.0-7.5 and room temperature and vortex mixed for several minutes. The resulting lipid dispersion appeared translucent with a slight bluish tinge typical of SUVs prepared by sonication of phospholipids. The ^{31}P NMR spectrum of this dispersion was also characteristic of SUVs, showing partially resolved signals for outer and inner monolayer lyso-PC. The ability of these unilamellar vesicles to retain trapped contents was established using pyranin, a membrane-impermeable fluorescent dye. Inclusion of an equimolar amount of cholesterol in the lyso-PC/FA equimolar mixture did not have any effect on the spontaneous formation of vesicles from these dispersions in the pH range of 7.0-7.5. Similar results were observed for equimolar mixtures consisting of different chain length lyso-PCs ($C_{14:0}$ and $C_{18:0}$)) and oleic acid.

M-Pos257

MEASUREMENT OF MOLECULAR SHAPE PARAMETERS OF MEMBRANE LIPIDS IN OPTIMALLY PACKED, HIGHLY CURVED BILAYERS ((W.J. Baumann, V.V. Kumar and B. Malewicz)) Hormel Institute, University of Minnesota, Austin,MN 55912.

The dynamic shape of a membrane lipid affects membrane curvature, bilayer asymmetry, phospholipid packing and membrane stability. Thus, by optimizing membrane stability and lipid packing in bilayers of known asymmetry and curvature, we have been able to actually measure for the first time molecular shape parameters, such as head group areas, in individual leaflets of highly curved bilayers. The curvature of small unilamellar vesicles (SUV) is readily measured by freeze-fracture EM; the phospholipid distribution between leaflets is determined by ^{31}P NMR in the presence of paramagnetic ions (Pr^{3+}); optimal lipid packing is typically assessed by minimizing motional parameters, such as relaxations (T_2, T_1) of phospholipid head group phosphorus; membrane stability is optimized by monitoring barrier properties against ions (Pr^{3+}, Mn^{2+}) or small molecules (calcein, [^{14}C]glucose), and particularly by probing the "quality" of the bilayer surface in terms of its resistance to phospholipase A_2 attack as we can follow by ^{31}P NMR in real time. Application of this novel approach is illustrated on POPC/lysoPC and POPE/lysoPC SUV. The head group areas measured on individual leaflets of optimally packed, highly curved bilayers are very similar to those that have been measured on monolayers near the collapse pressure. (Supported by NIH grant HL08214, UofM Grant-in-Aid 15214, and The Hormel Foundation).

M-Pos258

CHAOTROPIC ANION - PHOSPHATIDYLCHOLINE MEMBRANE INTERACTIONS: AN ULTRA HIGH FIELD NMR STUDY. ((G.L. Jendrasiak, R. Smith, A.A. Ribeiro)) (Intro by B. Karvaly-Kuemmel) East Carolina University, School of Medicine, Greenville, NC 27858-4354, Duke University Medical Center, Durham, NC 27710.

NMR studies on the interaction of the linear chaotropic anions, SCN^- and $SeCN^-$, with sonicated egg phosphatidylcholine (EPC) vesicles have been carried out at field strengths up to 14.1 Tesla. At 600 MHz, both anions cause splitting or increased splitting of the choline $N^+(CH_3)_3$, CH_2N^+ and O_3POCH_2 H-1 resonances with $SeCN^-$ being somewhat more effective in this action than is SCN^-. No changes were observed in the glycerol CH_2OP and CH_2OCO H-1 resonances and the phosphate P-31 resonance of the head-group region. The C-13 spectrum was unchanged by the presence of the anions. After 18 hours of exposure to the anion, the H-1 resonance splittings but not the chemical shift values returned to those prior to anion exposure. Increasing the temperature of the vesicles decreased the anion induced splitting, but, upon return to the beginning temperature, the chemical shifts did not return to their original values. The results are considered in terms of the "molecular electrometer" model recently developed by Seelig and co-workers.

M-Pos259

PHASE PERCOLATION IN THREE-COMPONENT LIPID BILAYERS: EFFECT OF CHOLESTEROL ON AN EQUIMOLAR MIXTURE OF TWO PHOSPHATIDYLCHOLINES.

((+Paulo F. Almeida, ++Winchil L.C. Vaz, and +T.E. Thompson)) +University of Virginia, Charlottesville, VA 22908, USA and ++Max-Planck Institute for Biophysical Chemistry, Goettingen, FRG.

The lateral diffusion of a phospholipid fluorescent probe is studied in lipid bilayers of dimyristoyl phosphatidylcholine/distearoyl phosphatidylcholine/ cholesterol composed of an equimolar mixture of the two phosphatidylcholines and variable fractions of cholesterol, using fluorescence recovery after photobleaching. The fractions of solid and fluid phases at equilibrium at each temperature were estimated from the excess heat capacity curves obtained with differential scanning calorimetry. The diffusion results are interpreted in terms of percolation of the fluid or solid phases. Fluid domain sizes are estimated from the behavior of the fluorescence fractional recovery. Addition of cholesterol causes a shift in the percolation threshold to smaller fractions of fluid phase; the average size of the fluid-phase domains does not change. *(Supported by grants GM-14628 and GM-23573 from the NIH and by the Max-Planck-Institute für Biophysikalische Chemie).*

M-Pos260

INFLUENCE OF PHOSPHATIDYLETHANOLAMINES ON BILAYER STRUCTURE. Gregory W. Hunter and Thomas C. Squier. University of Kansas, Lawrence, KS 66045-2106.

To better understand the mechanism in which phosphatidylethanolamine (PE) regulates the transport properties of many integral membrane proteins, we have used frequency-domain fluorescence spectroscopy to investigate the rotational dynamics of TMA-DPH in binary mixtures of dioleoylphosphatidylethanolamine (DOPE) and dioleoylphosphatidylcholine (DOPC). Utilizing unilamellar vesicles (diameter ≈ 100 nm), we find that physiological concentrations of PE (●) alter both membrane lipid packing order (see figure) and rotational dynamics. In order to differentiate steric effects of the small PE headgroup from specific electrostatic effects, we have compared the influence of PE on bilayer structural properties with that of N-methylated derivatives of PE [N-methyl PE (□) and N,N-dimethyl PE (■)]. Both methylated PE's have virtually no effect on membrane dynamics. These results indicate a unique ability of PE to modulate the physical properties of the bilayer.

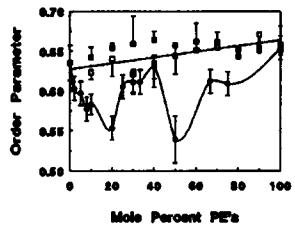

M-Pos261

A TIME-RESOLVED FLUORESCENCE SPECTROSCOPIC COMPARISON OF PHOSPHOLIPID BILAYERS CONTAINING MIXED CHAIN POLYUNSATURATED PHOSPHOLIPIDS.

((Charles D. Niebylski and Norman Salem, Jr.)) Laboratory of Membrane Biochemistry and Biophysics, DICBR, NIAAA, NIH, Bethesda, MD 20892

Phospholipid species containing 18:0 at sn-1 and polyunsaturates at sn-2 predominate in the brain. Time-resolved fluorescence anisotropy (using the single photon counting method) was employed to measure the rotational correlation time (ϕ) and limiting anisotropy (r_∞) of bilayer probes in unilamellar vesicles containing various polyunsaturated fatty acids. Small unilamellar vesicles composed of 100% 1-18:0,2-X-PC (phosphatidylcholine), where X= 18:1n9, 18:2n6, 18:3n6, 20:4n6, 20:5n3 or 22:6n3, were prepared and co-dispersed with the probe 1,6-diphenyl 1,3,5-hexatriene (DPH) or 1(4-trimethylammonium-phenyl)6-phenyl-1,3,5-hexatriene (TMA-DPH). As expected, in the liquid-crystalline phase (20°C and 37°C), the 18:0/18:1-PC membranes were more ordered than those containing 18:2n6, and both 18:1- and 18:2-containing vesicles were more ordered than those containing species with 3 or more double bonds. At ≥20°C, there were no significant differences between the ϕ and r_∞ values of either probe in vesicles containing 20:4, 20:5 and 22:6, all were in equally disordered states at or above 20°C. As the vesicles approached the gel-state (5°C), the rotational correlation times for DPH decreased significantly for each successive increase in unsaturation. The faster correlation times in 18:0/22:6-PC indicate a less ordered environment immediately next to the probe molecules. However, the limiting anisotropy of DPH reached a minimum value with the 18:2n6 species (.023) and then showed significant increases with further unsaturation with 20:4n6(.034), 20:5n3(.039) and 22:6n3(.044). TMA-DPH exhibited the same trends in time-resolved order parameters for these species at 5°C. These studies suggest that mixed-chain polyunsaturated phosphatidylcholines organize into structures with a high degree of local acyl chain disorder and yet maintain a tight packing of phospholipids on a global scale. Membranes composed of a variety of polyunsaturated species may thus contain unique structures capable of a multiplicity of states due to their flexible and dynamic charcteristics.

M-Pos262

ANISOTROPY OF T2 RELAXATION IN MULTILAMELLAR DISPERSIONS AND ORIENTED BILAYERS OF PURE AND MIXED LIPID SYSTEMS ((M. A. Monck*, C. Morrison†, P.cullis*, and M. Bloom†)). * Dept. of Biochemistry, † Dept. of Physics, U.B.C. Vancouver, Canada V6T 1Z3.

^{2}H NMR methods have been used to examine possible mechanisms of T2 relaxation in multilamellar dispersions and oriented bilayers of various pure and mixed phospholipid systems. The use of deuterium labelling in lipid membranes provides a convenient probe for obtaining motional and geometrical information on lipids in this environment. Since T2 relaxation times are sensitive to relatively slow motions ($\tau \approx 10^{-3} - 10^{-6}s$) on the NMR timescale it is possible to derive information about slow motional processes (surface undulations, diffusion and/or collective motions) which can contribute potential relaxation mechanisms in a lipid environment.

The orientation dependence of T2 relaxation rates in some lipid dispersions studied has indicated that surface undulations provide a potent relaxation mechanism in such systems. However, the orientation dependence found in oriented multilayers disagrees with the existing theory for surface undulations and suggests that such a mechanism is not solely responsible for T2 relaxation processes here. Results from individual and mixed lipid systems will be presented and the significance of these results will be discussed.

M-Pos263

PHOSPHOLIPID HEADGROUP COMPOSITION INFLUENCES ACYL CHAIN PACKING FREE VOLUME OF LIQUID CRYSTALLINE BILAYERS. ((Andrew P. Mone and Burton J. Litman)) Department of Biochemistry, University of Virginia Health Sciences Center, Charlottesville, VA 22908

To explore the role of phospholipid headgroup composition in determining the acyl chain packing free volume of a membrane bilayer, the time resolved anisotropy of the hydrophobic membrane probe DPH was measured in a series of large unilamellar vesicles. While maintaining the same acyl chains, the headgroup composition of the vesicles was varied. Membranes with 0, 25, 50 and 75 mole % of POPE or POPS in POPC were studied at 15, 25 and 37 °C. In this report, the fluorescence anisotropy of DPH is characterized by a fractional volume parameter (f_v), which models the volume available for reorientation of the probe within the hydrophobic regions of the bilayer and hence reflects the bilayer acyl chain packing free volume. POPE and POPS decrease f_v and increase the mean average fluorescent lifetime relative to the values measured for DPH in pure POPC vesicles. The relative value of f_v changes with headgroup composition in the order PC > PS > PE. Furthermore, at a given temperature f_v is a linear function of the mole % POPE or POPS. Dynamic fluorescence measurements were also made upon DPH in a series of rhodopsin containing vesicle samples. The presence of rhodopsin in these bilayers suppressed f_v and somewhat damped out the headgroup associated variation in this parameter. In these protein containing membranes f_v is again largest in POPC/rhodopsin (100:1). However, unlike the protein free vesicles, f_v in POPE/POPC/rhodopsin (50:50:1) is somewhat greater than f_v in POPS/POPC/ rhodopsin (50:50:1). (Supported by NIH grant EY00548).

M-Pos264

ATOMIC FORCE AND FLUORESCENCE MICROSCOPIES OF DEPOSITED MONOLAYERS OF L-α-DIMYRISTOYL-PHOSPHATIDIC ACID ((J.M. Mikrut*, J.B. Ketterson#, P. Dutta# and R.C. MacDonald*)) *Department of Biochemistry, Molecular Biology and Cell Biology, Northwestern University, 2153 Sheridan Road, Evanston, IL 60208, #Department of Physics and Astronomy, Northwestern University, 2145 Sheridan Road, Evanston, IL 60208. (Spon. by Ruby MacDonald)

Monolayers of L-α-dimyristoyl-phosphatidic acid (DMPA) with ~1% of the fluorescent dye DP-NBD-PE were deposited onto glass substrates and examined using atomic force and fluorescence microscopies. Companion films, containing no fluorescent dye, were prepared and examined using atomic force microscopy only. The films were transferred to the substrates at surface pressures which fall in the liquid-solid coexistence region in the phase diagram. For the films containing DP-NBD-PE, both atomic force and fluorescence microscopies can easily distinguish between the solid and liquid phases. The atomic force images show the solid phase to be uniform, relatively flat and ~2.5 nm higher than the lowest regions of the liquid phase. The liquid phase shows height variations on the order of 2.5 nm. The samples without DP-NBD-PE showed similar liquid and solid regions. The similarities and differences between the two types of films will be discussed in conjunction with the possible role which the dye plays in affecting the formation of the solid phase.

M-Pos265

FLUIDITY GRADIENTS IN INTERDIGITATED BILAYERS AS REVEALED BY MIXED-ACYL PHOSPHATIDYLCHOLINES LABELED WITH *N*-(9-ANTHROYLOXY) FATTY ACIDS. ((J.T. Mason)) Dept. of Cellular Pathology, Armed Forces Institute of Pathology, Washington, D.C. 20306-6000.

A series of 1-decanoyl-2-stearoyl-phosphatidylcholine molecules were synthesized where the stearic acid chain was labeled with an *n*-(9-anthroyloxy) moiety at either the 2, 6, 9, 12, or 16 position. The profiles of anisotropy at 316nm versus position for these probes (incorporated at a level of 0.5mol%) in C(18)C(18)PC (noninterdigitated) and C(18)C(10)PC (mixed interdigitated) bilayers was determined. For the C(18)C(18)PC bilayer in the gel or liquid-crystalline phases, a progressive and almost linear decrease in anisotropy is observed as the terminal methyl group is approached. In contrast, for the C(18)C(10)PC bilayer, the order profile decreases up to carbon 6, after which the anisotropy increases sharply and remains high until the terminal methyl group is reached. This unique fluidity gradient was observed in both the gel and liquid-crystalline phases. These results suggest that the mixed-interdigitated bilayer retains significant interdigitation of the lipid acyl chains in the liquid-crystalline phase. The temperature-dependence of the anisotropy of these probes in C(18)C(10)PC bilayers indicates that the probes partition preferentially into the liquid-crystalline phase. This effect is most pronounced for probes where the fluorescent label is located near the center of the acyl chain, the position of the terminal methyl groups in the mixed-interdigitated bilayer.

M-Pos266

BILAYER-BILAYER INTERACTIONS IN EQUILIBRIUM DISPERSIONS OF DMPC FROM SPECIFIC HEAT MEASUREMENTS.

N.L. Gershfeld[1], C.P. Mudd[2], K. Tajima[1], and R.L. Berger[3]
NIAMS[1], NCRR[2], NHLBI[3], NIH, Bethesda, MD 20892

We have measured the temperature dependence (25°-35°C) of the specific heat of dispersions of DMPC using a heat conduction calorimeter with very high sensitivity (± 0.00005 J/deg). Previous studies of the temperature dependence of the chemical potential of DMPC bilayers indicate that a dispersion consisting only of unilamellar vesicles forms spontaneously at a critical temperature T* of 29°C; at temperatures above and below T* the dispersion is multilamellar (1). The specific heat measurements show an anomaly between 28.80° and 28.96±0.01°C. We attribute this anomaly to the transformation from multilamellar dispersion to unilamellar vesicles at T* = 28.96°C. The free energy change of the transformation is equal to the cohesive energy between bilayers, and it is measured from ∫CpdT over this temperature interval. We obtained 3.20±0.03 J/mole or 0.008 ergs/cm^2 bilayer for this transformation, in agreement with other measurements of bilayer-bilayer interactions for neutral lipids (2,3). We also observed that the time $\underline{t}$ to reach equilibrium upon changing temperature increased dramatically between 28.80°C and T*, following the relation $\underline{t}$~(T*-T)$^{-1}$; this "slowing-down" near T* is a general characteristic of critical phenomena.

(1) N.L. Gershfeld, J. Phys. Chem., 93(1989)5256-5261. (2) R.P. Rand, V.A. Parsegian, Biochem. Biophys Acta, 988(1989)351-376. (3) E. Evans, M. Metcalf, Biophys. J., 46(1984)423-426.

M-Pos267

A DIFFERENTIAL HEAT CONDUCTION MICROCALORIMETER FOR SPECIFIC HEAT MEASUREMENT OF LIPID BILAYERS

C. P. Mudd[1], N. L. Gershfeld[2], R. L. Berger[3], and K. Tajima[2]
[1]NCRR, [2]NIAMS, [3]NHLBI, NIH, Bethesda, MD 20892

A heat conduction calorimeter has been developed for measuring small changes in heat capacity of milligram samples of membrane lipid dispersions as a function of temperature. The operation of the instrument is based on the principle that the thermal response of the sample to a short (10 sec), electrically generated heat burst is a function of the diffusivity of the sample. Modelling studies of the instrument's performance have revealed that the output response after the heat burst is a function of only ρC_p. Calibration of the instrument experimentally confirmed this behavior. This feature obviated the need to measure the thermal conductivity in order to determine C_p from the diffusivity equation, $\eta=\lambda/\rho C_p$. The calorimeter has the following characteristics: reproducibility of loading: ±400 μJ/deg-g; baseline stability: ±10 (μJ/deg-g)/36 hrs; resolution (±1 S.D.): ±50 μJ/deg-g; sample size 600 μl.

M-Pos268

THERMODYNAMICS OF LIPID-LIPID INTERACTIONS FROM GEL-FLUID PARTITIONING. ((Charles Spink and John O'Neil)) Chemistry Department, SUNY-Cortland, Cortland, NY 13045.

Using experimental data from differential scanning calorimetry (DSC), it is possible to evaluate the free energy, enthalpy and entropy of transfer of a bilayer solute from gel to fluid phase of model membranes of synthetic phospholipids. In this approach the variation of the melting temperature, Tm, of multi-lamellar vesicles with mole fraction of solute at low concentrations (Xs<0.04) is evaluated from the DSC transition curve. Using a "regular" solution model, the free energy of transfer is obtained. Also, the enthalpy of melting is carefully evaluated in the low mole fraction region, and by its concentration dependence the enthalpy of transfer is found. We are conducting a systematic study of various membrane lipid component mixtures, and report results of measurements on transfer data for low mole fractions of dilauryl-, dimyristryl- and distearoylphosphatidyl-cholines in dipalmitoylphosphatidylcholine bilayers. This series shows the thermodynamic consequences of introducing defects (chain mismatch) in the gel phase of the bilayer.

M-Pos269

DAUNOMYCIN ALTERS THE LAMELLAR TO HEXAGONAL (H_II) PHASE TRANSITION OF 1-PALMITOYL-2-OLEOYLPHOSPHATIDYLETHANOLAMINE. ((P.V. Escriba and J.A. Garcia-Sevilla)). University of the Balearic Islands, E07071 Palma de Mallorca, Spain. (Spon. by P.V. Escriba).

Anthracyclines are potent cytotoxic drugs, used in the treatment of a variety of solid tumors and leukemias. Their cytocidal action can be exerted by the sole interaction of the drug with the plasma membrane without penetrating the cell (1). We have studied the interaction of the anthracycline daunomycin (DNM) with large multilamellar vesicles of 1 mM 1-palmitoyl-2-oleoyl phosphatidylethanolamine (POPE) by differential scanning calorimetry (DSC) in a Microcal MC-2 calorimeter. Thermograms of POPE show two peaks: one at Tc=25.2°C (ΔH=5.5 kcal/mol), for the solid→liquid crystalline transition (main transition) and another one at T_H=69.5°C (ΔH$_H$=0.5 kcal/mol) for the lamellar→hexagonal phase (H_II) transition (L→H). In the presence of DNM, at drug:lipid molar ratios 1:10 to 1:1, the calorimetric parameters of the main transition changed slightly (Tc = 24.7°C and ΔHc = 6.5 kcal/mol for the highest concentration of DNM used). The L→H transition, conversely, was markedly altered by the presence of the anthracycline. The ΔH$_H$ value decreased in a concentration dependent fashion until total depletion for a drug:lipid molar ratio of 1:1. The T_H value increased in a concentration dependent manner up to 81.5°C for a drug:lipid molar ratio of 1:2. These results indicate an stabilization of the lamellar structure of the membrane promoted by DNM, which eventually avoids the L→H transition at high concentrations. Phosphatidylethanolamines (PEs) promote the *in vivo* occurrence of non lamellar structures, which there have been associated with physiological cellular events, such as the fusion of membranes and the membrane to cytoplasm translocation of proteins (2). The DNM:PE ratios in the plasma membrane of cells exposed to this drug are close to those used in these DSC experiments, according to the levels of PE found in the plasma membrane (3), the binding of DNM to membrane lipids (3) and the doses of drug used in chemotherapy (4). The alteration of the L→H transition could modify the interaction of peripheral proteins involved in signal transduction systems and the cell cycle (e.g. G proteins, protein kinases) with the plasma membrane, and could explain the cytotoxic effects of anthracyclines. References: (1) Tritton, T.R. and Yee, G. (1982) Science 217, 248. (2) Seddon, J.M. (1990) Biochim. Biophys. Acta 1031, 1. (3). Escriba, P.V., et al. (1990) Biochemistry 29, 7275. (4) Etievant C., et al. (eds.) (1990). In "New Concepts in Cancer". MacMillan Press. London.

M-Pos270

EFFECTS OF POLYETHYLENEGLYCOL-PHOSPHOLIPID CONJUGATES ON THE PHASE TRANSITION OF DIPALMITOYL PHOSPHATIDYLCHOLINE. ((F.K. Bedu-Addo and L. Huang)) Departments of Pharmaceutical Sciences and Pharmacology, University of Pittsburgh, Pittsburgh, PA 15261

It has been found that amphipatic polymers such as dioleoyl-N-(monomethoxy polyethyleneglycol succinyl)-phosphatidylethanolamine (PEG-PE) when incorporated into the liposome significantly increase its blood circulation time. We have investigated the effect of PEG-PE on the phase transition behavior of dipamitoyl phosphatidylcholine (DPPC) using high sensitivity differential scanning calorimetry. Various PEG-PE's of different PEG chain length and acyl chain compositions were prepared and incorporated into multilamellar vesicles of DPPC. The results to date showed that increasing quantities of PEG(5000)-dipalmitoyl phosphatidylethanolamine(DPPE) decrease the height and increase the width of the main transition peak of DPPC. By 6 mol%, a well defined small peak appeared at the low temperature side of the main transition peak. This appeared to diminish in size with increasing concentration, until at about 20 mol%, where the main transition peak was greatly reduced in height, broadened and developed shoulders on both sides. The pre-transition peak disappeared at about 10 mol% PEG(5000)-DPPE. These results indicate that PEG-DPPE, although having identical acyl chains as the matrix lipid DPPC, does not mix well with DPPC even at relatively low concentrations. The drug delivery implications of these data will be discussed. Supported by NIH grant CA24553.

M-Pos271

THE EFFECT OF CHOLESTEROL AND ANDROSTEONOL ON THE THERMOTROPIC PHASE BEHAVIOR OF PHOSPHATIDYLCHOLINE BILAYERS.

((T.P.W. MCMullen, R.N.A.H. Lewis and R.N. McElhaney, Department of Biochemistry, University of Alberta, Edmonton, Alberta, Canada T6G 2H7 (Spon. by B.D. Sykes).

Using HS-DSC we found that cholesterol incorporation into PC bilayers abolishes the overall chain melting enthalpy by 50 mol % cholesterol regardless of PC acyl chain length (13:0-21:0 PC). Two melting endotherms are observed as predicted by the 3.5 lipid/cholesterol molecule stoichiometry, a sharp component is seen between 0 and 22 mol % cholesterol, and a broad component from 1 to 50 mol %. In contrast, cholesterol incorporation in chain lengths shorter than 17:0 PC show a progressive increase in the broad component Tm and a significant decrease in cooperativity, while chain lengths above 18:0 PC show a progressive decrease in Tm and a lesser degree of curve broadening. This chain length-dependent effect has been documented in peptide/bilayer interactions and is called the hydrophobic mismatch effect. Androstenol incorporation into PC bilayers up to 50 mol % abolishes the transition enthalpy of 14:0 PC but not of 16:0 or 18:0 PC. Furthermore, the stoichiometric behavior of androstenol/PC is unlike that seen in cholesterol/PC mixtures. Increased androstenol incorporation in 16:0 and 18:0 PC also induces a new, lower temperature endothermic event. FT-IR experiments indicate this endotherm is not a chain melting event. (Supported by the Medical Research Council of Canada and the Alberta Heritage Foundation for Medical Research.)

M-Pos272

THE EFFECTS OF THE ANESTHETIC DIBUCAINE ON THE KINETICS OF THE GEL-LIQUID CRYSTALLINE TRANSITION OF DPPC MULTILAMELLAR VESICLES.

((W. van Osdol*, Q. Ye, M. L. Johnson and R. L. Biltonen))
*Laboratory for Molecular Pharmacology, NIH, Bethesda, MD; & Depts. of Biochemistry and Pharmacology, Univ. of Virginia, Charlottesville, VA.

The effects of the anesthetic dibucaine on the relaxation kinetics of the gel-liquid crystalline transition of dipalmitoylphosphorylcholine ($DC_{16}PC$) multilamellar vesicles have been investigated using volume perturbation calorimetry. The temperature and pressure responses to a periodic volume perturbation were measured in real time. Data collected in the time domain were converted to and analyzed in the frequency domain, using Fourier series representations of the perturbation and response functions. The Laplace transform of the classical Kolmogorov-Avrami kinetic relation was used to describe the relaxation dynamics in the frequency domain. The relaxation time of anesthetic-lipid mixtures, as a function of the fractional degree of melting, appears to be qualitatively similar to that of the pure lipid systems, with a pronounced maximum, τ_{max}, observed at a temperature corresponding to > 75% melting. τ_{max} decreases by a factor of ~ 2, as the nominal anesthetic/lipid mole ratio increases from 0 to 0.013, but exhibits no further change at higher mole ratios. However, the fractional dimensionality of the relaxation process, n, decreases from slightly less than 2 to ~ 1, as the anesthetic/lipid mole ratio increases from 0 to 0.027. At higher mole ratios n appears to be < 1. These results are interpreted in terms of the classical kinetic theory: low concentrations of dibucaine appear to reduce the average cluster size and cause fluctuating lipid clusters to become more ramified. At the highest concentration of dibucaine, where n < 1, the system must be kinetically heterogeneous.

M-Pos273

EFFECTS OF CORD FACTOR AND ITS ANALOGUES ON MEMBRANE BEHAVIOR.

((L.M.Crowe[1], T.Ioneda[2], B.L.Beaman[3], and J.H. Crowe[1])) Biophysics Group, UC Davis, Biochemistry Dept. University of Sao Paulo, Brasil[2], and Department of Medical Microbiology, UC Davis[3].

Cord factor (trehalose 6,6'-dimycolate) is produced by numerous pathogenic bacteria which persist intracellulary; its production has been linked to inhibition of fusion between the bacteria-containing phagosome and host cell lysosomes. We have shown previously that cord factor, incorporated into bilayers, inhibits calcium-induced fusion of negatively charged liposomes. Cord factor is not a single molecule but varies in both the mycolic acid portion and in the sugar headgroup. In an attempt to relate the structure of particular cord factors with infectivity and toxicity of bacterial strains, we are investigating the effect of various natural cord factors and synthesized glycolipid molecules on liposome behavior. We have looked at calcium-induced liposome aggregation, and changes in lipid phase transitions, membrane fluidity, and headgroup associated water. The results show that cord factor analogues with chains shorter than the natural mycolic acids produce minimal changes in DPPC phase transitions, significant increases in headgroup-associated water, and increased calcium-induced liposome aggregation. (Supported by grants DCB89-18822 from NSF and 5-RO1-AI20900-08 from NIH.)

M-Pos274

BULK-PHASE SEPARATION AND SOLVENT EFFECTS IN *RAC*-DIHEXADECYL-PHOSPHATIDYLCHOLINE-CHOLESTEROL MIXED BILAYERS.

((J.T. Mason and T.J. O'Leary)) Dept. of Cellular Pathology, Armed Forces Institute of Pathology, Washington, D.C. 20306-6000.

The properties of racemic di-*O*-hexadecylphosphatidylcholine (rDHPC) and cholesterol mixed bilayers in excess water have been studied by differential scanning calorimetry (DSC). Our DSC results indicate that dried films consisting of mixtures of these lipids hydrate to form a population of multilamellar liposomes in which cholesterol is distributed inhomogeneously between the concentric bilayers of the liposomes. This is designated as bulk-phase separation (interbilayer) as differentiated from lateral phase separation (intrabilayer). The degree of bulk-phase separation depends upon the method used to prepare and hydrate the mixed lipid film. Pronounced bulk-phase separation occurs when the lipids are rapidly frozen in benzene, lyophilized, and hydrated in water. However, the bulk-phase separation can be largely eliminated by hydrating the film in D_2O instead of water. Dried films prepared from chloroform/methanol (2:1) also hydrate to form liposomes that exhibit bulk-phase separation, but to a lesser extent than with the benzene films. This bulk-phase separation can only be eliminated by repeated freezing and thawing of the lipid suspension. These results suggest that cholesterol preferentially interacts with one of the isomers of rDHPC during the preparation of the dry film or during its subsequent hydration.

M-Pos275

MODIFICATION OF PHOSPHATIDYLCHOLINE BILAYER PERMEABILITY BY FREE FATTY ACIDS.

M. Langner, S.W. Hui, Dept. Biophysics, Roswell Park Cancer Institute, Buffalo, NY, 14263

The influence of free fatty acids on the permeability of phosphatidylcholine (PC) bilayers as a function of temperature was measured, using the fluorescence depletion of the membrane probe NBD-PE as a result of its reduction by dithionite. As expected, during DMPC phase transition, we observed an increase of dithionite permeability. When vesicles were formed from a mixture of DMPC and 7 mol % oleic acid, the dithionite permeability during phase transition was reduced. Stearic acid at the same concentration had no effect. The same results were obtained for different phosphatidylcholines and for different protocols of free fatty acid treatment. Similar results were observed when the quenching of pyrene-PC by iodide was measured. The increase of iodide partition into lipid bilayers was abolished by treatments of vesicles with unsaturated free fatty acids. When the membrane fluidity was measured by merocyanine 540 (MC540) fluorescence, there was no effect of free fatty acid treatment. The MC540 fluorescence intensity increased in the fluid phase DMPC as expected, despite the presence of free fatty acids in the membrane. Moreover, free fatty acids did not significantly alter the DMPC phase transition as measured by differential scanning calorimetry. We conclude that unsaturated, but not saturated, free fatty acids reduce lipid bilayer permeability for ions whereas the general thermodynamic properties of membranes are not altered.

M-Pos276

INTERACTION OF BILIRUBIN WITH 1,2-DIACYL-*sn*-GLYCERO-3-PHOSPHATIDYLCHOLINES: A DIFFERNTIAL SCANNING CALORIMETRIC STUDY

((Shaukat Ali and David Zakim, Department of Medicine, Division of Digestive Diseases, Cornell University Medical College, NY 10021)).

The IXa isomer of bilirubin intercalates between the polymethylene chains of lipid bilayers. To gain insight into the effects on the chains, we examined the thermotropic properties of multilamellar vesicles of DMPC, DPPC, and DSPC as a function of [bilirubin] in the range 0.1 to 8 mol%. The exact effects of bilirubin depended on the chain length of the lipids. But the general effects of bilirubin were the same in all systems. Bilirubin broadened and shifted to higher temperatures the main phase transition. This transition was not detected at higher concentrations of bilirubin, but in this setting a new phase with a highly enthalpic transition was detected. More importantly, the effects of bilirubin were fully developed at concentrations of 1 to 5 parts/1000. (Support NIH).

M-Pos277

BILAYER PACKING CHARACTERISTICS OF MIXED CHAIN PHOSPHOLIPID DERIVATIVES: RAMAN AND DSC STUDIES OF C(18):C(10)PC AND C(18):C(10)TMPC. ((M. M. Batenjany*, C. Huang§ and I.W. Levin*)) *Laboratory of Chemical Physics, NIDDK, NIH, Bethesda, MD 20892 and § the Biochemistry Dept., University of Virginia School of Medicine, Charlottesville, VA 22908.

The use of synthetic, interdigitated phospholipids is a convenient means to probe lipid bilayer packing characteristics in terms of acyl chain van der Waals interactions and hydrophobic hydration effects. Both vibrational Raman spectroscopy and high sensitivity differential scanning calorimetry (DSC) were used to analyze the bilayer interactions of two synthetic PC analogs in which the *sn*-1 and *sn*-2 acyl chains are comprised of 18 and 10 carbons, respectively. One derivative (C(18):C(10)PC) possesses the normal PC headgroup composition, while the second derivative contains an additional methylene group in the choline moiety; i.e. -P-O-$(CH_2)_3$-N$(CH_3)_3$ (C(18):C(10)TMPC). Hydrated preparations of C(18):C(10)PC are fully interdigitated at $T < T_m$ and adopt an orientation of three acyl chains per headgroup with the short *sn*-2 chains abutting one another, while the longer *sn*-1 chains position their terminal methyl groups at the water-lipid interface. For the C(18):C(10)TMPC analog, the increased size of the headgroup would be expected to shield the acyl chain terminal methyl groups from contact with the aqueous solvent. The Raman data indicate that the C(18):C(10)TMPC headgroup adopts an extended, *trans* orientation not observed for either the C(18):C(10)PC analog or hydrated PC's, in general. Both derivatives demonstrate a variability in their main phase transition temperatures (14.5-18 ° C), indicative of a metastable acyl chain packing arrangement. The C(18):C(10)TMPC analog demonstrated a two to four fold broader main transition profile than did C(18):C(10)PC. In agreement, the DSC data display a broader transition for C(18):C(10)TMPC and show two distinct transitions in the cooling profile of C(18):C(10)PC, but not C(18):C(10)TMPC. We report different acyl packing properties and integrated Raman intensities as a function of ionic strength in C(18):C(10)TMPC.

M-Pos278

STRUCTURAL AND FREE ENERGY INVESTIGATIONS INTO THE L_α-H_{II} TRANSITION FOR PE LIPIDS WITH 18 EFFECTIVE CHAINLENGTH TAILS

((P.E. Harper, S.M. Gruner)) Physics Dept., Princeton University, Princeton, NJ, USA ((R. N. A. H. Lewis, R. N. McElhaney)) Biochemistry Dept., The University of Alberta, Edmonton, Alberta, Canada

A series of seven 18-carbon effective chain length PE (phosphatidylethanolamine) lipids with L_α- H_{II} transition temperatures from 4°C to 88 °C were examined with X-ray diffraction and differential scanning calorimetry. Fourier reconstruction was used to determine the dimensions of the lipids in both phases. Earlier, interesting structural similarities at the phase transition had been observed for these lipids, despite the wide range of transition temperatures. (Lewis et al., Biochemistry 1989, 28, 541) This work expands and corrects the earlier observations, and presents a quantitative free energy theory for the phase behavior. It was found that the headgroup area at the water-lipid interface in the H_{II} phase was the same for all the lipids at a given temperature, and that the monolayer lipid length in the lamellar phase was roughly equal to the average lipid length in the hexagonal phase at the transition temperature. From this, one can infer that the phase transition is brought about when the length frustration(anisotropy) in the hexagonal phase is less than the headgroup area frustration in the lamellar phase. A quantitative model with one free parameter (the ratio of the area and length frustration energies) is fit to the data and shown to give the transition temperatures accurately to within 5°C . Supported by NSF , DOE (DE-FG02-87ER60522), NIH (GM32614) , MRCC, AHFMR

M-Pos279

CONFIGURATIONAL ENTROPY IS THE DRIVING FORCE OF ETHANOL ACTION ON MEMBRANE ARCHITECTURE

((D.C. Wang, N. Janes and T.F. Taraschi*))
Department of Pathology and Cell Biology
Thomas Jefferson University, Philadelphia, Pa 19107

A colligative thermodynamic framework has been developed that successfully describes the action of ethanol on membranes. Configurational entropy is the driving force of ethanol action on the membrane architecture. The action of ethanol and temperature originate in entropy and are equated through entropy. Membrane equilibria that are predicted to be most sensitive to the action of ethanol (where dilute concentrations of ethanol cause a perturbation equal to a large change in temperature) are those that exhibit a small ther-mal entropy change and a large difference in solute partitioning between membrane structures. Our model predicts that ethanol does not act on a single mem-brane structure, but on both structures in an equilibrium. The thermodynamic framework is applied to the action of ethanol on cooperative equilibria in a dipalmitoyl lecithin model membrane. Ethanol-induced perturbations are monitored by electron spin resonance (ESR) using the spin probe, TEMPO,. The agreement between predicted and experimental results is excellent. PHS AA07186, AA00088, AA07215, and AA07463.

M-Pos280

MODULATION OF IN-PLANE LIPID DOMAIN STRUCTURE IN BILAYERS BY SIGNAL PEPTIDES.

((M.B. Sankaram[1], L.M. Gierasch[2] and T.E. Thompson[1])) [1]University of Virginia, Department of Biochemistry, Charlottesville, VA 22908 and [2]University of Texas Southwestern Medical Center, Departments of Biochemistry and Pharmacology, Dallas, TX 75235

In two-component, two-phase lipid bilayers such as those formed from dimyristoyl phosphatidylcholine (DMPC) and distearoyl phosphatidylcholine (DSPC) the gel and fluid phases constitute a domain system. The structure of the domains is such that either the gel phase is disconnected to form isolated domains in a continuous reticular fluid phase matrix or *vice versa*. We have shown recently that (a) spin labelled lipids can be randomly distributed into the disconnected domains of either phase type, (b) the random distribution leads to a novel type of inhomogeneity for the first derivative line shapes of ESR spectra, (c) this inhomogeneity can be distinguished from more conventional types of inhomogeneities by measuring internally normalized intensity ratios on the ESR spectra, and (d) the intensity ratios can be used to determine average sizes for the disconnected gel and fluid domains (Sankaram et al., Biophys. J. 63: 340-349, 1992). In this work, we examine the effect of a hydrophobic transmembrane α-helical signal peptide of the outer membrane protein A from *Escherichia coli*, using the intensity ratio analysis of ESR spectra. A comparative analysis of the results obtained with phospholipid and peptide spin labels suggests that the presence in large numbers of peptide molecules in small fluid domains leads to a coalescence of the domains to form larger structures. *Supported by grants GM-14628, GM-23573 and GM-34962 from the NIH.*

M-Pos281

EFFECTS OF MODERATE PRESSURE ON THE GEL-LIQUID CRYSTALLINE TRANSITION OF BINARY PHOSPHATIDYLCHOLINE BILAYERS

((Qiang Ye, Kim K. Thompson, and Rodney L. Biltonen)) Department of Pharmacology, Univ. of Virginia, Charlottesville, VA 22908

The effects of hydrostatic pressure on the gel-liquid crystalline transition of multilamellar vesicles made of binary mixtures of dimyristoyl-phosphatidylcholine (DMPC), dipalmitoyl-phosphatidylcholine (DPPC), and distearoyl-phosphatidylcholine (DSPC) have been investigated with high pressure-differential scanning calorimetry. The overall phase transition processes have been found to be shifted towards higher temperature by pressure in a linear fashion for all three binary lipid systems studied. No significant change in the shape or the integrated area of the excess heat capacity function was observed with pressures up to 200 atm. A nominal transition temperature has been defined as that corresponding to the heat capacity maximum for binary lipid systems. In equimolar DMPC-DPPC and DPPC-DSPC mixtures, a single peak in the heat capacity function with respective transition half-widths of 3.5 and 2.5 °C was observed, and the pressure dependence of the nominal transition temperature was found to be 0.0228 ± 0.0003 and 0.0246 ± 0.0004 °C/atm, respectively. For an equimolar DMPC-DSPC mixture, two peaks in the transition heat capacity function were observed and the phase transition spans nearly 20 °C. The pressure dependence of the lower and upper nominal transition temperatures corresponding to the two heat capacity maxima was found to be 0.0250 ± 0.0002 and 0.0255 ± 0.0011 °C/atm, respectively. The fact that little change in the shape or the integrated area of the heat capacity function by pressure was observed indicates that moderate pressures up to 200 atm do not change the lipid-lipid interactions between unlike nearest neighbors or the phase transition enthalpy of binary lipid mixtures. (Supported by grants from the NIH and ONR).

M-Pos282

TITRATION CALORIMETRY STUDY OF THE INTERACTIONS OF ALCOHOLS WITH DIPALMITOYLPHOSPHATIDYLCHOLINE.

Fengli Zhang, Peter Guy, Tina Wu Leung and Elizabeth S. Rowe, Department of Biochemistry and Molecular Biology, University of Kansas Medical School, and VA Medical Center, Kansas City, MO 64128.

The thermodynamics of alcohol-lipid interactions were studied by using titration calorimetry. The alcohols used in this study were from butanol to nonanol, and the lipid used was dipalmitoylphosphatidylcholine(DPPC). The experiments were carried out at several temperatures at which the DPPC was in the L_α phase(45-60°C). The enthalpies, partition coefficients and the heat capacities of these interactions were obtained by fitting the titration calorimetry data to a model in which the alcohols are freely partitioning between the lipid and the aqueous phase. The results showed that the heat capacity changes of the alcohol-DPPC interactions are negative, and they are the same for the different alcohols. The enthalpies of the alcohol-DPPC interactions decrease with increasing temperature, as well as with increasing chain length of alcohol. The enthalpies are 1). positive for butanol; 2). negative for heptanol, octanol, and nonanol; 3). changing from positive to negative for pentanol and hexanol as temperature increases from 45 to 60°C. It is hard to measure the interactions for small alcohols, such as ethanol and methanol, due to the weak interaction and very large heat of dilution. The thermodynamic parameters of such interactions can be extrapolated by studying a series of higher chain length alcohols. (Supported by VA)

M-Pos283

"CAGED" AMINOPHOSPHOLIPIDS: SYNTHESIS AND CHARACTERIZATION OF NOVEL pH LABILE DERIVATIVES OF PHOSPHATIDYLETHANOLAMINE AND PHOSPHATDIYLSERINE.

D. C. Drummond and D. L. Daleke. Department of Chemistry, Indiana University, Bloomington, IN 47405.

A series of reversibly N-modified PS and PE derivatives have been synthesized by amidation of DOPS and DOPE with maleic, dimethylmaleic, citraconic, 3,4,5,6-tetrahydrophthalic, or phthalic anhydride. Representative yields for the citraconyl DOPS (C-PS) and citraconyl DOPE (C-PE) derivatives were 78% and 77%, respectively. The yields of the remaining derivatives varied from 47% to 100%. The derivatives were purified using a combination of carboxymethyl cellulose cation exchange and high performance liquid chromatography. Tetrahydrophthalic PE and dimethylmaleic PE derivatives could not be isolated due to their instability. However, non-hydrolyzable, cyclic forms of these lipids were purified and characterized by mass spectrometry and NMR analysis. The remaining derivatives were characterized for acid lability. Release of the blocking group was induced by acid catalyzed cleavage of the amide bond linking the lipid and the blocking group. The pH dependence of cleavage of the PS and PE derivatives was determined by incubating lipid dispersions in buffers of varying pH at 37°C and physiological salt concentration for 1h. Hydrolysis was measured by phosphate analysis of TLC-separated products. Half-maximal cleavage for the C-PE and C-PS derivatives was observed at pH 5.5 and 6.5, respectively. Significant cleavage of the phthalic and maleic PE derivatives did not occur at physiologically relevant pH values (pH 5.5 - 8). The half time for cleavage of C-PE and C-PS at pH 5.5 was 140 min and 100 min, respectively. These "caged" phospholipids will be used in ongoing studies of aminophospholipid transport across biological membranes. They may also be useful in membrane-membrane fusion studies.

M-Pos284

EFFECT OF CHOLESTEROL ON PHOSPHOLIPID PHASE DOMAINS AS DETECTED BY LAURDAN GENERALIZED POLARIZATION.

((T. Parasassi, M. Loiero, M. Raimondi, G. Ravagnan and E. Gratton)) Istituto di Medicina Sperimentale, CNR, 00137 Roma, Italy, Laboratory for Fluorescence Dynamics, UIUC, Urbana IL 61801.

Spectroscopic properties of 2-dimethylamino-6-lauroylnaphthalene (Laurdan) have been used to detect phospholipid gel and liquid-crystalline phase domains coexistence in liposomes where phase segregation is known to occur. In vesicles composed of equimolar DLPC and DPPC at 20°C, Laurdan Generalized Polarization (GP) values show a characteristic behaviour as a function of wavelength. GP values increase with the increase of excitation wavelength and decrease with the increase of emission wavelength. In pure gel phase, GP values do not show any relevant dependence on wavelength while in pure liquid-crystalline phase the behaviour of GP values is opposite than that observed in the presence of domain segregation. The addition of 30 mol% cholesterol to the equimolar mixture of phospholipids renders the excitation and emission GP spectra similar to those obtained in pure liquid-crystalline phospholipids but with higher absolute values.

M-Pos285

MOLECULAR MOTIONS OF LIPID AND CHOLESTEROL MIXTURES VIA ^2H NMR T_1 RELAXATION.

((Clare Morrison and Myer Bloom)). Physics Dept. U.B.C., Vancouver, B.C. V6T 1Z1.

The molecular motions of the acyl chains of POPC and POPC/cholesterol model membranes in the lamellar phase were investigated using deuterium spin-lattice relaxation, T_{1z} and $T_{1\rho}$. The most general form of the orientation dependence of the relaxation rate for axially symmetric motions was used [1].

$$\frac{1}{T_i} = a_0 + a_2 P_2(\cos\beta) + a_4 P_4(\cos\beta) \qquad (1)$$

where β is the angle between the director (normal to the bilayer) and the static magnetic field and the $P_i(\cos\beta)$s are Legendre polynomials. The coefficients a_i are functions of the spherical order parameters, S_{20} and S_{40}, and reduced spectral densities, $j(\omega_0)$ and $j(2\omega_0)$, which depend of the type and rate of motion.

Oriented membrane samples were used to measure the orientation dependence of T_{1z} and $T_{1\rho}$. The data were fitted to equation 1 and the order parameters and reduced spectral densities extracted. Some possible models for the motions of POPC and POPC/Chol mixtures will be given. This analysis is an alternative to the method of simulating partially relaxed powder spectra using computer models.

[1] C. Morrison and M. Bloom, *J. Magn. Reson.* (in press).

M-Pos286

USE OF PERYLENE AND PERYLENE-PHOSPHATIDYLCHOLINE TO INVESTIGATE THE EFFECTS OF CHOLESTEROL ON LIPID BILAYER PACKING.

((Piotr Targowski, Salvatore H. Atzeni and Lesley Davenport)) Dept. of Chem., Brooklyn College of CUNY, New York 11210. (Sponsored by Nancy M. Tooney).

We have examined the time-dependent anisotropic rotational motions of perylene and perylene-phosphatidylcholine (Per-PC) as probes of lipid packing in anisotropic DMPC lipid bilayers. We previously reported (Biophys. J., Davenport & Ri, 57:483a) that by using selective excitations the steady-state polarized fluorescence emissions, of disc-like perylene (D_{2h} symmetry) embedded in DMPC SUVs, reveal in-plane rotational rates which are sensitive to the physical state of the lipid and which in the presence of cholesterol (20 mole%) appear more restricted. Out-of-plane probe motions in the gel phase however, appear invariant to temperature and/or cholesterol. Time dependent polarized decays have been obtained for perylene in DMPC SUVs using 410nm excitation ($S_0 \rightarrow S_1$), at five temperatures below and up to the lipid T_c (23°C). Using global data fitting procedures linking preexponential (β) terms (allowed from symmetry considerations), our data shows a fast in-plane motion (ϕ_{ip}) which is somewhat temperature dependent and a hindered motion which at low temperatures in the gel lipid is best represented by an r_∞ term. With addition of cholesterol (20 mole%), ϕ_{ip} appears relatively unchanged. However, a second slower rotational time (ϕ_{op}) insensitive to temperature is observed in addition to an r_∞ term. For Per-PC, where the probe is anchored to the Sn'2 position of the phospholipid, as expected both these slipping 'in-plane' motions and out-of-plane motions appear to be retarded. Interpretations of these data in terms of heterogeneous lipid packing are being considered. Further studies of rotational motions of these fluorophores using the $S_0 \rightarrow S_2$ transition at 256nm, and the effects of cholesterol are in progress. (Supported in part by the AHA-NYC Affiliate and NSF DMB 9006044).

M-Pos287

USE OF DANSLY-LYSINE AND MC540 TO MONITOR CHOLESTEROL-INDUCED CONDENSATION OF PHOSPHOLIPID MEMBRANES.

((William Stillwell*, Stephen R. Wassall#, Alfred C. Dumaual* and William D. Ehringer*)) Departments of Biology* and Physics#, Indiana University-Purdue University at Indianapolis, Indianapolis, IN 46202

We employ the water-soluble fluorescent membrane surface probes dansyl-lysine and merocyanine (MC540) to follow the cholesterol-induced condensation of phospholipid bilayer membranes. As these dyes partition from water into membranes their fluorescence increase dramatically. However, upon incorporation of cholesterol the fluorescence is reduced in relation to the extent of membrane concensation, indicating the dyes are being excluded from the membranes. Five mixed chain phospholipids were tested. Surface area/pressure measurements on a Langmuir Trough indicate that monolayers composed of 18:0, 18:1 PC and 18:0, α18:3 PC are condensable by cholesterol while monolayers composed 18:0, γ18:3 PC; α18:3, α18:3 PC and 18:0, 22:6 PC are not. Fluorescence measurements made with dansyl-lysine and MC540 agreed with the monolayer measurements. We conclude that under appropriate conditions these dyes may be used to monitor cholesterol-lipid interactions in membranes.

M-Pos288

THE VESICLE-MICELLE TRANSITION OF EGG PHOSPHATIDYLCHOLINE-CHOLATE MIXTURES: PROBING THE TRANSITION REGION.

((A. Walter and D.E. Dewey)) Dept. Physiol. & Biophys., Wright State Univ., Dayton, OH 45435 (Sponsored by R. Putnam).

CryoTEM images show that the structural transitions of egg PC-sodium cholate mixtures proceed from vesicles to large bilayer sheets to cylindrical micelles (CMM) and finally small mixed micelles (SMM) as the fraction of cholate increases (Walter et al., Biophys. J. 60:1315). Here we characterize this transition using several fluorescent probes and rate/density centrifugation. Vesicles were prepared from egg PC dispersed in a 150 mM NaCl buffer (pH 7.2) by freeze/thaw extrusion. Sodium cholate stock solutions were prepared from recrystallized cholic acid and titrated with NaOH to pH 7.2. PC/cholate mixtures were equilibrated 24 hrs prior to any measurements. Light scattering intensity was measured to indicate the degree of solubilization of each sample. Cholate-induced ANTS/DPX leakage occurred precipitously at an R_e (cholate/PC) of 0.23 to 0.27 and probably indicated the vesicle/sheet transition. PRODAN, a dielectric sensitive fluorescent probe, was distributed in a more hydrophobic environment when the egg PC/cholate mixtures formed CMM than when vesicular or SMM structures were present. Rate/density centrifugation showed this intervening region contains at least two types of structures, one of which is significantly more dense than vesicles or small mixed micelles. (AHA-Ohio #MV-91-13)

M-Pos289

CHARATERIZATION OF THE BILE SALT INDUCED STRUCTURAL CHANGES IN THE PHOSPHOLIPID HEAD GROUP IN THE VICINITY OF THE VESICLE TO MIXED MICELLE TRANSITION. ((Joel M. Moore*, Anne Walter#, and Timothy S. Wiedmann*)), University of Minnesota, Department of Pharmaceutics, Minneapolis, MN,* Wright State University, Department of Physiology and Biophysics, Dayton, OH.#

Interaction of bile salts with phospholipids are of fundamental importance particularly in the intestinal absorption of hydrophobic therapeutic agents and, under pathological conditions, the formation of gallstones. An understanding of the structural/dynamic changes induced by bile salts on the head group of phospholipids is important for predicting the solubilization of cholesterol and other compounds by these lipid aggregates. Phosphorus NMR spectra have been obtained on a series of mixtures prepared by diluting a mixture of dimyristoyl phosphatidylcholine (DMPC) and sodium cholate (NaC) with additional NaC in order to span the vesicle-mixed micelle transition. Particle size and dispersity were determined by a Nicomp particle size analyser. As the NaC/DMPC mole ratio increased, there was a progressive decrease in the 31P NMR chemical shift anisotropy. Within a narrow range between the lamellar and mixed micellar phases, a superposition of apparently symmetric and asymmetric spectra was evident. In addition, particle size decreased as the fraction of bile salt increased as determined from the fraction of lipid giving rise to the isotropic signal. These data extend the detailed examination of the structural phase boundaries for the phospholipid-bile salt mixtures. (See accompanying abstract, A. Walter).

M-Pos290

TRANSMEMBRANE TRANSFER OF FLUORESCENT-LABELED LYSOPHOSPHOLIPIDS ACROSS THE BRUSH-BORDER MEMBRANE OF RABBIT INTESTINE. ((Z.Zhang and J.W.Nichols)) Dept. of Physiology, Emory Univ. School of Medicine, Atlanta, GA 30322

Previous experiments have demonstrated that at least 20% of the lysophospholipids produced in the intestine from the hydrolysis of ingested and biliary phospholipids are absorbed intact. Since the transfer of lysophospholipids across artificial phospholipid bilayers is very slow, some mechanism that facilitates transmembrane transfer is predicted to account for the efficient absorption of intact lysophospholipids. We have investigated the transmembrane transfer of a fluorescent, head-group labeled lysophospholipid N-(7-nitro-2,1,3-benzoxadiazol-4-yl)monoacyl phosphatidylethanolamine (N-NBD-lysoPE) across the membranes of isolated brush border membrane vesicles (BBMV) from the rabbit intestine. The transfer of N-NBD-lysoPE from artificial phospholipid vesicles containing a nontransferable fluorescence quencher to the nonquenching bilayers of BBMV was recorded as an increase in fluorescence. Curve fitting of the recorded traces required two exponential terms to fit the data indicating that the N-NBD-lysoPE was transferring into two distinct pools. We hypothesized that the first and second pools reflected the outer and inner leaflets of the BBMV bilayer, respectively. Transfer to the second pool could be eliminated by trapping rhodamine-labeled BSA inside the BBMV. Since rhodamine-labeled BSA binds and quenches N-NBD-lysoPE, this result supports the conclusion that the second pool reflects transfer to the inner leaflet of the BBMV. Protease treatment of the BBMV inhibits N-NBD-lysoPE transfer to the inner leaflet inferring protein-mediated transmembrane transfer. (Supported by Am. Cancer Soc. grant BE-148)

M-Pos291

INTERBILAYER TRANSFER OF PHOSPHOLIPID-ANCHORED MACROMOLECULES VIA MONOMER DIFFUSION.

((John R. Silvius and M.J. Zuckermann)) Departments of Biochemistry and Physics, McGill University, Montréal, Québec, Canada

Fluorescence energy transfer has been used to monitor the interbilayer exchange of conjugates linking diacyl phosphatidylethanolamines (PEs) to hydrophilic macromolecules via an (S-bimanylmercapto)succinyl moiety. Conjugates linking a diacyl PE to various macromolecules, including methoxypolyethylene glycols (mePEGs), polylysine, aminodextrans and apotransferrin, exchange between large unilamellar phosphatidylcholine (PC) or PC/PE vesicles 5- to 25-fold faster than do conjugates linking the same PE to small hydrophilic residues. Kinetic analysis suggests that exchange proceeds via monomer transfer through the aqueous phase, without requiring intervesicle collisions or formation of micelles by the conjugate molecules. Estimated half-times for intervesicle transfer of macromolecular conjugates with saturated PE 'anchors' range from minutes (for di-C_{14} anchors) to at most a few tens of hours (for di-C_{18} anchors). Cis-unsaturation of the PE 'anchor' increases the rate of interbilayer exchange by roughly three- to fourfold for each cis-double bond present. These findings suggest that significant intermembrane exchange may occur, on a biologically meaningful time scale, for a variety of natural and artificial phospholipid-anchored proteins and other macromolecules unless the 'tethered' macromolecule itself, as well as the lipid anchor, has significant affinity for other membrane components. (Supported by the MRC of Canada and les Fonds FCAR du Québec).

M-Pos292

Effects of unsaturation on the membrane antioxidant activities of vitamin E. YJ Suzuki[1], M Tsuchiya[1], SR Wassall[2], VE Kagan[3] & L Packer[1]. [1]Dept Mol & Cell Biol, UC, Berkeley, CA 94720, [2]Dept Physics, IUPUI, Indianapolis, IN 46205 & [3]Dept Environ & Occup Health, U Pittsburgh, Pittsburgh, PA 15261.

Vitamin E is a physiological antioxidant which protects membranes from lipid peroxidation. In the present study, we compared two vitamin E constituents, *d*-α-tocopherol (αT) and *d*-α-tocotrienol (αT_3), whose structures differ by the presence or absence of unsaturation on the hydrocarbon tail, and attempted to correlate their antioxidant activities with their physicochemical influences on the membrane structure and dynamics. Chemiluminescence and fluorescence measurements demonstrated that αT_3, which has an unsaturated tail, possesses greater peroxyl radical scavenging activity than αT in liposomes, whereas both antioxidants had identical activity in hexane solution, suggesting that the antioxidant potency of αT_3 is imposed by the membrane environment. When αT and αT_3 were compared for their effects on membrane order using ^2H NMR and conventional ESR spin labeling, no differences were observed. Saturation transfer ESR spin labeling, on the other hand, revealed that αT_3 incorporation decreased the parameter C'/C (yields information on the motion around the long molecular axis) in the gel phase and increased the L"/L parameter (affected by the rotation of the long axis itself, wobbling motion) in the liquid crystalline phase. Determination of the ratio of correlation times of L"/L and C'/C suggested that αT_3 imposes more motional anisotropy of the membrane. αT_3 also exhibited a better collisional fluorescence quenching with *cis*-parinaric acid than αT in liposomes, suggesting a higher diffusional mobility of αT_3. Thus, the unsaturated structure of vitamin E causes stronger effects on membrane reorientational dynamics and higher diffusional mobility in membrane, and these may enhance the antioxidant potency. *Supported by NIH (CA47597), PORIM, and AHA California Affiliate*

M-Pos293

STRUCTURAL AND THERMODYNAMIC INVESTIGATION OF FILAMENT FORMATION IN A DIACETYLENIC PHOSPHOLIPID ((Mark A. Davies, B.R. Ratna, and Alan S. Rudolph*)) Dept. of Biochemistry and Molecular Biology, Georgetown University School of Medicine, Washington, DC 20007 and *Center for Biomolecular Science and Engineering, Code 6900, Naval Research Laboratory, Washington, DC 20375

Previous microscopic experiments with the polymerizable, diacetylenic lipid 1,2-bis (10,12-tricosadiynoyl)-sn-glycero-3-phosphocholine in ethanol/water solutions have revealed the formation of thin, undulating filaments upon cooling from 60°C. Infrared spectroscopy and differential scanning calorimetry were used to investigate the phase characteristics of this lipid in mixtures of ethanol and water in order to describe filament formation in a structural context and to explore the thermodynamics of their formation. Relative percentages of specific types of gauche conformers in the lipid acyl chains in filaments were determined. The formation of filaments is characterized by a transition observed upon cooling from 60°C as identified by DSC and FT-IR. The calorimetric transition temperature observed at the concentration of lipid at which filaments form (above 10 mg/ml) is approximately 54°C. Infrared spectroscopy has revealed that the population of various gauche conformer classes, particularly (kink+gtg) and double gauche forms, decreased upon formation of filaments with double gauche forms virtually absent at 38°C, the temperature at which the filaments collapsed. These results suggest that the filaments form from an isotropic to fluid lamellar phase transition as the lipid is cooled in the ethanol/water solution.

M-Pos294

QUANTITATIVE DETERMINATION OF ACYL CHAIN DISORDERING IN PHOSPHOLIPIDS BY AN ION CHANNEL PEPTIDE AS PROBED BY INFRARED SPECTROSCOPY

((Mark A. Davies)) Department of Biochemistry and Molecular Biology, Georgetown University School of Medicine, 3900 Reservoir Road NW, Washington, DC 20007

CH_2 wagging modes, occurring between 1370 cm^{-1} 1300 cm^{-1} in infrared spectra of hydrocarbon chains, are a sensitive probe of phospholipid acyl chain conformational isomerism, providing quantitative population distributions of acyl chain kinks, multiple gauche, and end gauche conformers. Formation of gauche conformers in acyl chains of hydrated dimyristoyl phosphatidylcholine (DMPC) in the presence of the ion channel Gramicidin A has been probed using infrared spectroscopy. Gramicidin A was incorporated into DMPC at mole ratios between 100:1 and 10:1 (lipid:peptide) using a solvent system of benzene/ethanol (95:5, v:v), which insured its insertion in head-to-head dimer form. Spectra were acquired between 15°C and 55°C. Both infrared and Raman spectra of the Amide I region of Gramicidin A in dimer form will also be presented.

M-Pos295

PHASE BEHAVIOR OF DIELAIDOYLPHOSPHATIDYLCHOLINE BILAYERS IN THE PRESENCE OF ETHANOL STUDIED BY EPR. ((L.A. Dalton and K.W. Miller)) Dept. Biological Chemistry and Molecular Pharmacology, Harvard Medical School, and Department of Anaesthesia, Massachusetts General Hospital, Boston, MA 02114.

Although the main gel to liquid crystalline phase transition, T_m, has been extensively studied in saturated lipids, unsaturated lipids have received less attention. We have used EPR to examine T_m of dielaidoylphosphatidylcholine [DEPC; di(C18:1*trans*Δ9)PC] bilayer vesicles containing 5-, 10- or 14-doxylPC probes. The phase transition is characterized by a loss in orientational order of the acyl chain segments at all 3 depths in the bilayer over a narrow range in temperature, e.g., 10-12°C for the 5-position. The magnitude of the decrease in order parameter for 10-doxylPC is 2 to 3-fold less than the change reported by the 5- and 14-doxylPC labels, reflecting the influence of the double bond. In the gel phase, the 10- and 14-doxylPC probes were mobile on the saturation transfer EPR (ST-EPR) time scale, but the 5-doxylPC probe possessed a 20 μsec correlation time from 0 to 10°C. Upon heating, subtle changes in the ST-EPR spectra of 5-doxylPC occurred, attributable to minor alterations in anisotropic motion. In contrast to saturated lecithins, where long axis rotation is present below T_m, in DEPC the ST-EPR correlation times for 5-doxylPC long axis rotation and segmental wobble decreased together at the T_m. Ethanol-induced isothermal melting also occurred in a concerted manner at all depths. *Work supported by NIAAA grant AA07040.*

M-Pos296

LATERAL DIFFUSION IN AN ARCHIPELAGO: SINGLE-PARTICLE DIFFUSION.

((Michael J. Saxton)) Institute of Theoretical Dynamics, University of California, Davis, California 95616.

Several laboratories have measured lateral diffusion of single particles on the cell surface, and these measurements may reveal an otherwise inaccessible level of submicroscopic organization of cell membranes. Pitfalls in the interpretation of these experiments are analyzed. Random walks in unobstructed systems show structure that could be interpreted as free diffusion, obstructed diffusion, directed motion, or trapping in finite domains. To interpret observed trajectories correctly, one must consider not only the trajectories themselves but also the probabilities of occurrence of various trajectories. Measures of the asymmetry of obstructed and unobstructed random walks are calculated, and probabilities are evaluated for random trajectories that resemble either directed motion or diffusion in a bounded region.

Statistical fluctuations in Monte Carlo calculations of the diffusion coefficient are examined as a model for fluctuations in measurements of the diffusion coefficient by single-particle tracking. The variation in diffusion coefficient among random walks for a fixed configuration of obstacles is much greater than the variation among configurations of obstacles for a fixed area fraction of obstacles. The distribution in diffusion coefficients for different random walks is so broad that excluding "bad," apparently nondiffusive, trajectories may bias the determination of the diffusion coefficient. (Supported by NIH grant GM38133.)

M-Pos297

Location Models for Potential-Sensitive Hydrophobic Ions, Anti-HIV and Anti-*Pneumocystis Carinii* Compounds in Model Membranes: A NOESY NMR Spectroscopy Study - D. J. Gill, S. Chandrasekaran, and J. C. Smith, Dept. Chemistry and LCBS, Georgia State Univ., Atlanta, GA 30303 USA - The location(s) assumed by the potential-sensitive, hydrophobic ions tetraphenylborate (TPB^-) and tetraphenylphosphonium (TPP^+) in small 1,2-dimyristoyl-*sn*-glycero-3-phosphocholine (DMPC) and egg phosphatidyl choline (PC) unilamellar vesicles prepared at 10 mM and 50 mM concentrations, respectively, has been investigated using two-dimensional, phase-sensitive NOESY NMR spectroscopy. Prominent cross peaks between the TPB^- and TPP^+ phenyl protons and those of the DMPC fatty acid methylene, terminal methyl, and choline N-methyl groups are observed at mixing times as low as 100 ms when these probes are present in the vesicles at 5 to 8 mol percent. The same cross peak pattern was observed when residual HOD signal suppression was carried out by a binomial pulse sequence or with a decoupler pulse prior to data acquisition; use of the decoupler thus does not appear to introduce a detectable signal due to spin diffusion in these measurements. At a mixing time of 100 ms, cross peaks between the probe phenyl protons and those of the vinyl groups of the 9,10 unsaturated DMPC derivative were readily observed in vesicles prepared with this unsaturated lipid. These observations suggest a two site location model for the probes: a "deep" site including the methylenes approximately in the middle of the chain to the terminal methyl group and a primarily surface location in which the probe interacts with the lipid head groups. Preliminary volume integration results suggests that the deep probe location is the dominant one at the low mol percentages employed in these experiments. Similar work on the location of a number of anti-HIV and anti-*pneumocystis carinii* compounds of the porphyrin, diamidine, and pyrimidine classes in both egg PC and DMPC vesicles is in progress. Support: AI 27196

M-Pos298

ION MOVEMENTS IN LIPID BILAYERS STUDIED BY THE PHOTOGATING EFFECT. ((K. Sun and D. Mauzerall)) Rockefeller University, New York, NY 10021.

The photogating effect is the increase in conductivity of tetraphenyl boride ions (TPhB) by photoformation of porphyrin cations inside the lipid bilayer. It is ascribed to cancellation of space charge and to an Ion-Chain mechanism (Drain and Mauzerall, BJ, in press). The halogenated tetraphenyl borides (XTPhB) show larger conductance increases of well over two orders of magnitude. This is attributable to their more rapid translocation rates, 10^{-4}s, compared to that of unsubstituted TPhB, 10^{-2}s. Support for the Ion-Chain mechanism, wherein clusters of hydrophobic boride anions and porphyrin cations form a bridge for transmembrane hopping of boride ions, is shown by the large increase in mobility of the porphyrin cation in the presence of XTPhB. This is measured by the decrease in lifetime of the pulsed photogating effect when an electron donor is added to the side opposite that containing the electron acceptor. The lifetime decreases from >5s to 0.5s with 10 μM ferrocyanide if 4 μM ClTPhB is present. In agreement porphyrin cations of limited mobility such as chlorophyl a or polar porphyrins show only small photogating effects. This research was supported by NIH GM 25693.

M-Pos299

USE OF MONTE CARLO SIMULATIONS TO STUDY LATERAL ORGANIZATION OF LIPIDS IN PYR-PC/DMPC MEMBRANES

Istvan P. Sugar,* Daxin Tang and Parkson Lee-Gau Chong**
*Depts of Biomath. Sci. and Physiol./Biophys., The Mount Sinai Medical Center, New York, N.Y. 10029
**Dept. of Biochem., Meharry Medical College, Nashville, TN 37108

Pyrene excimeric fluorescence data on two-component Pyr-PC/DMPC membranes have recently been interpreted in terms of lipid regular distribution into hexagonal super-lattices at critical Pyr-PC concentrations (D. Tang and P.L.-G. Chong, 1992, Biophys.J. in press). We further studied the lateral distribution of Pyr-PC molecules at different temperatures and concentrations by means of Monte Carlo simulations.

Regular distribution of pyrene-labeled hydrocarbon chains into hexagonal super-lattice was obtained when the following three conditions were satisfied simultaneously: (1) critical concentration of the pyrene-labeled chains, (2) temperature which is lower than a critical one, and (3) negative energy parameter W. $W = E_h - (E_g + E_m)/2$ where E_h is the nearest neighbor interaction energy between pyrene-labeled and unlabeled hydrocarbon chains. The interaction energy between two hydrocarbon chains is inversely proportional to the 5th power of the interchain distance. The number of defects in the regular distribution increases with increasing temperature, while at a critical temperature the long-range order of the hexagonal super-lattice disappears. Between two critical concentrations of X_1 and X_2 two different hexagonal super-lattices coexist which are characteristic to the 1st and 2nd critical concentrations, respectively. (Supported by ARO.)

M-Pos300

USE OF FLUORESCENT MEMBRANE PROBES TO DISTINGUISH UNMODIFIED T27A TUMOR CELLS FROM THOSE MODIFIED BY DOCOSAHEXAENOIC ACID. ((William Stillwell, Alfred C. Dumaual,William D. Ehringer, and Laura J. Jenski)) Department of Biology, Indiana University-Purdue University at Indianapolis, Indianapolis, IN 46202

Here we employ the murine non-B, non-T leukemia cell line, T27A, as a rapidly growing cell to test our hypothesis that incorporation of docosahexaenoic acid (22:6Δ4,7,10,13,16,19) into membranes induces lateral phase separation producing DHA-rich, cholesterol-poor and DHA poor, cholesterol-rich domains. We have enriched the T27A cells with DHA by fusing then with small unilamellar vesicles composed of 18:0, 22:6 PC/18:0, 22:6 PE (1:1). We monitor DHA uptake by gas chromatography and measure DHA-alterations in plasma membrane structure by the fluorescent membrane surface probes dansyl-lysine and merocyanine (MC540) and the membrane interior probes laurdan and pyrene. These probes clearly demonstrate DHA-dependent spectral shifts which may indicate alterations in membrane structure. Associated with these changes we also report DHA-dependent changes in the expression of various epitopes on histocompatibilioty antigens as monitored with monoclonal antibodies. These experiments imply to us that DHA may have a profound effect on basic membrane structure.

M-Pos301

CALCULATION OF RESONANCE ENERGY TRANSFER EFFICIENCIES AND DONOR LIFETIMES FOR PROTEIN-LINKED DONORS AND BILAYER-DISTRIBUTED LIPID ACCEPTORS IN BIOLOGICAL MEMBRANES. ((D.B. Zimet, J.R. Abney, B.J-M. Thevenin, A.S. Verkman and S.B. Shohet)) CVRI and Dept. Lab. Med., UCSF, San Francisco, CA 94143.

Fluorescence resonance energy transfer (RET) is a well-established method for measuring distances in biological systems based on models of donor and acceptor distribution. For complex membrane systems in which fluorescent donors are linked to membrane proteins and fluorescent acceptors are linked to lipids distributed in the bilayer, donor and acceptor positions are defined statistically. Thus, statistical techniques such as Monte Carlo simulations must be used to model donor and acceptor distributions, and numerical techniques used to solve the associated RET equations. In this study, equilibrated protein positions were generated by Monte Carlo simulations for various protein-protein interactions and protein densities between 0 and 50% area fraction. Donor fluorophores were located either centrically or eccentrically with respect to the proteins to which they were attached, and either in or above the plane of the membrane. Acceptor positions were generated randomly for a given protein distribution by treating the acceptors as noninteracting point particles. From a generated donor and acceptor ensemble, the fluorescent lifetime and energy transfer efficiency for each donor in the ensemble were calculated to generate a characteristic distribution of lifetimes and an average transfer efficiency. Because a distribution of lifetimes contains more information than the average lifetime of a distribution, these histograms provide a superior method of matching a model with a real system. By analyzing in concert the data from this model with experimental data from both steady-state RET and multiharmonic frequency-domain lifetime measurements, it will be possible to obtain novel information concerning the distribution of donors as well as the separation between donors and acceptors in biological systems.

M-Pos302

EFFECTS OF PRESSURE ON SUBMICROSECOND LIPID DYNAMICS USING A LONG LIVED FLUORESCENCE PROBE. ((Lesley Davenport and Piotr Targowski)) Department of Chemistry, Brooklyn College of CUNY, New York 11210.

The effects of applied external pressure (0-1.2kBar) on submicrosecond lipid motions in lipid bilayers have been studied using coronene, a long-lived (τ_{av}~200ns) planar fluorescence probe. We previously reported using temperature dependence (Biophys. J., Targowski et al., 61:A503) that polarized fluorescence emissions from coronene (D_{6h} symmetry) depend on slow *out-of-plane* rotations only, which make this molecule sensitive to chain disordering events occurring well after the decay of most other fluorescence probes used in studies of membrane dynamics. We interpreted this system using a 'gated' lipid fluctuation model which invokes a *distribution* of lipid order and 'melting' rates, derived from Landau phase transition theory. We have now modified this model by including a pressure dependent term in the free energy expansion. Other thermodynamic parameters (e.g heat capacities) for the lipid system under investigation are inherent to the model. Steady state fluorescence emission anisotropies, <r>, obtained for coronene labeled dimyristoylphosphatidylcholine (DMPC) ULVs (1:200; probe to phospholipid molar labeling ratio) at 25°C and 30°C, were measured as a function of increasing pressure. The pressure induced lipid phase transition for DMPC SUVs and LUVs at 30°C, is shifted to higher pressure values ($P_{1/2}$=0.60 and 0.45 kBar, respectively) than for corresponding DPH labeled samples ($P_{1/2}$=0.35 and 0.33 kBar, respectively). This suggests that an increased pressure is required to hinder slow (submicrosecond) lipid motions detected only using a long lived fluorescence probe and which occur well below the normally reported 'gel-fluid' lipid phase transition. This is in agreement with our previous studies and predicted by our lipid order distribution model. Studies of pressure effects on peptides and other integral membrane components using our modified 'gated' lipid fluctuation model are in progress. (Supported in part by the AHA-NYC Affiliate and NSF DMB 9006044).

M-Pos303

DIFFERENTIAL POLARIZED FLUOROMETRIC STUDIES OF DPH IN ARCHAEBACTERIAL POLAR LIPID E LIPOSOMES ((Glendora Spencer, Lihua Wei and Parkson L.-G. Chong)) Dept. of Biochemistry, Meharry Medical College, Nashville, TN 37208

Differential polarized phase fluorometric methods were used to investigate the anisotropic rotational diffusion of 1,6-diphenyl-1,3,5-hexatriene (DPH) in polar lipid fraction E (PLFE) liposomes. PLFE was isolated from the thermoacidophilic archaebacterium, *Sulfolobus acidocaldarius*, grown at 70-75 °C. The decay of DPH emission in PLFE liposomes is best described by a two exponential decay law. There is no distinct phase transition in these liposomes. The r_∞ value decreases monotonically from 0.18 at 30 °C to 0.05 at 65 °C. The r_∞ of 0.05-0.06 at temperatures >58 °C are close to the r_∞ values reported in the fluid, liquid-crystalline state of the "normal" phospholipid vesicles. These results suggest that *Sulfolobus acidocaldarius* will gain a membrane fluidity equivalent to the fluid, liquid-crystalline state of "normal" lipids only when a higher temperature (e.g. >58 °C) is reached. This conclusion is consistent with our previous work of pyrene-PC lateral diffusion in the same membranes. Taken together, our studies demonstrate that the high growth temperature (>58°C) may be essential for the proper function/structure interaction in *Sulfolobus acidocaldarius* archaebacterial membranes. (Kao *et al.* (1992) BBRC in press). (Supported by NSF-RIMI and NIGMS).

M-Pos304

MOBILITY OF MEMBRANE COMPONENTS DETERMINED BY RECORDING TRAJECTORIES OF TETHERED FLUORESCENT MICROBEADS. ((M. Fein, F. Chuang, M. Sassaroli, R. DaCosta, H. Väänänen, J. Eisinger and J. Unkeless)) Mount Sinai School of Medicine, New York, NY 10029.

We have developed a methodology for attaching small (≈ 30 nm) fluorescent beads to specific membrane components and analyzing the bead trajectories recorded by intensified video fluorescence microscopy. Streptavidin was covalently coupled to carboxyl-modified fluorescent latex beads (Molecular Probes "Fluobeads") and is linked to the biotinylated monoclonal antibody or, preferably, its monovalent Fab fragment. Initial experiments employed a supported bilayer (SBL) on glass, but data were also obtained for receptors in membranes of immobilized living cells. The mean square displacement, $\langle r^2 \rangle$, of a bead was found to be proportional to diffusion times (t) over tens of seconds and the the relation $\langle r^2 \rangle = 4Dt$ was used to obtain the effective lateral diffusion coefficient, D. For the GPI-anchored Fcγ receptor (FcR) in an egg lecithin:cholesterol 80:20 SBL, values of D for 21 different beads ranged from 0.3 to 1.0 $\mu m^2/s$ with $\langle D \rangle \approx 0.6\ \mu m^2/s$. This is 2-3 times greater than D for another GPI-anchored protein, Thy-1, in the membrane of a murine thymocyte, as determined from the photobleaching recovery rate. Bead tracking provides a new tool for studying transport and signalling of receptors and how these are modulated by membrane composition and interaction with other proteins.

M-Pos305

KINETICS OF SPECTRIN AND BAND 4.1 BINDING TO PHOSPHOLIPID MODEL MEMBRANES. ((A.E. Mc Kiernan[1], R.C. MacDonald[3], R.I. MacDonald[3], & D. Axelrod[1, 2])) [1] Biophys Res Div, [2] Dept Physics, U. Mich., Ann Arbor, MI 48109, & [3] Dept Biochem, Mol & Cell Biol, Northwestern U., Evanston, IL 60208.

A number of factors affect spectrin binding to planar phospholipid model membranes supported on glass. These factors include the presence of negatively charged phosopholipids in the membrane, buffer ionic strength, and the presence of band 4.1 in the bulk solution. We have measured the equilibrium binding constants and desorption rates (k_{off}) of fluorescent labeled spectrin dimers (F-spectrin) using prismless total internal reflection/fluorescence recovery after photobleaching (TIR/FRAP) microscopy on model lipid membranes consisting of either phosphatidylcholine (PC) and phosphatidylserine (PS) molecules (75:25mol%) or entirely of PC. Both low ionic strength (L) and high ionic strength (H) cases were examined. Preliminary results indicate the equilibrium binding of spectrin alone to the PS membrane is 4 times stronger in L than in H. The average k_{off} (~10/s) for reversible binding is slower (by a factor of 1.4) in L vs. H, and at least 50% of the binding in L is irreversible on the time scale of several seconds, whereas none is irreversible in H. Spectrin (in L) binds to PS membranes 2.6 times more strongly than to all-PC membranes. However, spectrin (in H) binds 2.0 times less to PS than to all-PC. In the all PC membrane, k_{off} is approximately the same for both ionic strengths. For the PS membrane, addition of band 4.1 does not significantly enhance equilibrium spectrin binding in L, but does enhance binding by a factor of 3 in H. Although 4.1 does not significantly affect spectrin k_{off} to PS, it induces a significant irreversible fraction in H. Kinetic studies of fluor-labeled 4.1 will also be presented. NSF DMB8805296 (DA); UM PSD fell. (AM); NIH P01 HL45168 (RM)

M-Pos306

KINETICS OF ELECTRICAL BREAKDOWN OF LIPID BILAYERS. ((M.Winterhalter, K.H.Klotz and R.Benz)), Lehrstuhl für Biotechnologie, Biozentrum am Hubland, D-8700 Würzburg, FRG. (Spon. by R.Podgornik)

The kinetics of pore formation followed by mechanical rupture of bilayer lipid membranes were used to investigate the influence of incorporation of macromolecules into membranes. Control membranes, made from Diph PC (Diphytanoyl Phosphatidylcholine) or Diph PC/CpCl (Cetylpyridium Chloride), were charged to sufficiently high voltages to induce mechanical breakdown [1]. The subsequent decrease in membrane voltage was used to calculate the conductance. At the following step, macromolecules of interest (Pluronic 68, Polyacrylamide) were added into the aqueous phase. We observed that for macromolecules with strong membrane binding affinity the conductivity characteristics were significantly different from the control. Macromolecules with no membrane binding affinity did not alter these characteristics.

[1] C. Wilhelm, et al., Biophys. J. (1993) in press.

This work was supported by the Deutsche Forschungsgemeinschaft (SFB 176)

M-Pos307

COMMUNICATION IN THE CYTOSKELETON (S.R. Hameroff,[1] J. Dayhoff,[2] R. Lahoz-Beltra,[3] S. Rasmussen,[4] A. Samsonovich,[1] D. Koruga[1]) [1]University of Arizona, Tucson, AZ; [2]University of Maryland, College Park, MD; [3]Universidad Complutense, Madrid, Spain; [4]Los Alamos National Laboratories, Los Alamos, NM.

The cytoskeleton [microtubules (MT), actin, intermediate filaments, MT-associated proteins (MAPs), centrioles, etc.] structurally and dynamically organizes cell activities. Coupled to external cellular events by membrane linked proteins (fodrin, ankyrin, spectrin, etc.) and second messenger/protein kinase systems which phosphorylate MAPs and other cytoskeletal elements, the cytoskeleton "communicates" among membranes, nucleus, organelles, and different cell regions. Some experimental evidence (e.g. Vassilev et al, *Biochem Biophys Res Comm* 126:559, 1985) and numerous theoretical models (e.g. Rasmussen et al, *Physica D* 42:428, 1990) predict signaling and information processing in MT and MT-MAP networks. The latter include coherent (acousto-conformation) phonons, solitons, symmetry transitions, free energy minimization and quantum effects. We review these possible mechanisms and show how they could serve functional roles such as communicative signaling, memory, computation, growth, differentiation, adaptation, and synaptic regulation in cells ranging from protozoa to cortical neurons.

M-Pos308

NEUROHORMONAL REGULATION OF PKC ISOZYMES IN ISOLATED CARDIOMYOCYTES ((M. Puceat, R. Hilal-Dandan, L.L. Brunton and J.H. Brown)) Dept Pharmacology, UCSD, La Jolla, CA 92093

We investigated the effects of neurohormones which accelerate PI turnover and of phorbol myristate acetate (PMA) on PKC isozymes distribution (membrane *vs* cytosol) in both neonatal and adult rat ventricular myocytes. Using Western blot analysis with antibodies raised against α, β and ϵ-PKC, we found that myocytes isolated from neonatal or adult rat hearts mainly contained α and ϵ isoforms. In resting conditions, 50 and 70% of α and ϵ-PKC respectively were identified in a crude membrane fraction prepared from neonatal myocytes. In adult cells, 20 and 50% of α and ϵ-PKC respectively were found in membrane fraction. In both cell types, phenylephrine (10-100 µM in the presence of 1 or 10 µM propranolol) and ATP (50 µM) doubled membrane-associated immunoreactive ϵ-PKC. The effect was maximal within 0.5-1 min and returned towards control value within 15 min in the sustained presence of the agonists. In adult myocytes endothelin (0.1 µM) and carbachol (100 µM) exerted a similar effect on ϵ-PKC. Ionomycin (10 µM) was inactive. PMA (0.1 µM) increased membrane-associated immunoreactive ϵ-PKC by 4 and 7 fold in adult and neonatal cells respectively. This occurred within 0.5-1 min and was sustained up to 15 min. PMA also increased membrane-associated α-PKC but to a much less extent than ϵ isoform. None of the agonists increased membrane-associated α-PKC. We are using selective down-regulation of these isoforms to investigate their role in cardiac hypertrophy and *in vivo* protein phosphorylation.

M-Pos309

ANGIOTENSIN II INDUCES ARACHIDONIC ACID MOBILIZATION IN CARDIAC MYOCYTES. ((A.Lokuta, C.Cooper, S.T.Gaa, T.B.Rogers)) Univ. of Maryland School of Medicine, Dept. of Biological Chemistry., Baltimore, MD 21206

Arachidonic acid (ARA) has been reported to regulate cardiac K^+ channels (Kim *et al., Science 244*, 1174 (1989)). The present goal was to determine if hormones stimulate ARA release in heart cells. We have found that 100 nM angiotensin II (AngII) increases ARA mobilization in serum-free cultured neonatal rat myocytes with a biphasic time course (Fig. 1) This AngII specific response is dose-dependent (EC_{50}= 0.2 nM). It is effectively blocked by several AngII receptor antagonists: peptides Sar[1],Leu[8]-AngII ($IC_{50}\approx$ 3nM) and CGP ($IC_{50}\approx$ 7nM), and nonpeptides EXP3880 ($IC_{50}\approx$ 2nM) and DuP753 ($IC_{50}\approx$ 100nM). AngII-induced ARA accumulation is not blocked by antagonists of other important receptor types found in cardiac myocytes. A plausible hypothesis for these data is AngII receptors are coupled to a Ca^{2+}-dependent phospholipase A_2 activation. It was found that two known PLA_2 inhibitors, mepacrine (80 µM) and p-amylcinnamoylanthranilic acid (100 µM), and the Ca^{2+}-buffering agent EGTA (2.0mM), completely blocked AngII-evoked [^{3}H]ARA release. These data suggest that in addition to the well known phospholipase C activation, AngII also stimulates PLA_2 in cardiac cells. Thus, an important hormonal mechanism for short term regulation of cardiac ion channels, and other possible long term cell changes, may include ARA as a signalling molecule.

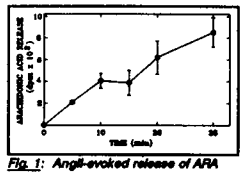

Fig. 1: AngII-evoked release of ARA

M-Pos310

SIGNAL TRANSDUCTION IN CILIARY SYSTEMS : THE EFFECT OF EXOGENOUS ATP ON INTRACELLULAR FREE CALCIUM IN HUMAN NASAL EPITHELIUM. ((A. Korngreen, Z. Priel)) Department of Chemistry, Ben-Gurion University of the Negev, Be'er-Sheva, 84105 Israel.

The signal transduction cascade that leads from the extracellular stimuli to the change in the beat pattern of the cilia is strongly coupled to the calcium ion which is an important second messenger in this cascade. Extracellular adenosine 5'-triphosphate (ATP) strongly enhances the ciliary beat frequency. A model was developed (T. Weiss et al, J. Membrane. Biol., 127, 185-193, 1992) which suggest that exogenous ATP interacts with a membrane receptor in the presence of Ca^{2+}, a cascade of events occurs which consequently open the calcium-activated potassium channels, which then leads to a change in membrane potential. The cilia respond to these changes in an enhancement of their activity. One of the predictions of this model is the rise in cytosolic calcium concentration.

A fura-2 microspectrofluorimeter was used to measure intracellular calcium transients in human nasal epithelia. A sharp rise in intracellular free calcium was observed after the addition of micromolar concentrations of ATP. The concentration of cytosolic calcium changed from a resting value of 50±20 nM (n=11) to a value of 610±80 nM (n=4) at 10µM of ATP at which the effect was maximal. This effect was investigated with various channel blockers and external conditions. These preliminary results verify on of the predictions of the above model and deepen our understanding of the signal transduction cascade in ciliary cells.

M-Pos311

MANGANESE-ENTRY PATHWAYS IN RAT MAST CELLS. ((Cristina Fasolato, Markus Hoth and Reinhold Penner)) Max-Planck-Institut für biophysikalische Chemie, Am Fassberg, D-3400 Göttingen, Germany.

A large number of studies on Ca^{2+} influx in non-excitable cells employs Mn^{2+} as a tracer for Ca^{2+} by measuring Mn^{2+}-induced quenching of Fura-2 fluorescence. We provide here electrophysiological data showing that, in mast cells, the calcium-specific current activated by depletion of intracellular calcium stores, I_{CRAC}, supports a small but measurable Mn^{2+} current. The influx of Mn^{2+} can be detected either by direct measurement of the current or by monitoring the Mn^{2+}-quenching of the Fura-2 fluorescence, however conditions favoring one type of measurement preclude the other. This confirms that I_{CRAC} is a ubiquitous mechanism for Ca^{2+} influx in non-excitable cells. Mn^{2+} quenching of Fura-2 fluorescence occurs also during activation of other two ionic currents: a small current through non-specific cation channels of 50-pS unitary conductance and a distinct cationic current of large amplitude. In addition to these influx pathways, Mn^{2+} can be taken up into calcium stores and be released subsequently by Ca^{2+}-mobilizing agonists.

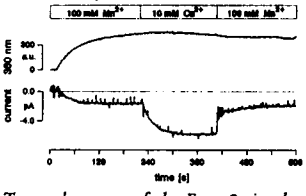

Temporal pattern of the Fura-2 signal (at 360 nm) and the activation of the manganese current by depletion of calcium stores with Ins(1,4,5)P_3.

M-Pos312

CALCIUM RELEASE-ACTIVATED CALCIUM CURRENT (I_{CRAC}) IN NON-EXCITABLE CELLS. ((Markus Hoth, Cristina Fasolato and Reinhold Penner)) Max-Planck-Institut für biophysikalische Chemie, Am Faßberg, D-3400 Göttingen, Germany. (SPON. by R. Hedrich).

In many cell types Ca^{2+} release is followed by Ca^{2+} entry across the plasma membrane. Here we characterize the highly Ca^{2+} selective current I_{CRAC} (Calcium Release-Activated Calcium current) that is activated by depletion of Ca^{2+} stores and could be responsible for long lasting elevated Ca^{2+} plateaus. It was found so far in a variety of non-excitable cells including mast cells, RBL-2H3 cells, hepatocytes, thyrocytes and fibroblasts. I_{CRAC} was dependent on the extracellular Ca^{2+} concentration with an apparent K_D of 3.3 mM. Its selectivity for Ca^{2+} over monovalent cations appeared to be in the same range as for voltage-activated Ca^{2+} channels. It was inhibited by all other divalents (Mn^{2+}, Ba^{2+} and Sr^{2+} blocked by permeation). Complex kinetics were obtained removing all the extracellular Ca^{2+}. While all features of I_{CRAC} are compatible with an ion channel mechanisms, there was no significant increase in current noise associated with its activation (see figure).

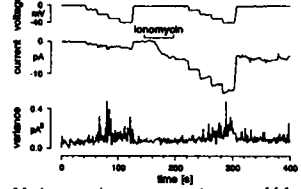

No increase in current variance could be observed during and after activation of I_{CRAC} at different holding potentials (Ca^{2+} stores were depleted by ionomycin).

M-Pos313

UPTAKE, INTRACELLULAR DISTRIBUTION, AND SECRETION OF ANSAMYCINS BY HEP G2 CELLS. Kenneth S. Leonards and Chii-Whei Hu, Research Dept., Pharmaceuticals Div., CIBA-GEIGY Corp., Summit, NJ, 07901 USA

The ansamycins are mono-pivaloyl oxazole derivatives of rifamycin, which have a very high affinity for lipoprotein particles and have been shown to have marked hypolipidemic properties in animals. In the present study, we employed Hep G2 cells to determine whether the ansamycins can enter hepatic cells directly and, if so, their fate. To accomplish this, we measured the uptake of radiolabelled CGS 24565 by Hep G2 cells in the absence of exogenous lipoproteins. We found that the ansamycin was taken up by the cells in a linear fashion for 6-7 hrs at 37°C (rate=142 picomoles/mg cell protein/hr). To determine the intracellular distribution of CGS 24565, the labelled cells were isolated and fractionated on sucrose gradients. We found that the compound was concentrated in only two fractions, a high density fraction containing mitochondrial membranes, potentially free compound or HDL, and a very light density non-membrane associated lipid fraction composed of triglycerides, free fatty acids, cholesterol esters, cholesterol, and phospholipids. With time, the compound was found to move from the denser to the lighter fraction. At 40 hrs post exposure, we found that the ansamycin was being resecreted intact into the extracellular medium where it was found as a component of newly synthesized and secreted lipoproteins. These results suggest that the ansamycins could be a valuable tool for examining intracellular lipid pools.

M-Pos314

INVOLVEMENT OF MITOCHONDRIA IN THE GENERATION OF Ca^{2+} SIGNAL BY ATP-RECEPTOR OF *EHRLICH ASCITES TUMOR CELLS (EATC)*. ((V. P. Zinchenko, and *P. Paucek)). Institute of Cell Biophysics Academy of Science, Pushchino, Moscow Reg., 142292, Russia; *Department of Pharmacology, Medical College of Ohio, Toledo, OH 43600

Involvement of mitochondria in Ca^{2+} redistribution in intact cells at the receptor activation was studied. It is now clear that the activation of purinoceptors of *EATC* is mobilized Ca^{2+} from Endoplasmic Reticulum (ER). The mobilization results in increased free Ca^{2+} concentration in cytosol. We have measured Ca^{2+} transport in mitochondria using NADH fluorescence from activated cells after ATP addition. The mitochondrial transport process is slower then Ca^{2+} changes in cytosol. Ca^{2+} mobilized from ER is intercepted by mitochondria and induced NADH reduction. The Ca^{2+} concentration changes in mitochondria have transient character. We found, however, that tetraphenylphosphonium (TPP^+) blocked Ca^{2+} efflux in mitochondria. The cells pretreated with TPP^+ induced irreversible accumulation of Ca^{2+} in mitochondria only when cells are activated by ATP. Mitochondria can accumulate 30% of Ca^{2+} released from ER.

M-Pos315

Ca-BUFFER CAPACITY IN MYXICOLA AXOPLASM. ((N.F. Al-Baldawi, M. A. Laflamme, and R.F. Abercrombie)) Department of Physiology, Emory University School of Medicine, Atlanta, GA 30322.

When Ca^{2+} serves its physiological role of intracellular messenger, it typically enters the cytoplasm through discrete channels at specific locations such as the surface membrane or internal storage sites. To accurately determine the cytoplasmic Ca-buffer capacity, however, it is desirable to elevate $[Ca^{2+}]$ uniformly and instantaneously. A system consisting of extracted cytoplasm from the giant neuron of a marine worm, Ca-specific "mini" electrodes, the photo-releasable "caged Ca" compound Nitr-5 (Tsien and Zucker, Biophys J. 50: 843-853), and a shuttered 75 watt zenon lamp was used to measure buffer capacity. In the absence of cytoplasm, complete photolysis of the chelator (in 0.3 M KCl, 0.01 M HEPES, pH 7.5) increased its Ca dissociation constant (K_d) ~20 times as determined from titration measurements. The percent conversion of Nitr-5 upon photolysis was calculated from the increase in $[Ca^{2+}]$ and was not influenced by the Ca/Nitr-5 mixture. The relative $[Ca^{2+}]$ increase, however, was maximal at a Ca/Nitr-5 mixture of ~4/6 that gave a pre-photolysis $[Ca^{2+}]$ of ~1 μM, consistent with the K_d's of the photolyzed and unphotolyzed forms of the chelator. The endogenous cytoplasmic buffer capacity was calculated from the change in $[Ca^{2+}]$ when Nitr-5 was mixed with Myxicola axoplasm (167 μM final concentration) and exposed to light. The Ca-binding capacity (change in endogenously bound Ca/change in free Ca) ranged from ~50 to ~200. Supported by NIH NS-19194.

M-Pos316

MOBILE AND IMMOBILE CALCIUM BUFFERS IN BOVINE ADRENAL CHROMAFFIN CELLS. ((Zhuan Zhou and Erwin Neher)) Max-Planck-Institut für biophy-sikalische Chemie, Am Faßberg, D-3400 Göttingen, Germany. (Spon. by D. Schild)

The calcium binding capacity (κ_S) and mobility of endogenous mobile buffers in bovine chromaffin cells preloaded with fura-2 was measured during nystatin perforated patch recordings followed by whole-cell recording, and the time course of changes in κ_S was registered during periods up to one hour. Rapid changes (within 10 to 20 seconds) of κ_S, as would be expected, if highly mobile organic anions contributed significiently to calcium buffering, were not observed upon transition to whole-cell recording. However, approximately half of the cells investigated displayed a drop in κ_S within 2 to 5 minutes, indicative of the loss of soluble Ca-binding proteins in the range 8-42 kDaltons. The average Ca-binding capacity κ_S (differential ratio of bound calcium over free calcium) was 9 ± 7 (mean$\pm$SEM) for the slowly mobile component and 31 ± 10 for the fixed component. It was concluded that a contribution of 7 from highly mobile buffers would have been detected, if present. Thus, this value can be considend as an upper bound to highly mobile Ca-buffer. Both mobile and fixed calcium binding capacity appeared to have relatively low Ca-affinity, since κ_S did not change in the range of Ca concentrations between 0.1μM and 3μM.

M-Pos317

DEPLETION OF INTRACELLULAR CALCIUM STORES ACTIVATES A LANTHANUM INHIBITABLE CALCIUM CURRENT IN AN EPITHELIAL CELL LINE (MDCK).

((P. Dietl)) Department of Physiology, University of Innsbruck, A-6020 Innsbruck.

In many cell types, receptor-mediated Ca^{2+} release from intracellular Ca^{2+} stores is followed by a sustained entry of Ca^{2+} across the plasma membrane. The pathway for this Ca^{2+} entry mechanism, however, has been only scarcely characterized by electrophysiological means. Here, a La^{3+} inhibitable ($IC_{50} \approx 1\mu M$) Ca^{2+} current is described using the whole cell patch clamp technique. This current is highly selective for Ca^{2+} over other cations ($Ca^{2+} >> Na^+, Ba^{2+}, Mn^{2+} >> K^+, Ni^{2+}$, choline$^+$). It is inwardly rectifying, not voltage-gated and not inhibited by nifedipine or Cd^{2+}. The current is quiescent with a pipette Ca^{2+} concentration of 1 μM but activated by excess of EGTA (10mM) in the pipette. To assess the role of intracellular Ca^{2+} stores in the regulation of the Ca^{2+} current, thapsigargin, an inhibitor of the endosomal Ca^{2+} ATPase, was applied. Thapsigargin (1μM) activated the La^{3+} inhibitable Ca^{2+} current independent of the pipette Ca^{2+} concentration. Extracellular ATP (10μM), via phosphoinositide breakdown, releases Ca^{2+} from intracellular stores. It caused activation of the Ca^{2+} current, when the Ca^{2+} buffer capacity of the pipette was high (10mM EGTA). This event was delayed with regard to activation of Ca^{2+} dependent K^+ channels, indicating that ATP induces Ca^{2+} release prior to activation of the Ca^{2+} current. Accordingly, inositol 1,4,5 trisphosphate (10μM in the pipette) also activated the La^{3+} inhibitable Ca^{2+} current, whereas 1,3,4,5 tetrakisphosphate had no effect on this current. It is concluded that depletion of intracellular Ca^{2+} stores activates a non-voltage-gated Ca^{2+} current by a yet unknown mechanism.

M-Pos318

Ca^{2+} RELEASE AND Ca^{2+} INFLUX IN XENOPUS OOCYTES FOLLOWING EXPRESSION OF A 5-HYDROXYTRYPTAMINE RECEPTOR. ((A.B. Parekh, M. Foguet*, H. Lübbert* and W. Stühmer)). Max-Planck-Institute für biophysikalische Chemistry, Am Faßberg, D-3400, Göttingen, Germany and *Preclinical Research, Sandoz Pharma ltd, Basel, Switzerland.

We have expressed a novel 5-Hydroxytryptamine (5-HT) receptor, cloned from rat stomach fundus, in *Xenopus* oocytes and monitored subplasmalemmal cytosolic free Ca^{2+} through the endogenous Ca^{2+}-activated Cl^- current. Following brief exposure to 5-HT (1 min), a rapid inward current with superimposed oscillations (50-800 nA) was observed followed by a long-lasting secondary inward current (20-80 nA, 10-40 min duration). Both phases of the current were abolished by heparin. The oscillations were still observed in Ca^{2+}-free solution (albeit lower frequency) but were insensitive to ryanodine. Caffeine reduced the currents but did not evoke a current itself. The secondary current was sensitive to changes in the external Ca^{2+} concentration and dramatically reduced by external Cd^{2+}. Similar results were obtained following injection of IP_3-F, an IP_3 analogue not metabolised to IP_4. The Ca^{2+} influx pathway can also be activated independently of IP_3 by depleting the internal store either by ionomycin or intracellular injection of EGTA. Moreover, the Ca^{2+}ATPase inhibitor thapsigargin greatly prolongs the duration of the secondary current activated by 5-HT. These results suggest that IP_3 has two roles, namely releasing Ca^{2+} from internal stores (which evokes the oscillations) and also activation of Ca^{2+} influx (which refills the stores). This Ca^{2+} influx is triggered by IP_3-store emptying.

M-Pos319

CELL VOLUME CHANGES ARE ACCOMPANIED BY ARTIFACTUAL CHANGES IN INTERNAL CALCIUM AS MEASURED BY FURA-2 FLUORESCENCE. ((L.M. Bolchkin and G. Matthews)) Dept. Neurobiology, SUNY, Stony Brook, NY 11794.

Volume regulation in single rat retinal pigment epithelial cells was investigated using whole-cell patch-clamp recording combined with fura-2 measurements of $[Ca]_i$. Hypotonic external solution elicited swelling, accompanied by an apparent increase in $[Ca]_i$ calculated from the ratio of fura-2 fluorescence at 340 and 380 nm. However, the observed changes in the ratio could be attributed to alterations in fura-2 fluorescence unrelated to binding of Ca. Increase in $[Ca]_i$ normally leads to an increase in fura-2 fluorescence at 340 nm and a decrease at 380 nm, but "Ca-responses" during volume changes were due mostly to a decrease at 380 nm, with little or no change in fluorescence at 340 nm (see Fig.). This behavior may result from two competing influences that arise upon swelling: 1) an increase in the amount of dye in the cell, which increases fluorescence proportionally at all wavelengths, and 2) a decrease in internal viscosity, which should decrease fluorescence preferentially at longer wavelengths (Poenie, M., 1990, Cell Calcium, 11, 85-91), producing an artifactual increase in the 340/380 ratio. Consistent with this interpretation, the swelling-induced "Ca-response" was unaffected by buffering of $[Ca]_i$ with 5 mM K_2EGTA/5 mM CaEGTA in the patch pipette (see Fig.); such strong buffering abolished genuine increases in $[Ca]_i$ of comparable magnitude elicited by ionomycin. The "Ca-response" upon swelling is within the range reported for a variety of physiological stimuli and might occur in any situation in which volume changes are a primary or secondary consequence of a physiological stimulus. (NIH Grant EY08673)

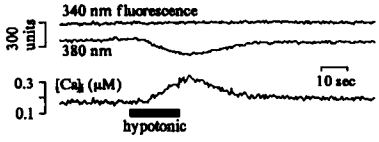

M-Pos320

CYTOPLASMIC Ca^{2+} DEPENDENCE OF THROMBIN-INDUCED Ca^{2+} INFLUX AND RELEASE IN HUMAN PLATELETS. ((J.G. Cantave and D.H. Haynes)) Department of Molecular & Cellular Pharmacology, University of Miami School of Medicine, Miami, FL 33101

The initial rates of Ca^{2+} influx and release from intracellular stores were determined by a method involving use of three different intracellular quin2 concentrations ($[Q]_T$). The method was calibrated by measuring the initial rate of increase in calcium-quin2 complex (d[Ca-Q]/dt) after addition of 2 mM external Ca^{2+} and 1 μM ionomycin to Ca^{2+}-depleted platelets. A plot of d[Ca-Q]/dt against $[Q]_T$ was hyperbolic. Initial rates of passive influx in the absence of ionomycin were lower but showed a similar $[Q]_T$ dependence. When repeated with thrombin to stimulate the influx, high values of d[Ca-Q]/dt were observed, but the $[Q]_T$ dependence was biphasic, showing a decrease for $[Q]_T$ between 1.0 and 2.0 mM. This shows that > 1.0 mM quin2 inhibits thrombin-stimulated Ca^{2+} influx. Measurements of initial rate and extent release of Ca^{2+} from the dense tubules of Ca^{2+}-replete platelets also show that high quin2 inhibits the thrombin-stimulated process. These results suggest that thrombin-induced Ca^{2+} influx and release are dependent on the instantaneous level of $[Ca^{2+}]_{cyt}$ which can be transiently attenuated by intracellular quin2. Absolute rates and extents were calculated in m mole Ca^{2+}/liter cell volume. Support: FL/AHA and NIH HL 38228, HL 07188

M-Pos321

ADRENERGIC STIMULATION INCREASES CYTOPLASMIC PH IN BROWN FAT CELLS. ((S.C. Lee, J. Hamilton, T. Trammell, P.A. Pappone & B. Horwitz)) Dept. of Animal Physiology, Univ. of Calif., Davis, CA 95616

Measurements of cytoplasmic pH in brown adipose tissue have demonstrated pH_i increases in response to adrenergic stimulation. We have measured pH_i in isolated brown fat cells to determine whether the cytoplasmic alkalinization is elicited by hormone acting on brown fat cells directly and whether pH_i changes are integral to the thermogenic response of the cells. We used BCECF and fluorescent imaging techniques to measure pH_i in acutely isolated hamster and rat brown fat cells and in primary cultures of rat brown fat cells. Stimulation of hamster cells with norepinephrine elicited significant (>0.05 units), reversible pH_i increases in both high bicarbonate and bicarbonate-free solutions. Alkalinization of pH_i occurred also in response to the α-adrenergic agonist phenylephrine and in some cases to the β-adrenergic agonist isoproterenol. Although our rat cells are thermogenically competent, pH_i responses were seen only rarely in either acutely isolated or cultured neonatal rat cells stimulated under identical conditions. We conclude that isolated brown fat cells are capable of responding to adrenergic stimulation with increases in pH_i, but that such increases may not be essential for hormone-elicited thermogenesis. (Supported by DK32907, DK35747, and GM44840)

M-Pos322

EFFECTS OF PHORBOL ESTERS ON REGULATION OF pH IN NEONATAL RAT VENTRICULAR MYOCYTES. ((T.A.Kohout and T.B.Rogers)) Dept. of Biol. Chem., Univ. of Maryland School of Medicine, Baltimore MD 21201 (Spon. by M. Kirby)

Mechanisms of intracellular pH (pH_i) regulation by protein kinase C (PKC) were studied in spontaneously beating neonatal rat ventricular myocytes using single cells loaded with the fluorescent pH indicator BCECF-AM. As shown in the figure application of phorbol ester, TPA (100 nM), resulted in an alkalinization of the cell by 0.08±0.01 pH units (pHU). To understand the underlying mechanisms the intrinsic activities of the major pH_i regulators were measured. The Na^+/H^+ exchanger activity, using an NH_4Cl prepulse technique, was 1.10 ± 0.06 mM/min and the HCO_3^-/Cl^- exchanger flux was 0.68 ± 0.09 mM/min, using a Cl^- removal protocol. The intracellular buffering capacity (β) was 14.0 ± 0.85 mM/pHU. These results are similar to those seen in adult myocytes. Application of TPA did not change β but did increase the ion fluxes through both antiporters; the H^+ flux via the Na^+/H^+ increased 88 ± 32% whereas the HCO_3^- flux increased 13 ± 4%. The increase in Na^+/H^+ exchanger activity compared to that of the Cl^-/HCO_3^- exchanger is consistent with the alkalinization observed in the figure above. In PKC-depleted cells TPA did not activate either exchanger, supporting the view that the effects are specific and mediated by PKC activation. This is the first report that PKC may modulate the activity of the Cl^-/HCO_3^- antiporter. These results reveal that control of pH_i may be an important target of PKC in neonatal cardiac myocytes.

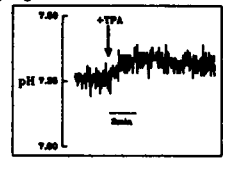

MITOCHONDRIAL MEMBRANE CHANNELS

M-VCR3

INTERNAL COMPARTMENTATION OF THE RAT-LIVER MITOCHONDRION. ((M. Marko, A. Leith, B. McEwen, P. Penczek, D. Barnard, B. McEwen, J. Frank, C.A. Mannella)) Wadsworth Center for Laboratories and Research, New York State Dept of Health, Albany, NY 12201-0509, and Dept of Biomedical Sciences, The University at Albany, State Univ of New York.

There is considerable uncertainty about the internal organization of the mitochondrion, e.g. the shape of the inner membrane and the nature of its contacts with the outer membrane. We have reconstructed isolated rat-liver mitochondria that have been conventionally fixed, osmicated and embedded in Epon. Single-axis tilt series (2° increments) were recorded from 0.4-0.5 μm-thick sections (stained with uranyl) over ranges of +/- 60° (or greater) with the Albany HVEM at 1.0 MeV. Alignment of the projections was achieved with an interactive scheme using colloidal gold particles and reconstruction was done by a simultaneous iterative reconstruction technique (SIRT). Mitochondria in the "condensed" state contain large intracristal compartments that are connected to each other and to the outside by narrow tubes. "Orthodox" mitochondria, on the other hand, appear to contain only tubular cristae, some of which are very long and branched. (Supported by NIH grants RR01219, R01-GM40165, R01-GM29169 and NSF grant DMB-89-16315.)

M-Pos323

ISOLATION AND PURIFICATION OF A VDAC CHANNEL-MODULATING PROTEIN FROM CALF LIVER MITOCHONDRIA. ((Ming Yao Liu and Marco Colombini)) Labs of Cell Biology, Dept. of Zoology, University of Maryland, College Park, MD 20742

The mitochondrial channel, VDAC, mediates metabolic flux across the mitochondrial outer membrane. In different conformational states, VDAC channels show different selectivity and permeability. The VDAC modulator, a soluble mitochondrial protein, has been demonstrated to dramatically increase the voltage dependence and induce the channels to enter a low conductive closed state. We have isolated and functionally purified this modulating protein by a combination of preparative isoelectric focusing, gel filtration chromatography, high performance liquid chromatography, and native gel electrophoresis. The purified protein migrated as a single band of 54 kDa on SDS-polyacrylamide gel with silver staining. However, the VDAC modulator was estimated to be about 100 kDa by gel filtration under reducing conditions. After isoelectric focusing, the modulating activity was found at pI 5.1. In addition, a new, more potent activity was found at pI 4.8. This fraction caused the channels to become virtually non-conducting when tested on the reconstituted bilayer system. By controlling the opening and closing of VDAC, the modulator could play an important role in the regulation of mitochondrial metabolism. (Supported by ONR)

M-Pos324

BLOCKAGE OF MITOCHONDRIAL PORINS WITH POLYANIONS

((Oscar Moran)) Istituto di Cibernetica e Biofisica, CNR. Via Dodecaneso, 33, 16146 Genova, Italy

Polyanionic substances, like dextran sulphate and Konig polyanion, induce a closure of the mitochondrial porin channel incorporated in planar membranes. This phenomenon consists on an increase of the steepness of the voltage dependence and/or a decrease of the half activation potential at positive voltages when added to the reference (ground) side of the membrane. This was explained as an interaction between the polyanionic substance and the gating mechanism of the channel. We re-interpreted the data, in terms of a simple voltage dependent blockage of the channel. We assume that the dissociation constant of the polyanion K, is a function of the potential with the form: $K = K(0)\ exp\ [z\partial VF/RT]$, where K(0) is the dissociation constant at zero mV, z is the apparent charge of the blocker, ∂ is the electrical distance from the reference side of the membrane, V is the membrane potential and F, R and T have the usual meanings. We calculated a set of parameters to simulate the experimental data.The best results are obtained when the binding site is very near to the membrane surface, and z is very high (see figure).

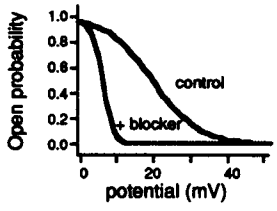

M-Pos325

CHARACTERIZATION OF THE MITOCHONDRIAL [^{125}I]-IODO-PHENYLARSINE OXIDE RECEPTOR.

((Robert D. Hoffman# and Maureen W. McEnery*)) Case Western Reserve University School of Medicine Departments of #Pathology, *Physiology and Biophysics and *Neuroscience, Cleveland, Ohio 44106

This report introduces [^{125}I] PAO as a selective, covalent, high affinity probe of cysteine residues. [^{125}I] PAO binds to kidney homogenate with a B_{max} of 1.7 pmol/ug and an apparent Kd of 345 nM. The binding is saturable, pH dependent, and covalent (with a $t_{1/2}$ of dissociation greater than 10 hr at room temperature). Upon subcellular fractionation of rat kidney, liver and brain, the [^{125}I] PAO binding site is enriched in the mitochondrial fraction; and, with further submitochondrial fractionation, is enriched 8-10 fold in inner membranes with an apparent Kd of 157 nM. The pharmacology of [^{125}I] PAO binding implicates highly reactive and accessible cysteine residues. PAO (1 uM) inhibits the initial rates of inorganic phosphate (^{32}PI) uptake in rat kidney while similar concentrations of PAO are without effect upon ^{3}H-ADP and ^{45}Ca uptake. Mitochondrial proteins (Triton X-100 extract) were fractionated on a PAO-affinity resin and bound proteins were eluted with β-mercaptoethanol. Western analysis of the resulting fractions indicates that the phosphate carrier binds tightly to the PAO-resin (elutes with greater than 10 mM β-mercaptoethanol), while VDAC, in contrast, flows through the PAO-affinity resin. The SDS-PAGE profile of [^{125}I] PAO-prelabelled mitochondrial membranes evidences a major (approx) 30 kDa protein in the absence of reducing agents. ^{125}PAO may be used as a probe of cysteine residues involved in the transport of phosphate via the mitochondrial phosphate carrier.

M-Pos326

SPERMINE IS AN INHIBITOR OF THE PERMEABILITY TRANSITION OF ISOLATED HEART MITOCHONDRIA.

((R.G. Lapidus & P.M. Sokolove)), Department of Pharmacology, Univ. of MD Medical School, Baltimore, MD 20201, USA.

The polyamine spermine (Sp) is widely recognized as a stabilizer of mitochondrial function. It has been reported, for example, to enhance Ca^{2+} retention and to overcome the effects of mitochondrial aging on membrane potential. Many of the effects of spermine could be explained if Sp were an inhibitor of the mitochondrial permeability transition (PT). Using a variety of triggering agents, we have monitored the PT in mitochondria isolated from rat heart *via* (1) Ca^{2+}-dependent swelling, (2) Ca^{2+}-dependent pyridine nucleotide [NAD(P)H] oxidation, and (3) the triggered release of Ca^{2+} from preloaded mitochondria. By all three criteria, Sp (2 mM) inhibited the PT. The transition triggered by *t*-butyl hydroperoxide, carboxyatractylate, phenylarsine oxide and elevated Ca^{2+} was completely suppressed; that elicited by elevated inorganic phosphate levels (P_i) was partially inhibited. A C_{50} of 0.38 ± 0.06 (SD) mM was measured for inhibition of the Ca^{2+}-induced transition. The observation that inhibition was generally independent of triggering agent suggests that spermine acts at or near the pore itself rather than at the level of the diverse biochemical processes postulated to modulate pore opening. [Supported by the American Heart Association, MD Affiliate, and the Univ. of MD Graduate School, Baltimore.]

M-Pos327

SPERMINE INHIBITION OF THE PERMEABILITY TRANSITION OF ISOLATED LIVER MITOCHONDRIA: AN INVESTIGATION OF MECHANISM.

((P.M. Sokolove & R.G. Lapidus)), Dept. of Pharmacology, Univ. of MD Medical School, Baltimore, MD 21201, USA.

Our laboratory has recently reported that the polyamine spermine (Sp) is an inhibitor of the permeability transition (PT) of isolated rat heart mitochondria. In this study, we used Ca^{2+}-dependent swelling to monitor the PT of liver mitochondria with the intent of elucidating the mechanism of Sp action. Our results indicate that: (1) Sp acts at a site *outside* the mitochondria; inorganic phosphate, which is required for Sp uptake, is not required for inhibition. (2) Sp (2mM) both lowers the maximal extent of Ca^{2+}-induced swelling and increases the C_{50} for Ca^{2+}, *i.e.*, Sp does not simply compete for a Ca^{2+} site involved in the PT. (3) The PT of liver, *but not heart*, mitochondria is highly dependent on the ionic composition of the medium. In our standard assay buffer [100 mM sucrose, 50 mM KCl, 20 mM Mops-KOH (pH 7.2), supplemented with 0.2 mM KH_2PO_4 for liver or 1.7 mM for heart], Sp was a less effective inhibitor of the PT of liver than of heart mitochondria. Lowering the ionic strength or the free Ca^{2+} concentration increased the sensitivity of the liver mitochondrial PT to Sp while nullifying the ability of carboxyatractylate to act as a trigger. [Supported by the American Heart Association, MD Affiliate, and the Univ. of MD Graduate School, Baltimore.]

M-Pos328

INDUCTION OF THE PERMEABILITY TRANSITION OF THE INNER MITOCHONDRIAL MEMBRANE IN RAT THYMOCYTES BY CUMENE HYDROPEROXIDE.

((Tatyana I. Gudz, Iovanna G. Pandelova and Sergei A. Novgorodov)) Moscow State University, Moscow, Russia. (Sponsored by R.A. Altschuld).

The effect of the oxidant, cumene hydroperoxide (CuOOH), on the respiration of rat thymocytes was investigated. Thymocytes were incubated in a low - Ca^{2+} medium containing glucose. At concentrations below the level necessary to initiate lipid peroxidation (20-100 μM) CuOOH was found to have three effects on thymocytes: 1) CuOOH decreased the rate of uncoupled respiration attributed to mitochondrial substrate oxidation, 2) CuOOH inhibited the activity of the K^+, Na^+ - ATP-ase, and 3) CuOOH increased respiration in the presence of oligomycin. This later effect was blocked by the antioxidant nordihydroguaretic acid, and by cyclosporine A, which is an immunosuppresent and a potent inhibitor of the mitochondrial permeability transition, as it occurs in isolated mitochondria. It is concluded that CuOOH is able to cause the permeability transition in mitochondria in situ.

M-Pos329

PHOSPHOLIPASE A_2 REACTION PRODUCTS FACILITATE OPENING OF THE PERMEABILITY TRANSITION PORE.

((K.M. Broekemeier and D.R. Pfeiffer)) Hormel Institute, U. of MN Austin MN 55912.

The mitochondrial permeability transition is now thought to occur through the opening of a nonspecific pore in the inner membrane. Regulation of the pore appears complex and to involve several interacting effectors. The relationship between PLA_2 reaction products and pore regulation is examined here. Ca^{2+}-loaded mitochondria undergo the transition after addition of P_i. Exogenous linoleic acid increases the initial P_i-dependent swelling rate by ~10-fold and eliminates the biphasic character of the swelling curve normally seen with Ca^{2+} plus P_i. Maximal effect is seen at 10 nmol 18:2/mg protein, with half maximal effect at 1.5 nmol/mg (<1 mole % of total lipid). 16:0 is as effective as 18:2, while the corresponding C_{16} alcohol or alkane has no effect. LPL are less effective than FFA. No transition occurs with 18:2 and Ca^{2+} alone or with 18:2 and P_i alone. The addition of 18:2 (10 nmol/mg) does not prevent complete inhibition of the transition by CSA (1 nmol/mg). Endogenous FFA, generated by preincubation of mitochondria with Ca^{2+}, are as effective as exogenous FFA at facilitating pore opening. Addition of FFA causes a small decrease in $\Delta\psi$. When CCCP is substituted for FFA in amounts that cause the same decrease in $\Delta\psi$, no acceleration of the transition is observed. Thus, low levels of FFA do not cause the transition *per se* but facilitate induction by P_i. (Support: HL49182 & AHA, MN Affiliate.)

M-Pos330

PATCH CLAMP ANALYSIS OF A CATION-SELECTIVE CHANNEL ISOLATED FROM RAT LIVER MITOCHONDRIA.

((Germán Costa, Robert C. Murphy, and Joyce J. Diwan)) Biology Dept. & Center for Biophysics, Rensselaer Polytechnic Institute, Troy, NY 12180

A protein fraction showing bands on SDS polyacrylamide gels at 97, 77, 57, 53 and 31 kDa was isolated by affinity chromatography on immobilized quinine. Patch clamp recordings from membranes reconstituted with the affinity purified fraction indicate the presence of two channels. When bathed symmetrically in a solution of 150 mM KCl, 5 mM Hepes and 100 μM $CaCl_2$, excised patches of reconstituted vesicle membranes exhibit conductance increments of approximately 40 and 130 pS. The affinity column eluate was further fractionated by isoelectric focusing using a Rotofor Cell. Patch Clamp recordings from membranes reconstituted with a fraction containing protein of 57 kDa have indicated that this fraction contains the 40 pS channel (Paliwal, Costa & Diwan, Biochemistry 31:2223, 1992). In some studies, single channel currents were recorded initially from excised patches bathed on both sides with medium containing 100 mM KCl, and after perfusion to increase KCl in the bath to 400 mM. The positive reversal potential determined after perfusion indicates selectivity for the cation K^+ over the anion Cl^-. A rabbit has been injected for antibody production with the 57 kDa band blotted from an SDS polyacrylamide gel. Western blots show weak reactivity of the serum with the 57 kDa protein. (Supported by USPHS grant GM-20726)

M-Pos331

Ca^{2+} FLUX VIA THE PARTIALLY PURIFIED BEEF HEART MITOCHONDRIAL Ca^{2+} CHANNEL FOLLOWING RECONSTITUTION INTO PROTEOLIPOSOMES.

((S.-d. Zhou, G. Mironova and K. D. Garlid)). Department of Pharmacology, Medical College of Ohio, Toledo, Ohio 43699

We report the first Ca^{2+} flux measurements obtained on the reconstituted mitochondrial Ca^{2+} channel. The channel was extracted with ethanol (Mironova et al., J. Biophys. and Biochem., 1982), partially purified on a DEAE-cellulose column and functionally reconstituted into phospholipid vesicles. Fura-2 was used to measure Ca^{2+} uptake driven by a K^+ gradient in the presence of valinomycin. Ca^{2+} transport in the reconstituted system exhibited hyperbolic dependence on $[Ca^{2+}]$, in contrast to its behavior in intact mitochondria. The K_m was 20 μM, and the V_{max} was 130 μmol/mg protein/min, approximately 250-fold greater than that observed in intact mitochondria. La^{3+} exhibited competitive inhibition of Ca^{2+} uptake, and ruthenium red exhibited noncompetitive inhibition with an IC_{50} of 2-3 nM. Supported by NIH Grant HL 36573

EPITHELIAL PHYSIOLOGY

M-Pos332

BIOPHYSICAL EFFECTS OF THERAPEUTIC ULTRASOUND ON CELLULAR AND PARACELLULAR IONIC CONDUCTANCE ARE CALCIUM DEPENDENT.

((Anan M. Al-Karmi[1], Mumtaz A. Dinno[1], David A. Stoltz[1], Lawrence A. Crum[3], and John C. Matthews[2])) [1]Dept of Physics, [2]Dept of Pharmacology, Univ of Mississippi, University,MS 38677 and [3]Applied Physics Laboratory, Univ of Washington, Seattle, WA 98105.

Recently, we reported an important finding in which we presented evidence that ultrasound renders its therapeutic effects primarily via non-thermal mechanisms [Dinno *et al.* in Ultrasound Med. Biol. 15, 461-470 (1989)]. Cavitation and microstreaming seem to play a major role in the process. Therapeutic ultrasound is used to enhance the repair of soft tissue, muscle, etc., and since these cellular and paracellular repair processes are dependent on calcium, it becomes important to study the effects of ultrasound in the presence and the absence of Ca^{2+}. Using frog skin as a biological model the effect of therapeutic ultrasound (1 MHz at an intensity of 0.3 W/cm^2) was investigated in real time. Application of ultrasound for 2 minutes caused a significantly larger increase in total ionic conductance (G_t) in the presence of Ca^{2+} than in its absence (ΔG_t 1.01 vs. 0 .42 mS/cm^2) . However, the short circuit current decreased in both cases. It is of interest to note that in the recovery phase, the time constant for G_t to return to steady state was significantly longer in Ca^{2+}-free solutions (122 vs. 18 min .). This study demonstrates that the biological effects of ultrasound are calcium dependent. Furthermore, the recovery time constants confirm the findings of Cereijido and collaborators [Contreras *et al.* in Am. J. Physiol. 263, C313-C318 (1992)] which addresses the role of Ca^{2+} in the formation of tight junctions. [Work supported by the NIH under Grant No. 2-RO1-CA-39374-07.]

M-Pos333

EFFECTS OF ISOPROTERENOL, PROPANOLOL, DPC AND PROTEIN KINASE INHIBITORS ON CHLORIDE PERMEABILITY IN PRECONFLUENT CELLS.

((A.F.D. Mahlangu, Howard Friedman, Deborah Alpert and James A. Dix)) Department of Chemistry, State University of New York, Binghamton, NY 13902-6000

Preconfluent A6 cells grown on plastic and Millipore CM inserts exhibit a chloride permeability that is either absent or reduced in the confluent state. We investigated the regulation of the permeability by stimulation of beta-adrenergic receptors and phorbol ester pathway. Chloride permeability was assayed by monitoring iodide efflux using a fluorescence method. Cells were loaded with the halide-sensitive fluorophore, 6-methoxy-N-(3-sulfopropyl)quinolinium) (SPQ), then manipulated to give an outwardly directed iodide gradient. As iodide effluxed from the cell (in exchange for extracellular nitrate), SPQ fluorescence increased. The time constant of iodide efflux and the increase in the total fluorescence signal 4 min after stimulation was measured. The time constant for control cells was 170 sec, which decreased to 60 sec upon isoproterenol stimulation (10 μM). Treatment with DPC (a chloride channel blocker) at 1 mM increased the time constant to greater than 600 sec. The fluorescence signal increased by 200% upon treatment with isoproterenol. The isoproterenol-stimulated fluorescence increase was inhibited by 60% by preincubation with propanolol (100 μM) and by 58% by incubation with DPC (1 mM). Sphingosine (100 μM) increased the isoproterenol-stimulated enhancement by 30%. These results suggest that A6 cells in the preconfluent state posses chloride permeability which is regulated by cAMP and protein kinase C.

M-Pos334

COMPUTER SIMULATIONS OF *IN VIVO* FUNCTIONING OF AIRWAY EPITHELIA.

((Janet A. Novotny-Dura and Eric Jakobsson)) Department of Physiology and Biophysics and the National Center for Supercomputing Applications, University of Illinois, Urbana, IL 61801.

A dynamic model of an airway epithelium has been constructed including the membrane and paracellular transport processes commonly thought to be important for airway epithelial functioning. The behavior of this model has been explored for both the simulated experiments in the Ussing chamber and also for a more physiologically realistic *in vivo* situation involving continuous water transport and evaporation from the apical side. Open circuit voltages and short circuit current seen in the model are consistent with results reported for Ussing chamber experiments. We find that the dynamic behavior and system stability of the model *in vivo* are substantially different from behaviors seen in the Ussing chamber. The tissue functioning is a complex emergent property of sodium, chloride, and water permeabilities. We are exploring these interactions. In addition to providing insight into the basic science of airway epithelium function, this work will elucidate the physiology associated with the cystic fibrosis genetic defect. Supported by an FMC Industrial Partners Grant to the National Center of Supercomputing Applications.

M-Pos335

MEMBRANE DYNAMICS OF CILIATED CELLS : EXTRACELLULAR ATP MARKEDLY REDUCES MEMBRANE ORDER PARAMETER.

((E. Alfahel , A.H. Parola and Z. Priel))Department of Chemistry, Ben-Gurion University of the Negev, Beer-Sheva, 84105, Israel.

The cilia are projections of the cell surface and are covered with membrane which are continoues with the cell surface membrane. Ciliary membrane plays an important role in regulation and modulation of ciliary movement. It detects change of external parameters and transmitts them via second messengers to the interior of ciliated cells. The effect of extracellular ATP on mucus transporting cilia in a freshly excised frog palate was examined by the Fluoresence polarization (P) method of a membrane non-penetrating lipophilic probe 1-(4-trimethylammoniumphenyl)-6-phenyl-1,3,5-hexatriene,p-toluenesulfonate (TMA-DPH). The following results were obtained: (1) Fluorescence polarization values measured in ciliary cell membrane are uniquely lower than in other eucariotic cells. (2) Extracellular ATP (5μM-50μM) caused a decrease (maximum 20% at 10μM) in P. (3)The rapid drop (within 30 sec) in P values followed by a gradual (20 min) recovery approaching initial values.

(4) Quinidine (200μM) a potent blocker of potassium-calcium activated channels, completely abolished the above observed ATP effect. (5) Applying quinidine after adding extracellular ATP resulted in faster recovery. (6) Cytoskeleton reagents e.g. cytochalasin- β or colchicine reduced the external ATP effect, the combination of both, completely abolished it. The mechanistic implication of the above are discussed.

M-Pos336

REGULATION OF Cl CONDUCTANCE OF ZYMOGEN GRANULE MEMBRANES BY ADENOSINE NUCLEOTIDES. ((U. Hopfer & B. Jiang)) Depart. of Physiol. & Biophysics, CWRU, Cleveland, OH 44106

CFTR has been shown to be regulated by protein kinase A as well as ATP binding and possibly hydrolysis at its nucleotide binding regions. To evaluate whether Cl conductance of granule membranes is regulated in a similar manner, a previous study on the effects adenosine nucleotides on Cl conductance of zymogen granules (Thevenod et al., Biochem. J. 272: 119, '92) was extended. The preparative procedure was modified to activate the Cl conductance. Rat pancreatic zymogen granules were prepared by Percoll density gradients, but then washed free of Percoll. Cl conductance was assessed by lysis in isotonic KCl in the presence of a maximal dose of valinomycin to ensure a high K conductance. These washed granules have half-times of lysis between 10-20 min at 37^{O} in the standard lysis assay containing valinomycin. Cl conductance is inhibited 30-50% by 25 uM of the stilbene disulfonates SITS and DIDS. It is also inhibited by ATP, which is additive with the effect of the stilbene disulfonates. The inhibition by ATP is concentration, temperature, and time, but not Mg dependent. With 3 min preincubation in the presence of ATP, maximal inhibition varies between 50-80% with 2 apparent inhibitory sites with Ki values of 5 uM and 3 mM, respectively. In contrast, AMP-PCP, a nonhydrolyzable analog of ATP, stimulates Cl conductance about 2-fold at a concentration of 0.5 mM. 50 uM vanadate abolished both stimulation and inhibition by AMP-PCP and ATP, respectively. ADP and GTP at similar concentrations had no effect on Cl conductance. These results indicate that the Cl conductance on granule membranes is regulated differently than CFTR. Support NIDK-39658.

M-Pos337

ACTIN FILAMENTS MEDIATE PROTEIN KINASE A (PKA) ACTIVATION OF EPITHELIAL Na^+ CHANNELS. A.G. Prat*, A.M. Bertorello, D.A. Ausiello & H.F. Cantiello. Renal Unit, Mass. Gen. Hosp. & Dept. Med., Harvard Med. Sch., Charlestown, MA 02129.

We recently demonstrated that actin filament organization controls Na^+ channel activity in epithelial A6 cells (Am. J. Physiol., 261:C882-C888, 1991). In this report we used patch-clamp techniques to assess the role of PKA on apical Na^+ channel activity. Addition of arginine-vasopressin (AVP), IBMX, cAMP analogs or forskolin induced or enhanced Na^+ channel activity under cell-attached conditions. Further, PKA plus ATP induced and/or enhanced Na^+ channels in excised patches. To determine the role of the actin cytoskeleton on the AVP-activated Na^+ channels various maneuvers to modify actin filament organization were used. Addition of DNAse I (which binds to G-actin preventing its polymerization) inhibited PKA-induced channel activation but phalloidin treatment (2 hs) had no effect. In contrast, cytochalasin D-treatment (2 hs) prevented the PKA-dependent channel activation which was reversed by subsequent addition of actin. To test the role of actin phosphorylation mediated by PKA, G-actin was incubated with active or inactive PKA plus ATP in a polymerizing buffer for 60 min. Phosphorylated actin induced Na^+ channel activity in excised patches pretreated with PKA inhibitor, while actin polymerized in the presence of inactive PKA did not elicit channel activation in those conditions. Our results are consistent with a model in which PKA phosphorylates actin altering actin polymerization which can regulate Na^+ channel activity.

M-Pos338

ACTIVATION OF Na^+/H^+ EXCHANGER AND NaK2Cl COTRANSPORTER IN SINGLE ACINAR CELLS REQUIRES AGONIST-INDUCED FALL OF $[Cl^-]_i$. ((Marli A. Robertson and J. Kevin Foskett)) Div. Cell Biology, Hospital for Sick Children, Toronto, ON M5G1X8. (Spon. by C. Deber)

Muscarinic stimulation of salivary gland acinar cells causes a rise of $[Ca^{2+}]_i$ which rapidly (< 3 sec) activates K^+ and Cl^- channels. Simultaneous fluorescence determinations of $[Ca^{2+}]_i$ or $[Cl^-]_i$ and DIC imaging of cell volume in single cells indicated that Ca^{2+} activation of these channels causes KCl efflux, a fall of $[Cl^-]_i$ from 70 to 30 mM, and 25% cell shrinkage during the 15-30 sec following the $[Ca^{2+}]_i$ peak. At the peak of shrinkage, rapid (~30 mM/min) Na^+ influx became activated, as indicated by $[Na^+]_i$ determinations using SBFI. Inhibitors indicated that Na^+ influx is mediated by Na^+/H^+ exchange (60%) and NaK2Cl cotransport (40%). The 30 s lag between the rise of $[Ca^{2+}]_i$ and activation of Na^+ influx suggested that elevated $[Ca^{2+}]_i$ is not the signal to these Na^+ transporters. Osmotic shrinkage ± cell acidification only activated influx to 10% of the muscarinic rate, indicating that cell shrinkage or acidification (observed in HCO_3^- media) are not triggers. Activation of PKC was without effect. The muscarinic response was reconstituted only when $[Ca^{2+}]_i$ was rapidly elevated. Nevertheless, a rise of $[Ca^{2+}]_i$ was insufficient to activate the Na^+ transporters since activation of cells in 80 mM K^+_o, to block shrinkage, failed to activate Na^+ influx. Osmotic shrinkage of stimulated cells in 80 K^+_o did not activate Na^+ influx however, indicating that KCl loss, rather than cell shrinkage, was critical. Thus, activation of the Na^+/H^+ exchanger and NaK2Cl cotransporter requires a fall of $[Cl^-]_i$, likely due to an allosteric effect of Cl^- on the transporters or critical signal transduction components.

M-Pos339

MEMBRANE WATER PERMEABILITY OF APICAL-OUT EPITHELIAL CYSTS DERIVED FROM MDCK CELLS

((Rickey L. Rivers, James A. McAteer, Bret Conners, Andrew Evan and James C. Williams, Jr.)) Medical University of South Carolina, Anatomy & Cell Biology, Charleston, SC 29425; Indiana University, Anatomy, Indianapolis, IN 46202

Thin-walled apical-out cysts were produced by low density seeding of MDCK cells onto a non-adherent substrate (agarose). Cyst formation was greatly enhanced by adding cAMP (1mM) to the serum-supplemented culture medium. These spherical cysts ranged from 30 to 60 μm in diameter with a cell thickness of ~1μm. Water permeability was determined by osmotic challenge using a theta-tubing based rapid solution-switching system, combined with digital video microscopy. The rate of shrinkage of the cysts was determined by measuring diameters of individual cysts from digitized images taken at periodic time points (3 or 5 seconds between images) after osmotic challenge. The rate of cyst shrinkage then was used to calculate the membrane water permeability of the apical-out cysts. The osmotic water permeability for these apical-out cysts was found to be very low, 3.9 ±0.4 μm/s (N=7), a value similar to that for the mammalian distal nephron in the absence of antidiuretic hormone. Scanning electron microscopy showed these cysts to be relatively smooth thus making the apical surface area and volume measurements very accurate. By having a low water permeability with accessible apical membranes, these cysts provide a unique model for the study of water permeability of an intact renal-derived epithelium.

M-Pos340

Ca^{2+}-ACTIVATED K^+ AND cAMP-DEPENDENT Cl^- CURRENTS IN KIDNEY MTAL EPITHELIAL CELLS. ((L. Lu and W.B. Guggino)) Department of Physiology & Biophysics, School of Medicine, Wright State University, Dayton, OH 45435 and Department of Physiology, Johns Hopkins School of Medicine, Baltimore, MD 21205

A Ca^{2+}-activated K^+ current was characterized by its voltage-dependent and Ca^{2+}-dependent properties in rabbit medullary thick ascending limb (MTAL) epithelial cells. The reversal potential (E_K) was shifted from -85 mV to 0 mV with a slope of 46 mV per e-fold change when the extracellular K^+ ion concentration was increased from 2 mM to 140 mM. Similar to the big-conductance Ca^{2+}-activated K^+ channel (BK) studied with the single-channel patch clamp technique, the Ca^{2+}-activated K^+ current is blocked by charybdotoxin (CTX). The results suggest that the Ca^{2+}-activated K^+ current is the predominant large conductance and Ca^{2+}-dependent K^+ pathway in the MTAL cell apical membrane. A Cl^- current was also investigated in MTAL cells. This current was activated by stimulation of intracellular cAMP using forskolin and isobutyl-1-methylxanthine (IBMX). The current-voltage (I-V) relationship of the Cl^- current showed an outward-rectifying pattern in symmetrical Cl^- solution. The Cl^- selectivity of the whole-cell current was verified by tail current analysis in different Cl^- concentration bath solutions. Several Cl^- channel blockers were found to be effective in blocking the outward-rectifying Cl^- current in MTAL cells. These results suggest that the Cl^- channel in the apical or basolateral membrane of MTAL cells may be regulated by the cAMP-dependent protein kinase induced phosphorylation.

M-Pos341

ION SECRETION IN MALPIGHIAN TUBULES (MT) OF RHODNIUS PROLIXUS. ((B.M. Rodríguez and G. Whittembury)). CBB, IVIC. POB. 21827, Caracas 1020-A, Venezuela. (Spon. by E. González).

Upper segment of MT were dissected and perfused in vitro. Transepithelial, peritubular and apical potentials were measured with conventional microelectrodes in ion substitution experiments before and after stimulation of secretion with serotonin (5.2 μM). In unstimulated MT the main permeability of the peritubular membrane (Pm) is to K^+, which is 100% blocked by Ba^{2+} (2 mM). None of principal ions (Na^+, K^+ and Cl^-) are freely permeable through the apical membrane (Am). In stimulated MT, the Pm is aminly permeable to K^+, having a low permeability to Na^+ (10% nernstian-slope) and a higher permeability to Cl^- (25% of total permeability, 32 °C), which is 100% blocked by Diphenyl-amine-2-carboxilate (0.5 mM). The Am in stimulated MT is not freely permeable to Na^+ and Cl^-, but shows a low permeability to K^+ (11% nernstian-slope). The exit of ions at this membrane is active. We propose a cation pump for the exit of Na^+ and K^+ and the counter-transport Cl^-/HCO_3^- for the exit of Cl^-. The action of furosemide (0.8 mM) indicates that the Na^+, K^+ and Cl^- cross the Pm by a cotransport mechanism, only in stimulated MT. Experiments with ouabain (14 μM) in bathing media suggest that the Na,K-ATPase has an 18% participation in the generation of the peritubular potential. The transepithelial resistance was calculated to be between 1.3-2.9 kohm.cm^2. The ions K^+ and Cl^- are also permeable through a paracellular route.

M-Pos342

IMAGING ION MICROSCOPY EVIDENCE THAT LANTHANUM ENTERS THE CELLS AND RELEASES CALCIUM FROM THE GOLGI REGION. ((X. Zha and G. H. Morrison)) Department of Chemistry, Cornell University, Ithaca, NY 14853.

The effect of La^{3+} on LLC-PK_1 (porcine kidney epithelium derived) cells was investigated by ion microscopy, a quantitative imaging technique based on mass spectrometry. Cells were incubated with $LaCl_3$ for 10 min. (1 mM) or 30 min (0.1 mM), and intracellular calcium distributions were imaged by ion microscopy. Compared to control cells, a 10 min. incubation with 1 mM of La^{3+} released more than 0.1 mM of calcium from the Golgi complex while other cellular regions, such as nucleus and cytoplasm, remained largely unchanged. A 30 min. incubation with 0.1 mM of La^{3+} induced similar depletions in the Golgi calcium. These two experiments were repeated on cells that are pre-incubated with 1 mM ouabain. The presence of ouabain in the medium increased the loss of calcium from the Golgi by about 4 folds as compared to the one without ouabain. The La^{3+} effect, therefore, was amplified by Na^+ loading, indicating a possible involvement of an Na^+/La^{3+} exchanger. The integrity of the Golgi complex was maintained in all experiments as evidenced by NBD-ceramide fluorescence staining of the cells. Lanthanum was detected within cells by ion microscopy and its uptake was facilitated by the ouabain induced Na^+ loading. These results indicate that La^{3+} may effect cellular calcium homeostasis by actions other than a simple calcium antagonist.

Supported by NIH grant GM 24314.

M-Pos343

SOME ASPECTS OF ZINC TRANSPORT INTO PIG SMALL INTESTINE BRUSH BORDER MEMBRANE VESICLES. ((F.Tacnet, F.Lauthier and P.Ripoche)) DBCM/SBCe, CE Saclay, 91191 Gif/Yvette Cedex, France .

A specific and saturable carrier mediated process for the essential trace element, zinc, was already described in the intestinal brush border membrane (for review see Cousins (1985) Physiol.Rev., 65:238-309 ; Tacnet et al. (1990) BBA, 1024:323-330). Here, we looked for possible zinc pathways through other transport systems by measuring time-courses of ^{65}Zinc uptake across the intestinal apical membrane isolated in a vesicular form.

Although zinc uptake is strongly affected by pH (pH_{opt}=6.6), experiments in the presence or absence of proton gradients did not allow us to conclude in favor of a neutral $Zn^{2+}/_nH^+$ exchange mechanism.

A zinc uptake through the Cl^-/HCO_3^- exchanger, as those shown in the red cell membrane, was studied. Although zinc transport was enhanced in the presence of bicarbonate ions (or other low-affinity zinc-binding anions such as thiocyanates), no DIDS or DPC sensitivity was detected indicating that the intestinal anion antiporter is not a major route for zinc reabsorption.

By using the tripeptide GlyGlyHis, expected to be a high-affinity zinc ligand, we showed that zinc could be transported as a $[(GlyGlyHis)_n\text{-}(Zn)_n]$ complex, utilizing the H^+/peptide cotransport system, i.e., in conditions necessary for the secondary active transport of the peptide: inwardly directed H^+ gradients and membrane potential "negative inside".

These results suggest that complexes of zinc could be reabsorbed through the brush border membrane either via a zinc specific pathway (saturable carrier) or via existing carriers such as a neutral anionic exchanger or peptide (or amino acid) transporters.

M-Pos344

MODULATION OF POTASSIUM CHANNELS AND CALCIUM INFLUX IN ENDOTHELIAL CELLS BY CYCLOPIAZONIC ACID, A SARCOPLASMIC RETICULUM Ca^{2+}-PUMP INHIBITOR. ((E. Pasyk and E.E. Daniel)) McMaster University, Hamilton, Ontario.

We have used cyclopiazonic acid (CPA), a selective inhibitor of the Ca^{2+}-pump in sarcoplasmic reticulum (SR) of cultured bovine pulmonary endothelial cells to elucidate the role of Ca^{2+} stores in controlling K^+ channels and Ca^{2+} entrance using patch-clamp technology. As a consequence of the action of CPA, unbalanced leakage of Ca^{2+} from the intracellular stores occurs, causing transient elevation of cytosolic Ca^{2+}. This elevation is expressed by $[Ca^{2+}]_i$-induced outward K^+ current activation. Reduction of inwardly rectifying K^+ current also occurs. The effects of CPA on both K^+ currents shifts the membrane potential towards more negative values increasing the driving force for the external Ca^{2+}. We also showed that Ca^{2+} may enter the bovine pulmonary artery endothelial cells through nonselective cation channels (permeable for Na^+, K^+, Ca^{2+}) activated by stretch. CPA stimulates an influx of Ca^{2+} through these channels. CPA-induced increase of intracellular Ca^{2+} due to emptying of Ca^{2+} stores and subsequent influx of external Ca^{2+} may lead to the production of EDRF by endothelial cells which contributes to the relaxation of vascular smooth muscle. (Supported by MRC and PMA of Canada.)

M-Pos345

CORTICOSTERONE STIMULATES AMILORIDE-SENSITIVE SODIUM ENTRY IN XENOPUS LAEVIS LUNG ((L.M. Baxendale)) The Johns Hopkins Univ. Sch. Nursing, Baltimore, Md. 21287-1316.

Sodium (Na) absorption is integral for alveolar fluid reabsorption essential for optimal lung function. Xenopus laevis lung (XLL) resembles mammalian alveolar type II epithelial cells (ATII) (Fischer et al 1989) morphologically and functionally. Both systems exhibit active Na absorption via entry through amiloride-sensitive apical Na channels and exit via basolateral Na-K ATPase pumps. Harvest and preparation of ATII monolayers is a time and labor intensive procedure. XLL has a single epithelial cell type and does not require manipulation for study. Contrary to previous reports, we have found that large adult XLL does respond to β adrenergic agonists and other agents such as the glucocorticoid corticosterone (Corti) important in regulation of Na and fluid reabsorption in distal lung. Lungs of XL were excised, opened and mounted as a flat sheet on lucite rings in a modified Ussing chamber. Tissues were continuously perfused on both sides with a Ringer's solution containing (in mM): 100 Na, 2.4 K, 2.4 HCO_3, 2 Ca, 102 Cl, 5 D-glucose bubbled with room air pH 7.8 at 22° C. Initial values for open-circuit transepithelial voltage and resistance (Rt); and short-circuit current (Isc) were recorded. Essentially all of the Isc was amiloride sensitive (Ina). The tissues were short-circuited and Ina was allowed to equilibrate (7.1 ± 1.1 $\mu A/cm^2$). At this point, corticosterone (1 μM) was added to the basolateral bath. After several minutes,Ina increase to a plateau value of 13.7 ± 3.3 $\mu A/cm^2$ (t=192 minutes). Rt was slightly decreased in the presence of Corti (88.5 ± 2.5 % control). Glucocorticoid receptors are found on ATII cells and these data suggest XLL also shares this trait. These data indicate that XLL may be an alternative model system for ATII cells. Further, enhanced lung function observed in the presence of glucocorticoids (which enhance surfactant secretion) may also be augmented by stimulation of Na entry and therefore fluid reabsorption.

MEMBRANE RECEPTORS

M-Pos346

PURIFICATION AND CHARACTERIZATION OF THE HIGH AFFINITY HIT CELL SULFONYLUREA RECEPTORS ((D.A. Nelson, L. Aguilar-Bryan, S.W. Wechsler, A.S. Rajan and J. Bryan)) Depts. of Medicine and Cell Biology, Baylor College of Medicine, Houston, TX 77030

Sulfonylureas stimulate insulin secretion from pancreatic beta cells by binding with high affinity to a membrane protein, presumably an ATP-sensitive K^+ channel. HIT cell membrane proteins were photolabeled with an ^{125}I-labeled glyburide analog, solubilized with 1% digitonin and chromatographed on lectin, reactive dye and phenylboronate containing column beds. Further purification was done by electrophoresis. The major form of the receptor is a Con A-binding glycoprotein with an apparent MW of 140 kDa. This protein photolabels with an efficiency of ~1%. The 140 kDa band shifts mobility slightly upon digestion with Endoglycosidase F/N-glycosidase F (Endo F), yielding a polypeptide of ~137 kDa after N-linked carbohydrate removal. A second, minor, wheat germ agglutinin-binding form of the receptor is also present in HIT cells. This protein, with an apparent MW of 150 kDa, photolabels with low efficiency. Incubation of this form of the receptor with Endo F also yields a polypeptide of ~137 kDa, suggesting the two forms of the receptor contain similar polypeptides, but differ in carbohydrate content. This idea is supported by experiments in which each receptor is digested with Endo F, followed by V8 protease. The resultant peptides from each receptor have identical electrophoretic mobilities. Two radiolabeled peptides from the 140 kDa protein, of 49 and 66 kDa, are glycosylated at residue 9, the same position as in the intact polypeptide. This suggests that the N-terminus is extracellular, and that the sulfonylurea binding site is in the first one-third of the receptor protein.

M-Pos347

THE KINETICS OF RECEPTOR-MEDIATED CELL ADHESION UNDER FLUID FLOW. ((L.A. Tempelman, D. A. Hammer)) School of Chemical Engineering, Cornell University, Ithaca, NY 14853.

The physiological function of many cells is dependent on their ability to adhere via receptors to ligand-coated surfaces under fluid flow. For example, an early step in the leukocyte-mediated inflammatory response is the adhesion of neutrophils to endothelial cells under fluid stresses of 1 -5 dynes/cm^2. We have developed an experimental system to measure the kinetics of cell adhesion as a function of cell and surface chemistry and fluid flow. Using a parallel-plate flow chamber, we measure the binding of rat basophilic leukemia (RBL) cells preincubated with anti-DNP IgE to polyacrylamide gels to which 2,4 dinitrophenol (DNP) is covalently bound. We observe the spatial pattern of cell binding as cells travel from the DNP-free to the DNP-coated section of the chamber, as well as the total number of cells bound.

There is a rather narrow range of DNP densities, IgE coverages and shear rates for which the percentage of cells which bind changes. For example, with 4×10^4 binding sites on the cells and a ligand density of approximately 10^{10} sites/cm^2, adhesion ranged from 99 to 2.4 % for shear rates from 30 to 120 sec^{-1}. The spacial patterns of adhesion indicate that adhesion is a probabilistic process. Results for adhesion as a function of receptor number and ligand density will also be presented. Finally, we measured the adhesion of RBL cells to DNP-coated gels which were preincubated with anti-DNP IgE. Adhesion in this system results from the binding of the Fc_ε receptor to the Fc portion of IgE , a *higher* affinity interaction with a hundred fold *lower* forward reaction rate. Adhesion under flow in this system is very low, although static adhesion occurs readily. This demonstrates that the forward rate of reaction of the receptor-ligand pair is more important than its affinity in the regulation of adhesion under fluid flow.